



HAL
open science

Wireless Resource Allocation in 5G-NR V2V Communications

Thanh-Son-Lam Nguyen

► **To cite this version:**

Thanh-Son-Lam Nguyen. Wireless Resource Allocation in 5G-NR V2V Communications. Library and information sciences. Université Paris-Saclay, 2023. English. NNT : 2023UPASG052 . tel-04342129

HAL Id: tel-04342129

<https://theses.hal.science/tel-04342129>

Submitted on 13 Dec 2023

HAL is a multi-disciplinary open access archive for the deposit and dissemination of scientific research documents, whether they are published or not. The documents may come from teaching and research institutions in France or abroad, or from public or private research centers.

L'archive ouverte pluridisciplinaire **HAL**, est destinée au dépôt et à la diffusion de documents scientifiques de niveau recherche, publiés ou non, émanant des établissements d'enseignement et de recherche français ou étrangers, des laboratoires publics ou privés.

Wireless Resource Allocation in 5G-NR V2V Communications

*Allocation des ressources radio dans les
communications 5G-NR V2V*

Thèse de doctorat de l'université Paris-Saclay

École doctorale n° 580 : Sciences et Technologies de l'Information et de la
Communication (STIC)

Spécialité de doctorat : Sciences des réseaux, de l'information et de la
communication

Graduate School : Informatique et sciences du numérique

Référent : Université de Versailles-Saint-Quentin-en-Yvelines

Thèse préparée dans l'unité de recherche DAVID (Université Paris-Saclay, UVSQ), sous la
direction de Nadjib AIT SAADI, Professeur, le co-encadrement de Sondes KALLEL KHEMIRI,
Maître de conférence

Thèse soutenue à Versailles, le 18 septembre 2023, par

Thanh-Son-Lam NGUYEN

Composition du jury

Membres du jury avec voix délibérative

Toufik AHMED Professeur, ENSEIRB-MATMECA, Universités Bordeaux INP	Président
Adlen KSENTINI Professeur, EURECOM - Communication systems	Rapporteur & Examineur
Phillipe MARTINS Professeur, Télécom Paris	Rapporteur & Examineur
Tijani CHAHED Professeur, Télécom SudParis	Examineur
Thi-Mai-Trang NGUYEN Professeure, Université Sorbonne Paris Nord	Examinatrice

Titre : Allocation des Ressources Radio dans les communications 5G-NR V2V

Mots clés : V2X - V2V - 5G - NR - Numérolgie - Allocation des Ressources

Résumé :

Cette thèse doctorale explore l'amélioration de l'allocation des ressources sans fil dans les communications Vehicle-to-Everything (V2X), selon la norme 3GPP Release 16. Le domaine spécifique de notre recherche est la communication NR-V2X Sidelink, également connue sous le nom de communication New Radio-Vehicles to Vehicles (NR-V2V). Notre objectif est de formuler un nouveau protocole d'optimisation qui garantit non seulement des services de haute qualité (QoS) mais surpasse également les méthodologies existantes dans la communication NR-V2V.

Tout d'abord, nous introduisons la Configuration Physique Adaptative (APC), un algorithme basé sur la recherche conçu pour identifier la

configuration optimale de la couche physique à l'intérieur d'un ensemble de facteurs environnementaux, spécifiquement adaptée pour un schéma de communication de diffusion. Suite à cela, nous faisons évoluer l'APC vers une variante sensible à la radio (RA-APC), élargissant son champ d'action en incorporant une communication en unicast et en établissant une structure plus flexible pour les ressources PHY. Dans la phase finale, nous affinons encore RA-APC en intégrant un algorithme d'apprentissage automatique, spécifiquement un arbre de décision. Cette intégration met à jour les schémas au sein des facteurs d'entrée, augmentant ainsi à la fois la précision et l'efficacité du processus d'optimisation de l'allocation.

Title : Wireless Resource Allocation in 5G-NR V2V Communications

Keywords : V2X - V2V - 5G - NR - Numerology - Resource Allocation

Abstract :

This doctoral dissertation explores the enhancement of wireless resource allocation in Vehicle-to-Everything (V2X) communications, as specified by the 3GPP Release 16 standard. The specific area of our research is the NR-V2X Sidelink communication, also known as the New Radio-Vehicles to Vehicles (NR-V2V) communication. Our goal is to formulate a novel optimization protocol that not only guarantees high-quality services (QoS) but also outperforms existing methodologies in NR-V2V communication.

Initially, we introduce Adaptive Physical Configuration (APC), a search-based algorithm designed

to identify the optimal physical layer configuration within a set of environmental factors, specifically tailored for a broadcast communication scheme. Following this, we evolve APC into a Radio Aware variant (RA-APC), broadening its scope by incorporating unicast communication and establishing a more flexible structure for PHY resources. In the final phase, we further refine RA-APC by integrating a machine learning algorithm, specifically a decision tree. This integration uncovers patterns within the input factors, thereby augmenting both the accuracy and efficiency of the allocation optimization process.

Résumé

Cette thèse doctorale explore l'amélioration de l'allocation des ressources sans fil dans les communications Vehicle-to-Everything (V2X), selon la norme 3GPP Release 16. Le domaine spécifique de notre recherche est la communication NR-V2X Sidelink, également connue sous le nom de communication New Radio-Vehicles to Vehicles (NR-V2V). Notre objectif est de formuler un nouveau protocole d'optimisation qui garantit non seulement des services de haute qualité (QoS) mais surpasse également les méthodologies existantes dans la communication NR-V2V.

Premièrement, la thèse présente le concept de systèmes de Cooperative Intelligent Transport Systems (C-ITS) et ses deux technologies de communication les plus célèbres. Dedicated Short-Range Communications (DSRC) utilisent la technologie Wi-Fi, cependant Cellular Vehicle-to-Everything (C-V2X) est basé sur le réseau cellulaire, standardisé par 3GPP. Étant donné que la thèse se concentre sur le C-V2X, nous avons porté sur une étude approfondie de la norme 3GPP Release 16 (5G NR-V2X), en particulier NR-V2V. La recherche s'est concentrée sur les exigences de service, la qualité du service, le pilier de protocole, la couche physique, le mode d'allocation des ressources radioélectriques, et d'autres aspects pertinents, fournissant une compréhension de leurs capacités et fonctionnalités.

Deuxièmement, la thèse a examiné les aspects problématiques de l'allocation des ressources dans NR-V2X, y compris la portée limitée du spectre, la congestion des canaux radio, l'évolutivité et l'interopérabilité, etc. La thèse souligne l'importance de mettre en œuvre des stratégies d'allocation de la numérologie adaptative qui peuvent atténuer ces défis et optimiser l'utilisation des ressources.

Ainsi, cette thèse a fourni un examen approfondi de la littérature, de la recherche et des technologies existantes concernant la numérologie adaptative dans la communication V2X. Le manuscrit a examiné les différentes approches et algorithmes mentionnés dans la littérature, en soulignant leur valeur et leur limite dans les scénarios NR-V2X. Cette revue a fourni des informations précieuses sur l'état de l'art et a guidé l'élaboration du cadre de numérologie adaptative proposé.

Sur la base des conclusions de la recherche, la thèse a proposé trois contributions.

Tout d'abord, nous avons proposé un nouvel algorithme appelé Adaptive Physical Layer Configuration (APC), pour répondre aux exigences de l'allocation de ressources V2X. L'APC examine l'impact de la taille de sous-canal et de la numérologie sur le système dans l'approche de planification centralisée, dans laquelle l'allocation des ressources est gérée par le gNB, et la communication en mode de broadcast. L'objectif principal de APC est d'identifier les meilleures configurations de numérologie et de taille de sous-canal dans la couche physique (PHY) pour répondre aux exigences QoS les plus strictes pour la communication V2X. L'Adaptive Expected Serving Packet Rate (AESPR) a été intégré

au calendrier pour prévenir la présence du phénomène de la famine. Les résultats démontrent que notre proposition fonctionne bien pour maximiser la valeur de l'Effective Transmitted Packet (ETP) et réduire au minimum la famine pour les Logical Channels (LC) à faible priorité.

Ensuite, nous améliorons l'APC en tenant compte de l'état de l'environnement de radio. Notre deuxième contribution est Radio-Aware Adaptive Physical Layer Configuration (RA-APC). Nous avons étudié les effets de l'algorithme sur la communication Unicast et la flexibilité des ressources en termes de quantité de sous-canal. Notre proposition, RA-APC, a été validée par des simulations approfondies et a obtenu des améliorations significatives en matière d'ETP, de fiabilité et de latence. En outre, dans cette étude, nous avons examiné diverses combinaisons de numérogie et de taille de sous-canal lors de l'application de RA-APC.

Dans la phase finale, le temps de convergence nécessaire pour trouver une bonne numérogie et une taille de sous-canal peut être encore réduit en utilisant un modèle Machine Learning. Etant donné toutes les données d'observation, nous entraînons un Decision Tree sur les données générées par RA-APC pour estimer la valeur de sortie. Notre troisième contribution est l'RA-APC basé sur Decision Tree (DeTrAP). En plus, DeTrAP prend également en considération diverses densités et la nature dynamique des services V2X. Les résultats indiquent que DeTrAP dépasse le RA-APC en termes de performance réseau. Ceci est obtenu en réduisant le temps nécessaire pour déterminer la numérogie appropriée et la taille du sous-canal pour différents scénarios de densité et de service V2X.

Cette thèse a contribué à la question de la numérogie adaptative pour l'allocation des ressources de communication NR-V2X. Les résultats de la recherche et la méthodologie suggérée fournissent une étude compréhensive ainsi que des idées pratiques pour gérer les interférences, allouer efficacement les ressources et améliorer les performances globales des systèmes NR-V2X.

Acknowledgments

First of all, I express my most sincere gratitude to Professor **Nadjib AITSAADI** and Professor **Sondes KALLEL** for their guidance and mentorship. Without them, this thesis would not have come into fruition. They have set an inspiring example of a researcher that I aspire to grow into. I also want to thank **Cédric ADJIH** and **Ilhem FAJJARI** for their contribution to this research. I very much appreciate the advice and insights that they have generously shared with me throughout this thesis.

I had the honor to welcome five outstanding researchers to my thesis committee : Professor **Adlen KSENTINI** from EURECOM, Professor **Phillipe MARTINS** from Télécom Paris, Professor **Toufik AHMED** from Université Bordeaux, Professor **Tijani CHAHED** from Télécom SudParis, and Professor **Thi-Mai-Trang NGUYEN** from Université Sorbonne Paris Nord. Their challenging questions and insightful remarks have been valuable, which allowed me to gain a larger perspective on my research works.

During the four years of this thesis, I had the chance to meet and work with my colleagues at DAVID lab (Université de Versailles Saint-Quentin-en-Yvelines - Université Paris-Saclay). I genuinely enjoyed the discussions we have had together, that lightened the mood and challenged the mind all the same. Especially, I would like to thank **Hadi YAKAN**, who have not been only colleagues but have also become dear friends of mine, with whom I have shared both the joy and hardship of this four-year journey.

Finally, I could not have reached the destination without the unconditional love and unending support from **my family** and **my beloved**. I dedicate this thesis to them as a proof of my infinite gratitude to the people who love me most.

Contents

Abstract	ii
Résumé	iii
Acknowledgments	v
List of Figures	xii
List of Tables	xiv
List of Abbreviations	xv
1 INTRODUCTION	1
1.1 Cooperative Intelligent Transportation Systems (C-ITS)	1
1.2 Communications in C-ITS	3
1.2.1 WLAN-based DSRC	4
1.2.2 Cellular-based C-V2X	6
1.3 Thesis Problematic, Motivation and Contributions	8
1.4 Thesis Outline	12
2 LITERATURE STUDY	13
2.1 3GPP 5G NR-V2X Release 16	13
2.1.1 Architecture	13
2.1.2 Protocol Stack for NR-PC5	16
2.1.2.1 V2X application layer	17
2.1.2.2 Radio Resource Control (RRC) layer 3	18
2.1.2.3 Service Data Adaptation Protocol (SDAP) sublayer 2	19
2.1.2.4 Packet Data Convergence Protocol (PDCP) sublayer 2	19
2.1.2.5 Radio Link Control (RLC) sublayer 2	19
2.1.2.6 Medium Access Control (MAC) sublayer 2	20
2.1.2.7 Physical (PHY) layer 1	21
2.1.2.8 User Plane and Control Plane	22
2.1.3 Physical (PHY) layer for NR-V2X Sidelink	23
2.1.3.1 Operating bands and channel bandwidth	23

2.1.3.2	Numerology	24
2.1.3.3	Time domain	25
2.1.3.4	Frequency domain	26
2.1.3.5	Physical resource	28
2.1.3.6	Transport Block (TB) in detail	29
2.1.3.7	Link Adaptation : the Channel-state information (CSI)	35
2.1.4	Transport Block Size (TBS) determination	36
2.1.5	Service requirements and use cases for NR-V2X	39
2.1.5.1	LTE-V2X	39
2.1.5.2	NR-V2X	40
2.1.6	Resource allocation modes	43
2.1.6.1	Mode 1	43
2.1.6.2	Mode 2	45
2.1.7	QoS NR-PC5	49
2.1.7.1	PC5 QoS parameters	49
2.1.7.2	PC5 QoS characteristics	50
2.1.7.3	PC5 QoS Flow	51
2.2	NR-V2X resource allocation (RA) problematic and approaches	54
2.3	State-of-the-art on numerology in NR-V2X	57
2.4	Conclusion	61

3	A FLEXIBLE NUMEROLOGY CONFIGURATION FOR EFFICIENT RESOURCE ALLOCATION IN 3GPP V2X 5G NEW RADIO	63
3.1	Introduction	63
3.2	Problem formulation	64
3.2.1	System description	64
3.2.2	V2X application and traffic model	64
3.2.3	PHY layer	65
3.2.4	Mobility environment	66
3.2.5	Problem formulation	68
3.2.6	Performance evaluation parameters	70
3.2.6.1	Throughput	70
3.2.6.2	Latency	71
3.2.6.3	Reliability	71
3.2.6.4	Effective Transmitted Packet (ETP)	72
3.3	Proposal	72

3.3.1	Adaptive PHY layer Configuration (APC)	73
3.3.2	Resource Allocation Scheduler	75
3.3.2.1	Pre-emption method	76
3.3.2.2	Adaptive Expected Serving Packet Rate (AESPR)	78
3.4	Performance Evaluation	79
3.5	Conclusion	83

4 A NOVEL RADIO-AWARE AND ADAPTIVE NUMEROLOGY CONFIGURATION IN V2X 5G NR COMMUNICATIONS 85

4.1	Introduction	85
4.2	Problem formulation	86
4.2.1	System description	86
4.2.2	V2X application and traffic model	86
4.2.3	PHY layer	87
4.2.4	Mobility environment	88
4.2.5	Problem formulation	88
4.2.6	Performance evaluation parameters	91
4.3	Proposal	91
4.3.1	Radio-Aware Adaptive PHY layer Configuration (RA-APC)	92
4.3.2	Resource Management Algorithm	93
4.4	Performance Evaluation	97
4.5	Conclusion	100

5 DETRAP : A NOVEL AI/ML V2X 5G NR ADAPTIVE PHYSICAL LAYER CONFIGURATION 103

5.1	Introduction	103
5.2	Machine learning preliminaries	104
5.2.1	Machine learning	104
5.2.2	Decision tree learning	106
5.2.2.1	Training	106
5.2.2.2	Prediction	107
5.3	Problem formulation	107
5.3.1	System description	107
5.3.1.1	V2X application and traffic model	107
5.3.1.2	PHY layer	107
5.3.2	Problem formulation and performance parameters	109
5.4	Proposal : Decision Tree Adaptive Physical layer Configuration (DeTrAP)	110

5.5	Performance Evaluation	114
5.6	Conclusion	118
6	CONCLUSION AND FUTURE WORK	121
6.1	Conclusion	121
6.2	Perspectives	123
A	Appendix : Celtic Next SARWS Euroepan project : Real-time location-aware road weather services composed from multi-modal data	127
B	Appendix : Cellular network with OpenAirInterface platform	129
C	Appendix : Modulation and Coding Scheme tables	131
D	Appendix : Channel Quality Indicator tables	135
E	Appendix : Use Case Group Requirement Tables	139
F	Appendix : First stage SCI structure	143
G	Appendix : Transport Block Size determination	145
	Bibliographie	163

List of Figures

1.1	Cooperative Intelligent Transportation Systems (C-ITS) context [2]	1
1.2	V2X communication technologies	4
1.3	The 3 rd Generation Partnership Project (3GPP) Vehicle-to-Everything (V2X) Timeline	6
2.1	3GPP 5G NR V2X (NR-V2X) Release 16 architecture	14
2.2	3GPP NR-V2X Release 16 (R16) Uu interface	15
2.3	3GPP NR-V2X R16 PC5 interface	15
2.4	3GPP NR-V2X R16 Protocol Stack	16
2.5	V2X application layer functional model [29]	17
2.6	Three Radio Resource Control layer (RRC) states	18
2.7	SDAP with flows and SL-DRB	20
2.8	Medium Access Control Medium Access Control layer (MAC) sublayer structure	21
2.9	IP packet to MAC-PDU	22
2.10	User Plane and Control Plane	23
2.11	Frame - Subframe - Slot	26
2.12	Bandwidth - Bandwidth Part - Subchannel	27
2.13	Resource Element - Resource Block - Subcarrier	28
2.14	An example of Transport Block (TB) with subchannel size 10 Resource Block (RB)s	29
2.15	Structure of an example Transport Block with 2-symbol PSCCH, 2-symbol PSSCH-DMRS, without PSFCH	30
2.16	Structure of an example Transport Block with 3-symbol PSCCH, 3-symbol PSSCH-DMRS, and PSFCH	31
2.17	Structure of Physical Sidelink Broadcast Channel (PSBCH)	32
2.18	1 st -stage Sidelink Control Information (SCI) format	34
2.19	2 nd -stage SCI format	35
2.20	Sidelink Channel State Information	35
2.21	Resource Allocation mode	43
2.22	Procedure of Mode 2 resource allocation	45
2.23	Example of timeline of sensing and resource selection procedure triggered at time n .	46
2.24	Example of timeline of sensing and resource selection procedure triggered at time n , with re-evaluation at time z before $(m - T_3)$.	48
2.25	NR-PC5 QoS parameters and characteristic	49

2.26 NR-PC5 Per-Flow QoS Model	52
2.27 PC5 QoS Flow in V2X Application Layer point of view	53
3.1 System description	66
3.2 Latency components in PHY layer	71
3.3 Interact between APC and RA	73
3.4 RA step by step	76
3.5 Packet Sent (a) : without APC + without AESPR, (b) : without APC + with AESPR	81
3.6 Trade-off between Packet Sent and Reliability by APC	81
3.7 ETP by APC	82
4.1 System description	87
4.2 Interaction between Resource Management (RM) and Radio-Aware Adaptive Physical Layer Configuration (RA-APC).	91
4.3 Resource Allocation (RA) step by step	93
4.4 RA step by step (continue)	94
4.5 Packet sent +/- Radio awareness,	99
4.6 Reliability +/- Radio awareness	99
4.7 Effective Transmitted Packet (ETP) +/- Radio awareness	99
4.8 Balance state, ETP, and Packet Drop of all States	100
5.1 Three paradigms of machine learning	104
5.2 A decision tree	106
5.3 Two-step process	111
5.4 Interaction between RA and DeTrAP	113
5.5 The full algorithm of DeTrAP	113
5.6 Packet sent +/- DeTrAP	114
5.7 Reliability +/- DeTrAP	115
5.8 Performance of DeTrAP under Timer	117
6.1 Markov Decision Process	123
B.1 USRP B210	129
B.2 OAI platform	130

List of Tables

2.1	NR-V2X Sidelink (SL) operating bands in Frequency Range (FR)1	24
2.2	Channel bandwidths supported for NR-V2X band	24
2.3	Numerology	25
2.4	Maximum Resource Blocks configuration by bandwidth and numerology for NR-V2X SL [70]	28
2.5	Physical resource summary	30
2.6	Demodulation Reference Signal (DMRS) position [65]	33
2.7	N_{RE}^{DMRS} according DMRS Time Pattern [68]	37
2.8	Summary requirement use case group	42
2.9	Standardized PQI to QoS characteristics mapping	51
2.10	State-of-t	60
2.11	Number of subchannels related to SCS and subchannel size for n47	62
3.1	An example of User Cases V2X QoS requirement	65
3.2	3GPP 5G NR-V2X SL parameters	67
3.3	CQI/SINR mapping [113]	70
3.4	Number of Resource Unit (RU)s by Subcarrier Spacing (SCS) μ - Subchannel size W in n47 band - 40MHz bandwidth	74
3.5	State index by SCS μ - Subchannel size W	74
3.6	Simulation parameters	80
4.1	Simulation network parameters	98
5.1	3GPP 5G NR-V2X SL parameters	108
5.2	TabA for case 1	112
5.3	TabB for [case 1, density 100, input state 1]	112
5.4	TabC for [case 1, density 100, input state 1]	112
5.5	Simulation network parameters	116
5.6	Case by combination of LCs	117
5.7	Percentage of simulation achieved GS under Timer	118
C.1	MCS index table 1	132
C.2	MCS index table 2	133

C.3	MCS index table 3	134
D.1	CQI table 1	135
D.2	CQI table 2	136
D.3	CQI table 3	137
E.1	Performance requirements for Vehicles Platooning use case group	140
E.2	Performance requirements for Advanced Driving use case group	141
E.3	Performance requirements for Extended Sensors use case group	142
E.4	Performance requirements for Remote Driving use case group	142
G.1	Transport Block Size (TBS) for $N_{info} \leq 3824$	145

List of Abbreviations

Terme	Description
3GPP	The 3 rd Generation Partnership Project
4G	Fourth Generation
5G	Fifth Generation
5GC	5G Core
5QI	5G QoS Identifier
AESPR	Adaptive Expected Serving Packet Rate
AF	Application Function
AM	Acknowledged Mode
AMF	Access and Mobility Management Function
APC	Adaptive Physical layer Configuration
AS	Access Stratum
BLER	Block Error Rate
BS	Balance State
BSM	Basic Safety Message
BW	Bandwidth
BWP	Bandwidth Part
C-ITS	Cooperative Intelligent Transportation Systems
C-V2X	Cellular Vehicle-to-Everything
CAM	Cooperative Awareness Message
CG	Configured Grant
CN	Core Network
CoCA	Cooperative Collision Avoidance service
CP	Cyclic Prefix
CP-OFDM	Cyclic Prefix - Orthogonal Frequency Division Multiplexing
CPM	Collective Perception Message
CQI	Channel Quality Indicator
CRB	Common Resource Block
CSI	Channel State Information

Terme	Description
CSI-RS	Channel State Information Reference Signal
CSMA/CA	Carrier Sense Multiple Access Collision Avoidance
D2D	Device-to-Device
DC-GBR	Delay Critical - Guaranteed Bit Rate
DCC	Decentralized Congestion Control
DCI	Downlink Control Information
DENM	Decentralized Environmental Notification Message
DeTrAP	Decision-tree-based RA-APC
DG	Dynamic Grant
DL	Downlink
DMRS	Demodulation Reference Signal
DSRC	Dedicated Short-Range Communications
DT	Decision Tree
ECC	European Commission
EDCA	Enhanced Distributed Channel Access
EHF	Extremely High Frequency
EmerTA	Emergency Trajectory Alignment service
ETP	Effective Transmitted Packet
ETSI	European Telecommunications Standards Institute
EU	European Union
eV2X	enhanced Vehicle-to-Everything
FCC	Federal Communication Commission
FR	Frequency Range
GBR	Guaranteed Bit Rate
GDP	Gross domestic product
GFBR	Guaranteed Flow Bit Rate
GS	Good State
HARQ	Hybrid automatic repeat request
HD	Half-duplex

Terme	Description
ICI	Inter-Carrier Interference
IEEE	Institute of Electrical and Electronics Engineers
IoT	Internet of things
ISI	Inter-Symbol Interference
ITS	Intelligent Transportation Systems
LC	Logical Channel
LDCP	Low-Density Parity-Check
LoA	Levels of Automation
LTE	Long Term Evolution
LTE-V2X	4G LTE V2X
MAC	Medium Access Control layer
MBMS	Multimedia Broadcast Multicast Service
MCS	Modulation Coding Scheme
MDBV	Maximum Data Burst Volume
MDP	Markov Decision Process
MFBR	Maximum Flow Bit Rate
MIMO	Multiple Input - Multiple Output
ML	Machine Learning
mmWave	millimeter-wave
n38	NR band 38
n47	NR band 47
NEF	Network Exposure Function
NG-RAN	New Generation - Radio Access Network
NR	New Radio
NR-V2V	5G NR V2V
NR-V2X	5G NR V2X
NSA	Non-standalone
OAI	Open-Air-Interface platform
OFDM	Orthogonal Frequency Division Multiplexing

Terme Description

PC5	Proximity-based Communication 5
PCF	Policy Control Function
PDB	Packet Delay Budget
PDCCH	Physical Downlink Control Channel
PDCP	Packet Data Convergence Protocol layer
PDU	Protocol Data Unit
PER	Packet Error Rate
PFI	PC5 QoS Flow Identifiers
PHY	Physical layer
PQI	PC5 5G QoS Identifier
PRB	Physical Resource Block
ProSe	Proximity Services
PSBCH	Physical Sidelink Broadcast Channel
PSCCH	Physical Sidelink Control Channel
PSFCH	Physical Sidelink Feedback Channel
PSSCH	Physical Sidelink Shared Channel
PT-RS	Phase-Tracking Reference Signal
PUCCH	Physical Uplink Control Channel
QAM	Quadrature Amplitude Modulation
QoS	Quality of Service
QPSK	Quadrature Phase Shift Keying
R16	Release 16
RA	Resource Allocation
RA-APC	Radio-Aware Adaptive Physical Layer Configuration
RAN	Radio Access Network
RB	Resource Block
RE	Resource Element
RLC	Radio Link Control layer
RM	Resource Management
RP	Resource Pool
RRC	Radio Resource Control layer

Terme	Description
RSRP	Reference Signal Received Power
RSU	Road-Side Unit
RU	Resource Unit
RWS	Road Weather Stations
RX	Receiver
S-PSS	Sidelink Primary Synchronization Signal
S-SSB	Sidelink Synchronization Signal Block
S-SSS	Sidelink Secondary Synchronization Signals
SA	Standalone
SAE	Society of Automotive Engineers
SBCCH	Sidelink Broadcast Control Channel
SCCH	Sidelink Control Channel
SCI	Sidelink Control Information
SCS	Subcarrier Spacing
SDAP	Service Data Adaptation Protocol layer
SDR	Software Defined Radio
SDU	Service Data Unit
SEAL	Service Enabler Architecture Layer
SensIS	Sensor Information Sharing
SIB12	System Information Block 12
SINR	Signal to Interference Plus Noise Ratio
SL	Sidelink
SL-BCH	Sidelink Broadcast Channel
SL-DRB	Sidelink Data Radio Bearer
SL-SCH	Sidelink Shared Channel
SL-SRB	Sidelink Signaling Radio Bearer
SLRB	Sidelink Radio Bearer
SMF	Session Management Function
SNR	Signal to Noise Ratio
SPS	Semi-Persistent Scheduling
SR	Scheduling Request
STCH	Sidelink Traffic Channel

Terme	Description
TB	Transport Block
TBS	Transport Block Size
TC	Transport Channel
TM	Transparent Mode
TQ	Transmission Queue
TTI	Transmission Time Intervals
TX	Transmitter
UDR	Unified Data Repository
UE	User Equipment
UL	Uplink
UM	Unacknowledged Mode
URLLC	Ultra-Reliable Low Latency Communication
US	United States (of America)
USRP	Universal Software Radio Peripheral
Uu	The Radio interface between UTRAN and the User Equipment
V2B	Vehicle-to-Building
V2C	Vehicle-to-Cloud
V2D	Vehicle-to-Device
V2G	Vehicle-to-Grid
V2H	Vehicle-to-Home
V2I	Vehicle-to-Infrastructure
V2N	Vehicle-to-Network
V2P	Vehicle-to-Pedestrian
V2V	Vehicle-to-Vehicle
V2X	Vehicle-to-Everything
V2X AS	V2X Application Server
VAE	Application Enabler
WAVE	Wireless Access in Vehicular Environments
WLAN	Wireless Local Area Network
WQ	Waiting Queue

1 - INTRODUCTION

This thesis primarily engages with C-ITS, with a particular focus on the challenges pertaining to Cellular Vehicle-to-Everything (C-V2X) communication technology. As such, we initiate this academic endeavor by delineating the C-ITS context in the forthcoming section.

1.1 . Cooperative Intelligent Transportation Systems (C-ITS)

An investigation conducted by the European Commission (ECC) reveals that road congestion across Europe inflicts a financial strain approximating 1% of the Gross domestic product (GDP), translating to an annual expense exceeding 110 billion euros. Furthermore, the ECC's findings underscore the fact that health-related costs of air pollution, with road traffic as its primary contributor, escalate to several hundreds of billions of euros each year. The European Union (EU) has invested more than 60 billion euros in various projects to address this issue from 2014 to 2020 [1].

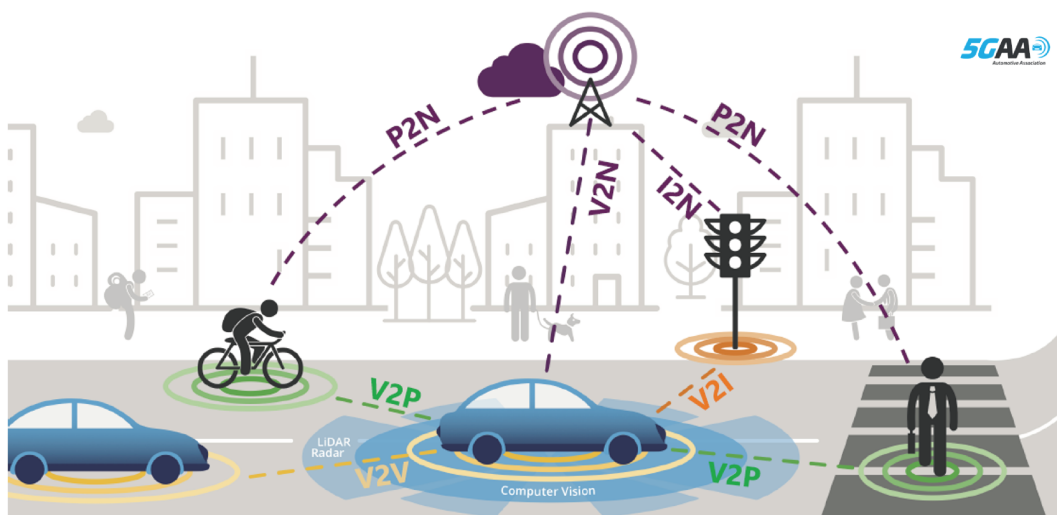


Figure 1.1 – C-ITS context [2]

The advancement of C-ITS plays a crucial part in accomplishing the ECC's goals. These include tackling the escalating issues of traffic congestion, energy utilization in transportation, and emissions across Europe. The advantages cover various aspects such as enhancing road safety, decreasing traffic, improving transportation efficiency, increasing mobility, driver comfort, ensuring service reliability, new infotainment experiences for passengers, minimizing energy consumption and environmental effects for global warming, and promoting economic growth etc. These can be achieved thanks to C-ITS's focus on cooperative communication and collaboration among vehicles, infrastructure, and other road users, as illustrated in Figure 1.1.

While C-ITS offer a multitude of benefits, they are not devoid of complexities tied to their implementation. Enumerated below are some of the prominent challenges associated with C-ITS deployment.

- International cooperation and harmonization are necessary for the deployment of C-ITS, especially for cross-border transportation and interoperability.
- Scalability is an important consideration for the deployment of C-ITS, as it must be able to handle a wide range of transportation scenarios and a large number of vehicles. Ensuring scalability to manage the rising data volume and connected vehicles is a challenging task. Efficient algorithms, protocols, and infrastructure are necessary to meet the demands of a complex and dynamic transportation environment.
- Security and privacy are important considerations in C-ITS as it involves the sharing of sensitive information such as real-time traffic data, driver behavior, and private information. It is crucial to ensure the security and privacy of this information to avoid unauthorized access, cyber attacks, etc. Building powerful encryption, authentication, and security systems is a significant challenge.
- The success of C-ITS requires reliable and efficient communication networks for transmitting data between infrastructure and vehicles. Establishing a trustworthy and secure communication system, encompassing wireless networks and roadside units, presents notable challenges, particularly in locations with suboptimal connectivity or within rural areas.

Addressing these challenges necessitates concerted efforts from diverse stakeholders, including governments, technology providers, vehicle manufacturers, and road authorities. Having delineated the challenges of C-ITS, we will delve deeper into the communication challenge, the primary focus of this thesis, in the subsequent section.

1.2 . Communications in C-ITS

The communication protocols employed in C-ITS bear significant similarity to those utilized in V2X communication. It encompasses all communication capabilities, mainly as :

- Vehicle-to-Vehicle (V2V) : the direct communication between vehicles and nearby vehicles to exchange data,
- Vehicle-to-Pedestrian (V2P) : communicate with e.g. bicycle, pedestrian on sidewalk,
- Vehicle-to-Network (V2N) : the communication between a vehicle and a V2X application service provider, server, services on the network
- Vehicle-to-Infrastructure (V2I) : Establish communication with entities such as traffic lights, base stations, and Road-Side Unit (RSU).

Furthermore, recent developments have led to the introduction of the following terms :

- Vehicle-to-Device (V2D) : Establishing a connection with electronic devices, such as Internet of things (IoT) devices.
- Vehicle-to-Grid (V2G), Vehicle-to-Building (V2B) also known as Vehicle-to-Home (V2H), mostly used for electric vehicles,
- Vehicle-to-Cloud (V2C) : similarly to V2N, connecting to cloud services, e.g. firmware update for vehicles.

It is crucial to take into account the definitions of both C-ITS and V2X. C-ITS is being developed in the EU and focuses mainly on cooperative scenarios, particularly V2V and V2I. However, V2X is a definition of all non-cooperative and cooperative scenarios, and it encompasses all forms of communication between vehicles and any element within a transportation context, including V2V, V2I, V2P, and V2N. The cooperative scenario involves the exchange of in-

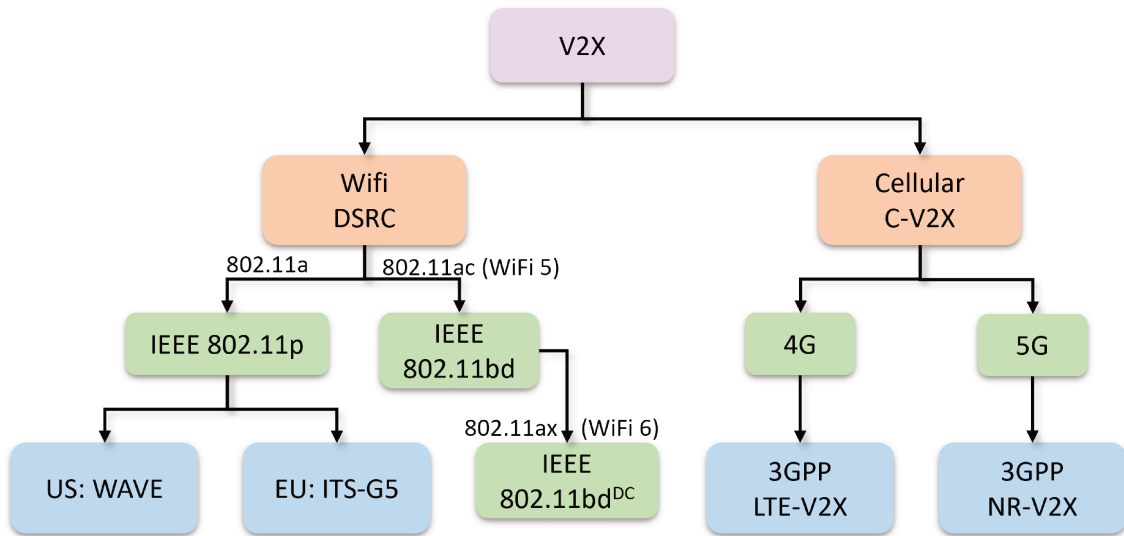


Figure 1.2 – V2X communication technologies

formation to enhance safety, while non-cooperative scenarios do not involve data exchange, such as remote driving in 3GPP or connecting to the cloud, etc. Moreover, C-ITS offers the whole protocol stack : application layer, facilities layer, network layer and access layer. In contrast, V2X mainly concentrates on communication technologies, which is the access layer. In the access layer, C-ITS can utilize V2X communication technologies. In the scope of this thesis, our focus is primarily on the access layer of C-ITS. Therefore, the term “V2X” is used in this thesis due to the V2X communication technology on access layer of C-ITS.

V2X, illustrated in Figure 1.2, fundamentally relies on two competing technologies : Wireless Local Area Network (WLAN)-based and cellular-based systems.

1.2.1 . WLAN-based DSRC

Dedicated Short-Range Communications (DSRC) was first introduced as a V2X technology in the Institute of Electrical and Electronics Engineers (IEEE)’s 802.11p [3] standard for its Physical layer (PHY) and MAC layers in 2010. This is a variation of the IEEE 802.11a. It is known as Wireless Access in Vehicular Environments (WAVE) [4] [5] in the United States (of America) (US) and ITS-G5 in Europe developed by European Telecommunications Standards Institute (ETSI) [6]. It facilitates two forms of communication : V2V and V2I communi-

cation. The infrastructure of a vehicular network refers to the RSUs that are positioned along the streets or highways.

Various spectrum management organizations, including the Federal Communication Commission (FCC) and the ECC, have assigned the 5.9 GHz radio spectrum band primarily for the use of DSRC-based applications in order to encourage the advancement of DSRC technology.

This standard allows relative velocity of up to 250 Km/hr, response times of approximately 0.1 second, and a communication distance of up to one kilometer. The 802.11p protocol employs Orthogonal Frequency Division Multiplexing (OFDM) with a 10 MHz channel bandwidth and 8 Modulation Coding Scheme (MCS) at the PHY layer, provides a maximum bit rate of 27 Mbps [7].

The WAVE protocol stack in the US consists of various components at each layer, including IEEE 802.11p at the PHY layer, IEEE 802.11p and IEEE 1609.4 at the MAC sublayer, IEEE 802.2 at the Logical Link Control sublayer, and IEEE 1609.3 at the Network layer [8].

In Europe, ETSI ITS-G5 adopts a comparable strategy to IEEE's, but incorporates additional functionalities onto the current WAVE components. At the MAC layer, 802.11p uses the Enhanced Distributed Channel Access (EDCA) protocol to enhance the Carrier Sense Multiple Access Collision Avoidance (CSMA/CA) standard Quality of Service (QoS). If the wireless channel's data load surpasses its capacity, implementing Decentralized Congestion Control (DCC) [9] mechanisms in ITS-G5 stations becomes necessary to regulate the channel load. These mechanisms are intended to fulfill the needs of Intelligent Transportation Systems (ITS) applications, particularly for road safety applications, by ensuring high reliability and low latency. Additionally, it includes a layer called "Facilities" that sits between the Network and Application layer in the stack. The EN 302-571 [10] standard has been harmonized by the ECC for C-ITS in the EU. The ITS-G5 technology introduces a service channel assignment that is categorized into four types :

- ITS-G5A is utilized for safety-related applications.
- ITS-G5B is used for applications that are not related to safety.
- ITS-G5C pertains to infrastructure-based broadband radio access networks operating in the 5.6 GHz frequency band.
- ITS-G5D is reserved for upcoming ITS applications.

Since 802.11p was created over 10 years ago, the improved PHY and MAC methods from 802.11ac (or WiFi 5) can be used to improve 802.11p. The IEEE 802.11 Next Generation V2X Study Group was established in March 2018 to achieve this goal. The IEEE 802.11bd [11] Task Group was established in January 2019 following a preliminary feasibility analysis. The IEEE 802.11bd standard is expected to provide better performance than the IEEE 802.11p. It can support twice the MAC throughput of 802.11p, allow relative velocity of up to 500 km/hr, and have a communication range twice as long as 802.11p. Another variant of 802.11bd, which is developed from 802.11ax (or WiFi 6), is called 802.11bd^{DC} and is under development.

We note that 802.11bd must be compatible with 802.11p in a backward manner. This means that devices using 802.11bd and 802.11p standards need to be able to communicate on the same channel. At the time of writing, this standard 802.11bd has not yet been released [12].

1.2.2 . Cellular-based C-V2X

Meanwhile, a competitor of WLAN-based DSRC is introduced. V2X bases on cellular technology called C-V2X, standardized by 3GPP. The development timeline summary is illustrated in Figure 1.3.

Dating back to year 2014, with the introduction of Proximity Services (ProSe) [13] for Long Term Evolution (LTE) in Release 12 [14] and 13 [15] based on Device-to-Device (D2D) communications, 3GPP began to develop their own C-V2X standard. The Proximity-based Communication 5 (PC5) interface was first defined.

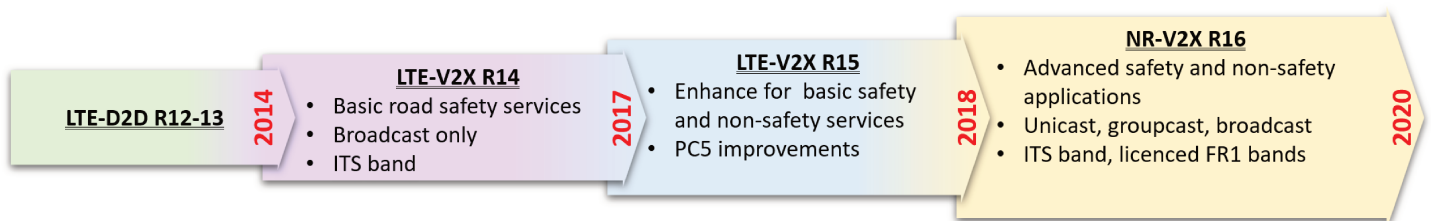


Figure 1.3 – 3GPP V2X Timeline

In 2017, 3GPP became a competitor in V2X by releasing 4G LTE V2X (LTE-V2X) [16] Release 14 [17] standard. This first cellular C-V2X standards based on the Fourth Generation (4G) LTE air interface can be called C-V2X Phase I. In LTE-V2X Release 14, the communication was expected to operate on the ITS 5.9 GHz band reserved with 10 MHz bandwidth.

Differently from DSRC that focused on V2V and V2I communications, LTE-V2X encompasses V2V, V2P, V2I and V2N [18] especially support for V2V services based on LTE SL. LTE-V2X has been developed to facilitate the exchange of basic safety messages between nearby users. These messages may include collision warnings, emergency brake warnings. LTE-V2X Release 14 has been designed to support basic road safety services, facilitate the exchange of basic safety messages between nearby users. These services rely on the broadcast transmission of small awareness messages such as Cooperative Awareness Message (CAM)s, Basic Safety Message (BSM)s, Collective Perception Message (CPM)s or Decentralized Environmental Notification Message (DENM)s etc.

LTE-V2X was further enhanced in Release 15 [19] in 2018, which can be called C-V2X Phase II. LTE C-V2X can fulfill V2X requirements, provided that vehicular density remains low [20]. Nonetheless, LTE C-V2X is insufficient for V2X applications with strict QoS requirements. The issue can be tackled with 3GPP Fifth Generation (5G) New Radio (NR), which is standardized in Release 15 [21][19].

Based on the study in Technical Report 38.885 [22] for new V2X applications with more stringent requirements, 3GPP profit the advances of newest cellular communication technology which is 5G NR air interface and released NR-V2X [23] R16 in 2020. The R16 [24] standards (called Phase III) by 3GPP specify architecture enhancements to accommodate advanced V2X services, application layer support for V2X services, and support for NR-V2X with NR SL.

The NR radio access technology offers wider bandwidth in both sub-6 GHz and millimeter-wave (mmWave) bands. Multiple numerologies enhance the frame structure's flexibility, leading to reduced transmission time intervals. Furthermore, NR-V2X encompasses novel functionalities such as Multiple Input - Multiple Output (MIMO), high modulation orders, and advanced channel coding. In addition, NR-V2X has introduced new feedback-based retrans-

missions, enhancements to communication options such as broadcast, unicast and groupcast, etc. These enhancements increase data rates, decrease latency, and improve spectral efficiency in V2X communication systems.

We note that NR-V2X is not backward compatible with LTE-V2X. According to 3GPP, the aim of NR-V2X design is to complement LTE-V2X, rather than replacing it. NR-V2X is intended to support enhanced Vehicle-to-Everything (eV2X) use cases that cannot be supported by LTE-V2X [22], e.g. autonomous driving.

In 2022, the Release 17 [25] standard was introduced by 3GPP. Additional radio spectrum has been allocated for V2X communication. The V2X service can utilize NR n14, NR band 38 (n38), NR band 47 (n47), and n79 bands. The 600 MHz bandwidth of n79 can enhance the infotainment and self-driving experience. The NR n14 band, which operates within the frequency range of 788 MHz to 798 MHz, expands transmission range. This is extremely helpful for the public safety services. 3GPP's focus in release 17 is to enhance power efficiency for pedestrian User Equipment (UE)s. This is the outcome of a study in [26], is specified in [27] and [28]. The V2X application has also been developed in this release [29][30][31] which is studied in [32] [33]. Multimedia Broadcast Multicast Service (MBMS) [34][35][36] was initially introduced in LTE-V2X, then removed in NR-V2X R16, and is currently being reintroduced. MBMS will facilitate multicast transmission for the downlink and send data to a V2X application on a group of vehicles. The upcoming release 18 [37] will introduce 5G Advanced next year (2024) with enhancements for V2X. However, we currently have very limited information.

1.3 . Thesis Problematic, Motivation and Contributions

A wealth of research has been conducted on DSRC since the advent of 802.11p over a decade ago, as highlighted in multiple studies such as [38] [39] [40] [41]. The evolution of 4G LTE cellular communication technology ushers in fresh challenges for the scientific community to tackle. On one hand, a majority of researchers advocate for the utilization of a singular technology or propose a hybrid solution. The latter amalgamates the benefits of both technologies with the aim of augmenting the efficiency and reliability of V2X com-

munication. For example, King et al. [42] tackle the problem of interoperability between these two technologies. Khan et al. [43] propose a two-level clustering scheme for efficient data dissemination by combining DSRC and C-V2X. Conversely, another approach involves drawing comparisons between these two distinct technologies. The authors in [44], [45], [46], [47], and [48] study and compare 802.11p and LTE-V2X. Meanwhile, Naik et al. [49] research on latest V2X communication technologies : 802.11bd and NR-V2X.

In spite of the robustness of DSRC's radio spectrum utilization for V2X short-range communication, its limited performance in high vehicle density scenarios has raised concerns regarding its widespread adoption. DSRC faces challenges such as limited mobility support, lack of advanced use case support for fully automated vehicles, limited coverage range, infrastructure, latency, and reliability. Insufficient progress in resolving standing issues with DSRC and recent advancements in cellular network technologies have inspired the research community to explore cellular-based V2Xcommunications.

The available literature indicates that C-V2X outperforms DSRC. Nevertheless, V2X use-cases have increasingly strict QoS requirements, particularly in advanced applications such as Ultra-Reliable Low Latency Communication (URLLC) V2X services. This matter is quite complex due to the dynamic nature of V2X services and traffic. In addressing this issue, the 3GPP NR-V2X proposes adaptable solutions including **numerology**, physical resources, and beyond. Recently, the research community has been concentrating on the allocation of resources in C-V2X that requires efficient management to avoid interference and collisions. However, there is a lack of research on the impact of numerology on the requirements of different V2X applications and whole system. For example, the scenario of "Emergency trajectory alignment" in the Advanced Driving use case group has very stringent requirements on latency and reliability. This service is aperiodic and has a highest priority. Meanwhile, "Cooperative driving for vehicle platooning Information exchange between a group of UEs" in Vehicles Platooning use case group is a periodic service without reliability requirement, and has a low priority. However, it requires a very high payload. We will address in depth this topic in section 2.1.5 on page 39. Each V2X service have specific requirements and behavior. The selection of numerology in the PHY layer and the scheduling of resources for V2X services by the scheduler are topics requiring further investigation.

Resource allocation in C-V2X is another complex issue. A challenge in resource allocation is balancing data traffic for various V2X services with differing characteristics. The starvation phenomenon of low-priority V2X service data is a problem when the scheduler prioritizes higher-priority V2X service data. There is a shortage of research on this topic.

One example of a 5G NR-V2X aperiodic, time-critical application is the Emergency Trajectory Alignment scenario. This service is part of the URLLC type and demands a very low latency of 3 milliseconds, high reliability of 99.999%, and a high data rate of 30 Mbps. Furthermore, we are interested to mention the Cooperative Collision Avoidance scenario of 5G NR-V2X as a case of a URLLC 5G NR-V2X periodic service. Finally, we include the Sensor Information Sharing scenario as a case of a low-priority 5G-V2X periodic service. The resource allocation algorithms suggested in the literature do not take into account the requirements of V2X applications. This thesis deals with the challenge at hand.

Therefore, the first contribution tackles these issues by examining how subchannel size and numerology impact the system in centralized scheduling approach, in which the resource allocation is managed by the gNB, and broadcast mode communication. In Chapter 3, we propose a novel brand-new algorithm known as the **Adaptive Physical layer Configuration (APC)**. Finding the optimal numerology and subchannel size configuration in the PHY that can accommodate the strictest V2X QoS is the primary objective of the APC algorithm. We also propose **Adaptive Expected Serving Packet Rate (AESPR)** used by scheduler to avoid starvation phenomenon issue.

Then, while taking channel state into account for the second contribution, we observe the same scenario with all combinations of numerology and subchannel size in unicast mode communication. In chapter 4, a proposal, namely **RA-APC**, is made.

Ultimately, we discern that it's possible to expedite the process of identifying an optimal numerology and subchannel size. This is accomplished by using machine learning and the dresults obtained in the second contribution. To shorten this convergence time, we propose the **Decision-tree-based RA-APC (DeTrAP)** scheme as the third contribution. We also take into consideration various densities. Chapter 5 details our DeTrAP algorithm.

Building upon the three aforementioned contributions, we have submitted the following three conference papers

1. Lam, N., Kallel, S., Aitsaadi, N., Adjih, C., & Fajjari, I., "A Flexible Numerology Configuration for Efficient Resource Allocation in 3GPP V2X 5G New Radio", in IEEE Global Communications Conference 2022. (accepted)
2. Lam, N., Kallel, S., Aitsaadi, N., Adjih, C., & Fajjari, I., "A Novel Radio-Aware and Adaptive Numerology Configuration in V2X 5G NR Communications", in IEEE International Conference on Communications (ICC) 2023. (accepted)
3. Lam, N., Kallel, S., & Aitsaadi, N., "DeTrAP : A Novel AI/ML V2X 5G NR Adaptive Physical Layer Configuration", in IEEE Global Communications Conference (GLOBECOM) 2023. (submitted)

Furthermore, we have three additional contributions in the context of C-ITS and cellular technology

1. Contribution as leader of one task in Celtic Next SARWS European project, explained in Appendix A on page 127.
2. Deploy 4G and 5G OpenAirInterface platform as described in Appendix B on page 129.
3. We have developed a simulator, dubbed 5GNRSidelinkSim, which is an expansion from its predecessor, LTEV2Vsim. 5GNRSidelinkSim is upgraded with 3GPP 5G NR-V2X R16 standard.

1.4 . Thesis Outline

The thesis is organized in six chapters as follows :

Chapter 1 is the current chapter and presents the context and challenges of the thesis. This chapter outlines the motivating factors behind the research performed in this thesis and its primary contributions.

Chapter 2 is the following chapter and provides an overview of 3GPP NR-V2X R16, which includes its architecture, protocol stack, resource allocation modes, QoS, service requirements and PHY layer resources. Furthermore, this chapter presents a literature review on NR-V2X resource allocation, as well as on numerology.

Chapter 3 on page 63 presents the first contribution as well as **APC** algorithm to find the best numerology and subchannel size in PHY layer.

Chapter 4 on page 85 moves to the second contribution and introduces **RA-APC** considering Unicast mode communication, channel state and density.

Chapter 5 on page 103 presents the third contribution with **DeTrAP** algorithm, based on data and machine learning.

Chapter 6 on page 121 concludes our researches and gives the overview of our on-going work, also perspective in short-term and mid-term.

2 - LITERATURE STUDY

Contents

2.1	3GPP 5G NR-V2X Release 16	13
2.1.1	Architecture	13
2.1.2	Protocol Stack for NR-PC5	16
2.1.3	Physical (PHY) layer for NR-V2X Sidelink	23
2.1.4	Transport Block Size (TBS) determination	36
2.1.5	Service requirements and use cases for NR-V2X	39
2.1.6	Resource allocation modes	43
2.1.7	QoS NR-PC5	49
2.2	NR-V2X resource allocation (RA) problematic and approaches	54
2.3	State-of-the-art on numerology in NR-V2X	57
2.4	Conclusion	61

For a comprehensive understanding of our proposed solutions, it's imperative to delve into the details of the 3rd Generation Partnership Project's (3GPP) 5th Generation (5G) New Radio Vehicle-to-Everything (NR-V2X) Release 16 (R16) standards. Additionally, an examination of contemporary research addressing both resource allocation and numerology issues is required.

In this chapter, we first present the context of our research, covering the overview of 5G 3GPP NR-V2X in section 2.1. Then, we detail literature review on RA in Section 2.2. Next, state-of-the-art on numerology is presented. Ultimately, we will wrap up with a succinct summary, paving the way to our initial contribution presented in the subsequent chapter.

2.1 . 3GPP 5G NR-V2X Release 16

2.1.1 . Architecture

In 3GPP NR-V2X R16, vehicle can communicate with i) other vehicles by using NR-PC5 interface and ii) 5G Core (5GC) or V2X Application Server (V2X

AS) using NR-Uu interface connecting to base station gNB. Figure 2.1 describes the interfaces and the Network Functions in 5GC that support for 5G V2X communication. Moreover, in this R16, 3GPP also defines and supports for three mode communications, which are Unicast, Groupcast and Broadcast. Whereas LTE-V2X supports only Broadcast transmission. We will take a quick look to some most important functions in 5GC that support for V2X below :

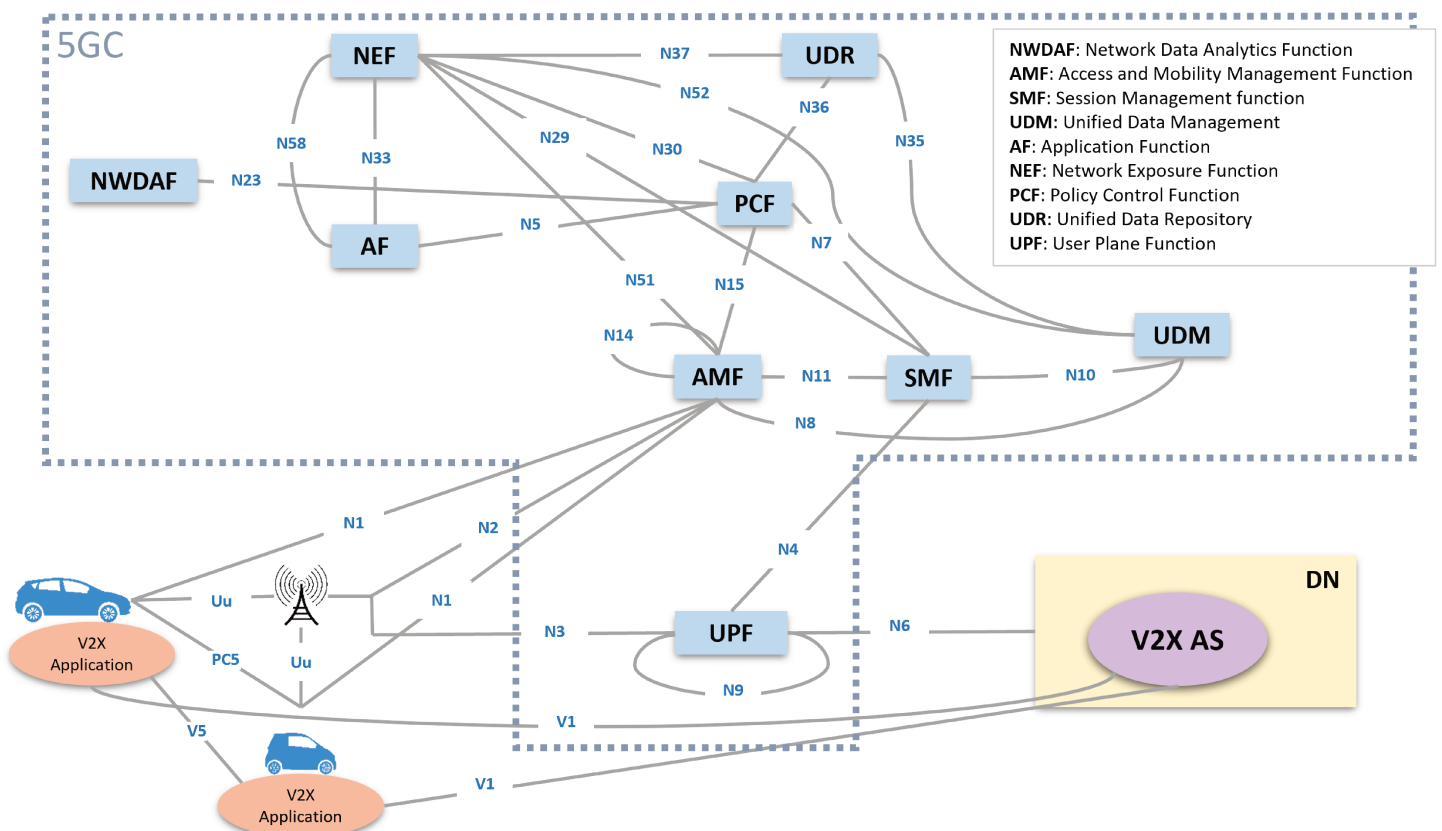


Figure 2.1 – 3GPP NR-V2X Release 16 architecture

- A V2X AS is an important part of the V2X ecosystem. It acts as a central platform for hosting, managing, and operating V2X applications that use V2X data and services. The primary role of a V2X AS is to facilitate the development, deployment, and operation of V2X applications. The latter encompass safety applications, traffic management systems, intelligent transportation services, etc. The server acts as a centralized node for V2X-related information, allowing applications to access, analyze, and utilize this data to provide services to users and the V2X

ecosystem. V2X AS can be inside 5GC (considered as Application Function (AF)) or a third-party component from outside.

- Network Exposure Function (NEF) is used as a gateway for third-party V2X AS update V2X service-related information of 5GC.
- Access and Mobility Management Function (AMF) and Session Management Function (SMF) maintain the activity of vehicles in the area.
- Unified Data Repository (UDR) refers to a centralized storage system that stores various V2X service parameters and related information such as PC5 QoS parameters, V2X service profiles UE information, etc.
- Policy Control Function (PCF) determines whether to provision V2X parameters for V2X communication.

And the reference points :

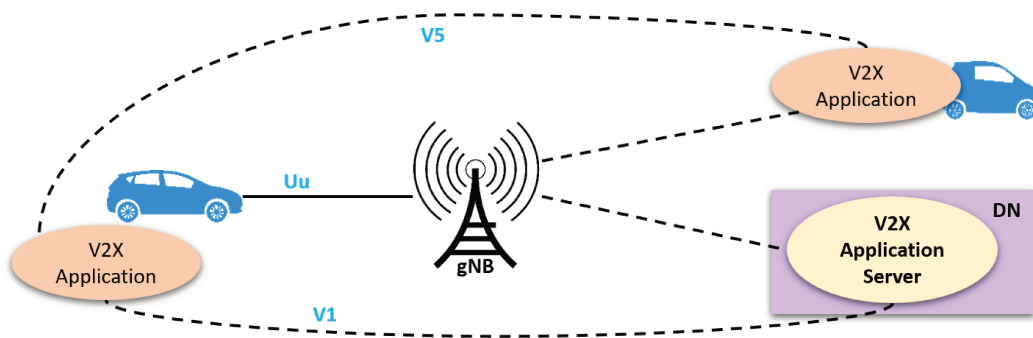


Figure 2.2 – 3GPP NR-V2X R16 Uu interface

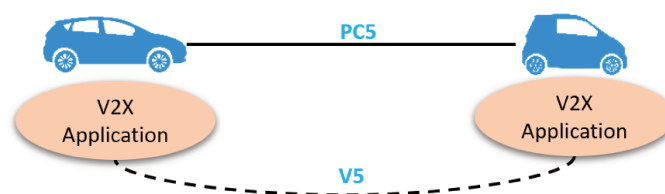


Figure 2.3 – 3GPP NR-V2X R16 PC5 interface

Vehicles communicate with i) other vehicles, ii) 5GC, and iii) V2X AS via reference points in the NR-V2X ecosystem. The The Radio interface between UTRAN and the User Equipment (Uu) (Figure 2.2) interface serves as the reference point connecting the UE and the New Generation - Radio Access Network (NG-RAN) or gNB, whereas NR-PC5 (Figure 2.3) roles as the reference

point between UEs that utilize 5G NR. The V1 interface acts as the reference point between the V2X Applications in the UE and the V2X AS, while the V5 is the reference point between the V2X Applications in the UEs.

2.1.2 . Protocol Stack for NR-PC5

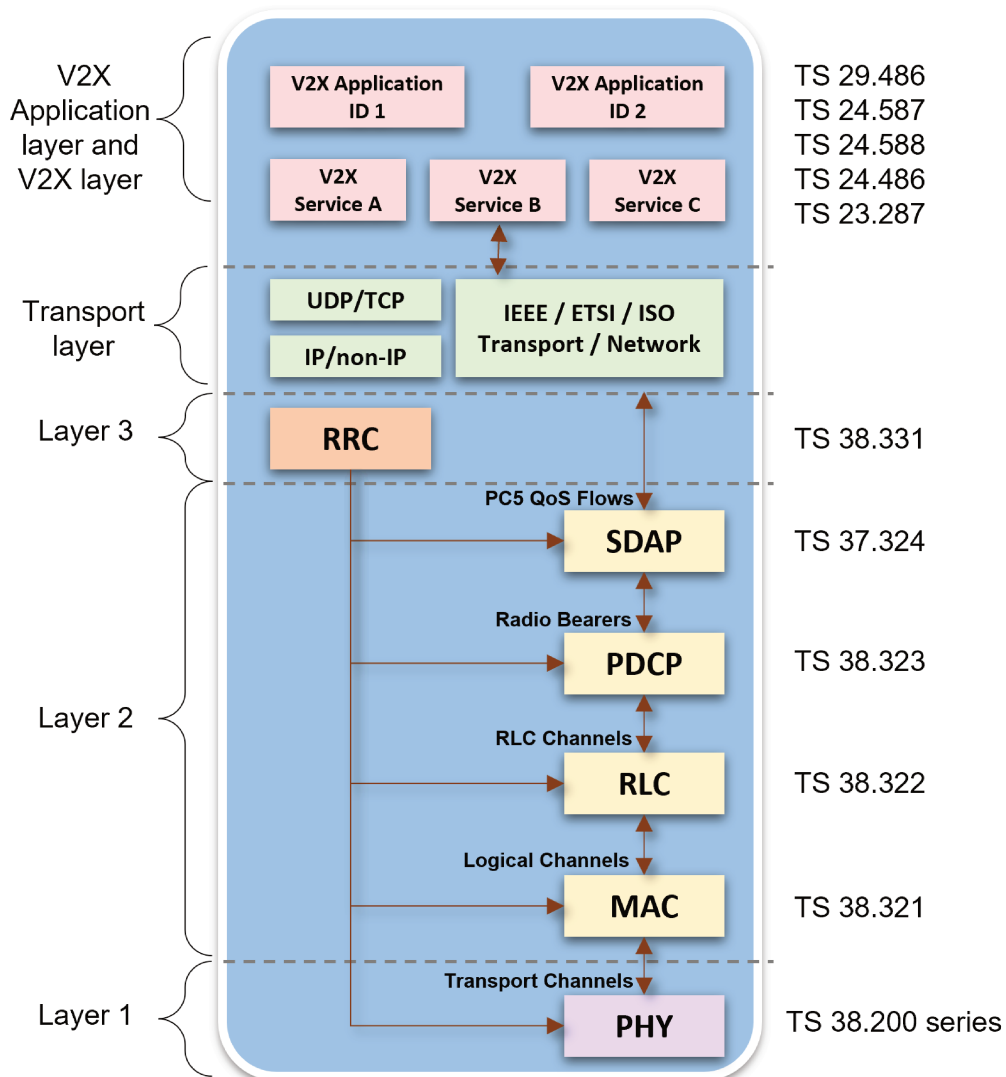


Figure 2.4 – 3GPP NR-V2X R16 Protocol Stack

In this R16, as illustrated in Figure 2.4, 3GPP reuses other standards for higher layer. 3GPP mainly focus only on Access Stratum (AS) layer. NR-V2X uses the same protocol stack as 5G. It defines the V2X Application Layer and

V2X Layer. Below that, there is the RRC layer 3, used in Control Plane. In layer 2, a new sublayer called Service Data Adaptation Protocol layer (SDAP) is added in 5G, also used in NR-V2X, followed by Packet Data Convergence Protocol layer (PDCP), Radio Link Control layer (RLC), MAC sublayers. The last layer is PHY layer. We will now provide a explanation of these layers, starting from the application layer and going down to the PHY layer.

2.1.2.1 . V2X application layer

In Release 16, 3GPP primarily focuses on the AS layer, which includes layer 3, layer 2, and layer 1. However, the 3GPP is planning to address the V2X Application layer in Release 17 [29]. Therefore, we are going to present an overview of the V2X application layer release 17, which will help us obtain a deeper knowledge of V2X according to specifications by 3GPP.

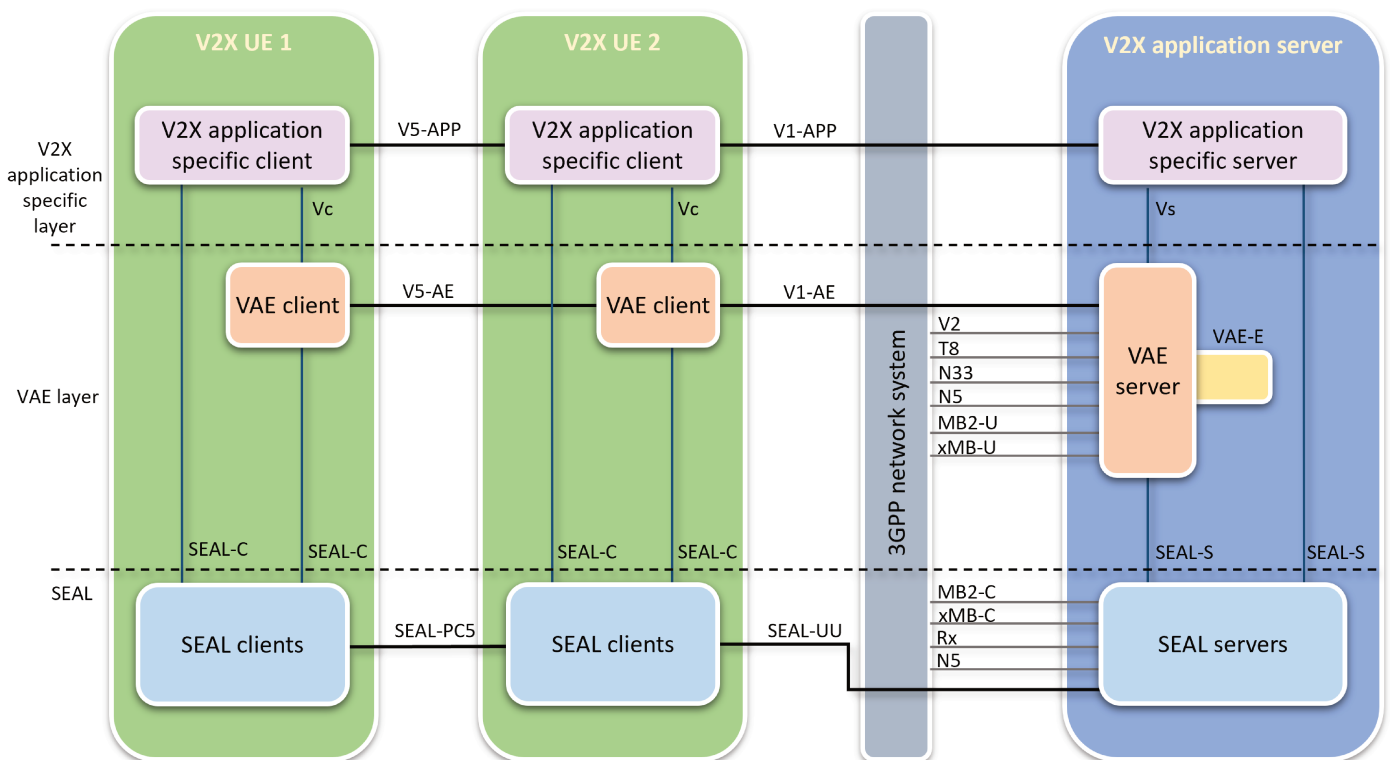


Figure 2.5 - V2X application layer functional model [29]

On the UE, the V2X application layer consists of the V2X Application Enabler (VAE) [30] [31] client, Service Enabler Architecture Layer (SEAL) [50] clients, and the V2X application specific client. The VAE client provides support func-

tions, while the SEAL client(s) offers SEAL services to the V2X application specific client through the reference point shown in Figure 2.5.

On the server, the V2X AS comprises the V2X application specific server, the VAE server [30] [31], and the SEAL servers [50]. Through the reference point shown in Figure 2.5, the VAE server provides support functions while the SEAL server(s) delivers SEAL services to the V2X application specific server.

The VAE layer offers support functions to V2X applications. These functions include registration, sending or receiving V2X messages, network monitoring reports, application level locations, and 3GPP system configuration information such as V2X User Service Description and PC5 parameters. In addition, SEAL provides various services including location management [51], group management [52], configuration management [53], identity management [54], key management [55], and network resource management [56].

2.1.2.2. Radio Resource Control (RRC) layer 3

RRC for SL [57][58] in NR-V2X is sit on top of AS layer, served on Control Plane in Uu and PC5 interface. This layer 3 configures SL resource allocation depending on information received from gNB. It also measures and reports to the system information related to SL. There are three RRC states : RRC_CONNECTED, RRC_INACTIVE and RRC_IDLE. A vehicle or a UE is in RRC_IDLE state if no connection to the operator has been established. Otherwise, it is in RRC_CONNECTED state or in RRC_INACTIVE state. These three states of RRC are shown in Figure 2.6.

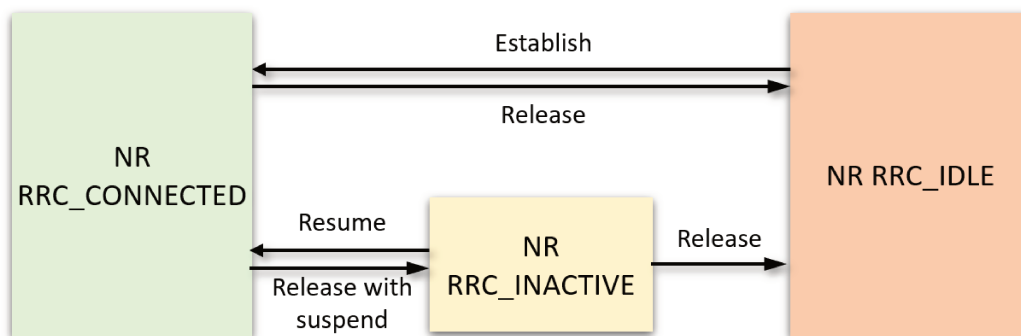


Figure 2.6 – Three RRC states

RRC in the UE will receive the System Information Block 12 (SIB12) [57], the most importance V2X system configuration, from the network via gNB. The SIB12 is especially defined and used for NR SL communication configuration, sent in RRCReconfiguration [57] message from network to vehicles. We must note that, for PC5 interface, PC5-RRC is a logical connection between two UEs and supported only for Unicast mode communication over PC5 interface. After establishment of a PC5 Unicast Link, a PC5-RRC is created and this PC5-RRC will be released when UEs finishes their Unicast connection.

2.1.2.3 . Service Data Adaptation Protocol (SDAP) sublayer 2

SDAP[59] is a sublayer for User Plane protocol stack that was first introduced in 5G NR. SDAP maps between a QoS Flow and a Sidelink Data Radio Bearer (SL-DRB). A flow (Figure 2.7) represents a unidirectional stream of data with specific QoS requirements, while a bearer provide the transport mechanism and resource allocation for carrying the data between the UEs, or between UE and the network. A UE can have maximum 2048 QoS Flows for NR-V2X SL communication, and maximum 512 Sidelink Radio Bearer (SLRB). We will come back with the flow again in section 2.1.7.3 on page 51.

Moreover, SLRB is divided into two groups : SL-DRB works on User Plane which begins from SDAP sublayer. The other is Sidelink Signaling Radio Bearer (SL-SRB) which is used for Control Plane.

2.1.2.4 . Packet Data Convergence Protocol (PDCP) sublayer 2

PDCP [60] sublayer is implemented in both Control Plane and User Plane protocol stack in NR. PDCP provides header compression, encryption, and integrity. In NR-V2X, PDCP sublayer does not support duplication for PC5 interface, and uses out-of-order delivery only for Unicast transmission.

2.1.2.5 . Radio Link Control (RLC) sublayer 2

RLC [61] sublayer in 5G is almost the same as LTE RLC. The RLC sublayer 2 in 5G NR may operate in Transparent Mode (TM), Unacknowledged Mode (UM), or Acknowledged Mode (AM). In the TM, the RLC sublayer transfers upper-layer data packets to the lower layers without segmenting or reassembling them. The UM transmits Protocol Data Unit (PDU) over the radio inter-

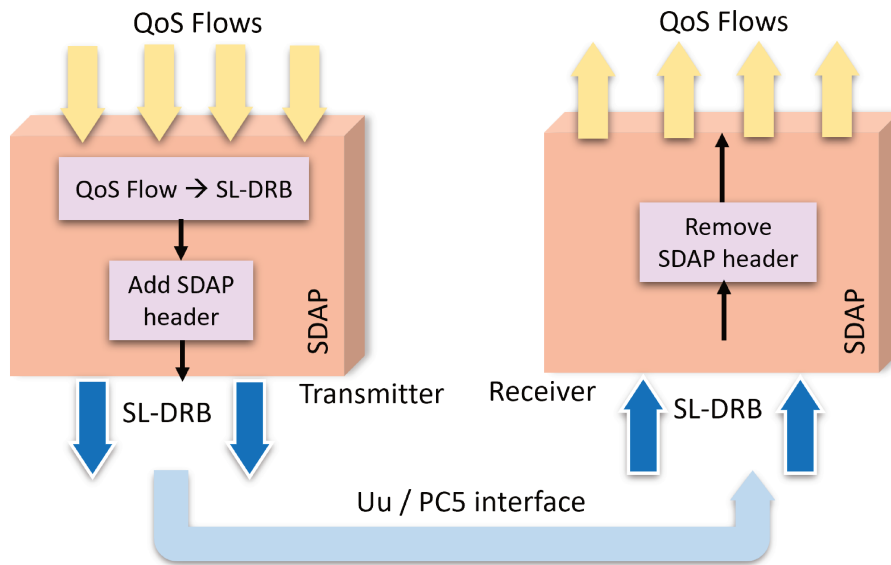


Figure 2.7 – SDAP with flows and SL-DRB

face without receiving any acknowledgment or carrying out error detection or recovery. Meanwhile, the AM is considered the most reliable mode within the RLC which offers segmentation, reassembly, error detection, and recovery mechanisms. In NR-V2X, both UM and AM are utilized in Unicast communication, while Groupcast or Broadcast communications work on UM. However, the TM is only utilized for broadcasting the control plane traffic, which is called Sidelink Broadcast Control Channel (SBCCH) in this layer.

2.1.2.6 . Medium Access Control (MAC) sublayer 2

MAC [62] sublayer in NR-V2X maps from Logical Channel (LC) to Transport Channel (TC) on PHY layer. It is necessary to note that an LC refers to a channel at the MAC layer that carries specific types of data or control information between the MAC layer entities of the transmitter and receiver. On the other hand, a TC is a channel at the PHY layer that carries user data and control information between the PHY layer entities of the transmitter and receiver. The number of LC in MAC sublayer for NR-V2X SL is maximum 512 LCs divided into three types : Sidelink Control Channel (SCCH) for control information on Control Plane, Sidelink Traffic Channel (STCH) for User Plane, and SBCCH (mentioned in section 2.1.2.5) for broadcasting system information on Control Plane.

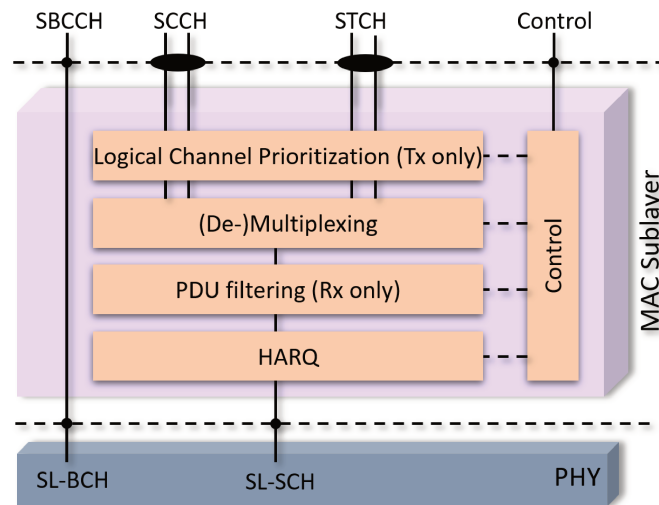


Figure 2.8 – Medium Access Control MAC sublayer structure

These two types of LC, SCCH and STCH, are mapped to Sidelink Shared Channel (SL-SCH) of TC, whereas SBCCH maps to Sidelink Broadcast Channel (SL-BCH) of TC. MAC sublayer also provides radio resource selection or scheduling, as well as multiplexing, etc.. Figure 2.8 shows the mapping from LC in MAC sublayer to TC in PHY layer.

Before continuing, let us briefly examine the process of transforming the packet from the higher layer to the MAC layer. In Figure 2.9, IP packets from higher layers are combined with a new header in the SDAP layer to form PDCP Service Data Unit (SDUs). Next, within the PDCP layer, these PDCP SDUs are appended with an additional header and transmitted to the RLC layer. After adding a header and changing into MAC SDUs, RLC SDUs are finally moved to the MAC layer. Some MAC SDUs are joined (multiplexed) into a MAC PDU, which is also known as a MAC TB. The MAC SDUs can originate from either the same bearer or a different bearer in higher layer, but they must have the same destination UE. Afterwards, MAC PDUs are transferred to the PHY layer and then transmitted to the receiving UE through the radio interface.

2.1.2.7. Physical (PHY) layer 1

[63][64][65][66][67][68][69] PHY layer sits at the bottom of the 3GPP 5G NR R16 protocol stack. The PHY layer offers a TC to MAC sublayer of Layer 2 and receives the control information from RRC layer 3 to do coding, data modulation, resource mapping and antenna mapping for sending or receiving

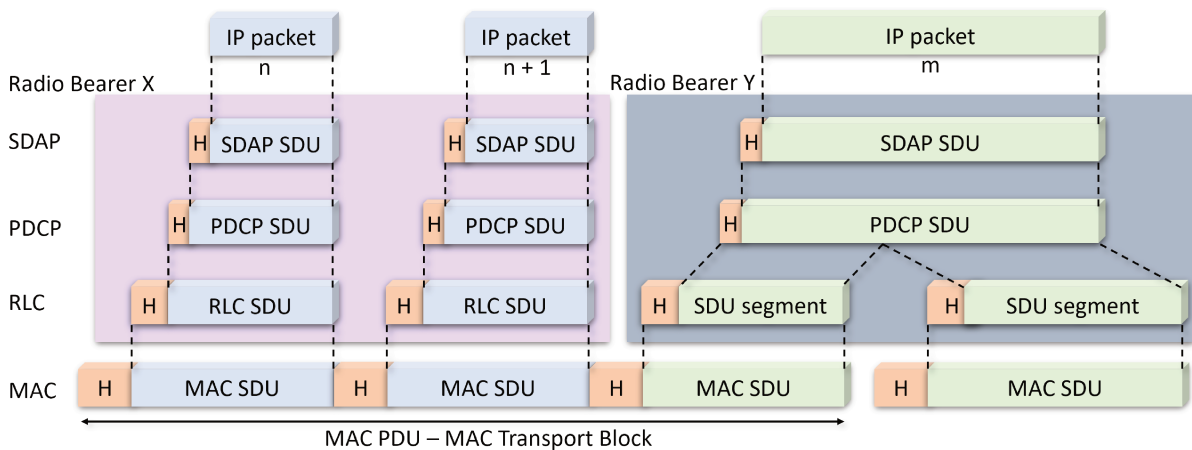


Figure 2.9 – IP packet to MAC-PDU

the data via antenna. We will go to detail of this layer in the next section 2.1.3 on page 23.

2.1.2.8 . User Plane and Control Plane

The Control Plane and User Plane are two separate planes in 5G NR-V2X that manage different aspects of communication.

The Control Plane in V2X is responsible for transmitting control signaling messages and control information between UEs or between the network and the UE. The Control Plane is mainly used to establish, maintain, and manage the connection between them.

The User Plane, also referred to as the data plane, is in charge of sending user data traffic between UEs or between the network and the UE. It is responsible for the transmission of user data packets, including voice, video, and other V2X application data. The User Plane guarantees the effective and reliable transmission of user data across the network. It is separate from the Control Plane and its main purpose is to transmit the data payload without being involved in control signaling or management operations.

The separation of the Control Plane and User Plane offers efficient and flexible communication in NR-V2X. It allows to manage and control the communication session using the Control Plane, while effectively transmitting data through the User Plane. This separation enables efficient resource allocation, scalability, and adaptability for various V2X service requirements.

As shown in Figure 2.10, in AS (layer 1, 2 and 3) of 5G NR-V2X protocol stack, SDAP is first defined and sit on top of User Plane in AS layer for SL-DRB bearer to transmit the data. Meanwhile, for the Control Plane, RRC from layer 3 is the first layer and use SL-SRB bearer for Control Plane to transmit control signaling and control information messages.

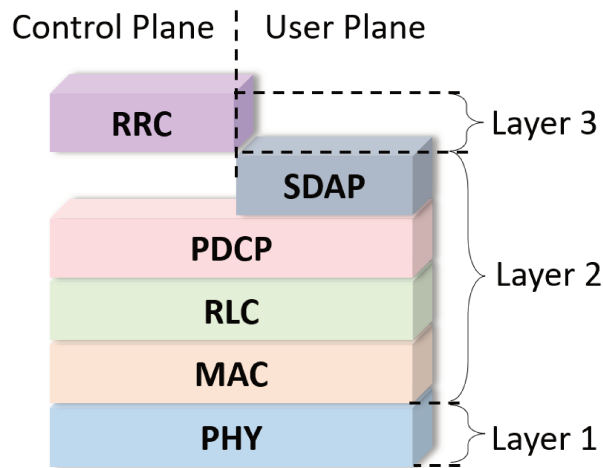


Figure 2.10 – User Plane and Control Plane

2.1.3 . Physical (PHY) layer for NR-V2X Sidelink

The most crucial aspect of our research will be carefully explained in this section. In fact, understanding this layer with its numerology, subchannel size, transport block, and other characteristics is mandatory for understanding our proposals. Let us begin with the Operating bands.

2.1.3.1 . Operating bands and channel bandwidth

The 3GPP R16 standard defines the frequency ranges for 5G NR, which include FR1 (410 MHz–7125 MHz) and FR2 (24250 MHz–52600 MHz). The FR2 frequency range can be referred to as the mmWave. In the context of NR-V2X, R16 standard focuses primarily on utilizing FR1. Specifically, it utilizes the unlicensed ITS n47 band and the licensed operating band n38 for NR SL. It should be noted, however, that the usage of the n38 band is subject to regional limitations. Table 2.2 and Table 2.1 [70] give you more information of n47 and n38 NR bands. Furthermore, the duplex mode for NR-V2X remains Half-duplex (HD), aligning with the approach adopted in LTE-V2X Release 14.

Additionally, it is important to mention that in Release 17, the NR-V2X ecosystem has been assigned two additional bands, which are n14 and n79. This band assignment aims to meet the stringent requirements of NR-V2X scenarios and enhance the user experience in V2X communication. The n79's 600 MHz bandwidth may improve the infotainment and self-driving experience, while the transmission range is increased by the n14 band, which uses the frequency range of 788 MHz to 798 MHz. This is enormously helpful for public safety services in V2X.

Table 2.1 – NR-V2X SL operating bands in FR1

NR Band	SL Transmission operating band (MHz)	SL Reception operating band (MHz)	Duplex mode	Interface
	low - high	low - high		
n38	2570 - 2620	2570 - 2620	HD	PC5
n47	5855 - 5925	5855 - 5925	HD	PC5

Table 2.2 – Channel bandwidths supported for NR-V2X band

NR Band	SCS kHz	5 MHz	10 MHz	15 MHz	20 MHz	25 MHz	30 MHz	40 MHz
n38	15	Yes	Yes	Yes	Yes	Yes	Yes	Yes
	30	-	Yes	Yes	Yes	Yes	Yes	Yes
	60	-	Yes	Yes	Yes	Yes	Yes	Yes
n47	15	-	Yes	-	Yes	-	Yes	Yes
	30	-	Yes	-	Yes	-	Yes	Yes
	60	-	Yes	-	Yes	-	Yes	Yes

2.1.3.2. Numerology

Numerology [65], as indicated in Table 2.3, is denoted as μ , which is a factor for SCS configuration and is represented by a SCS value. NR-V2X SL supports four μ value (SCS values). The supported values for μ in FR1 are 0, 1,

and 2, correspond to 15, 30, and 60 kHz glsSCS, respectively. For FR2, values 2 and 3 of μ are supported; these correspond to 60 and 120 kHz SCS, respectively. Furthermore, the utilization of Normal Cyclic Prefix (CP) (14 symbols) applies for all the numerology μ listed in Table 2.3. Nevertheless, Extended CP (12 symbols) is limited to use for the numerology μ value 2, corresponds to 60 kHz SCS. In the purpose of this thesis, we concentrate on researching FR1, which only accepts values 0, 1, and 2 of μ while utilizing Normal CP.

Table 2.3 – Numerology

μ	SCS kHz	FR	Cyclic Prefix	RB bandwidth	Symbols per slot	Slot per frame	Slot per subframe	Slot duration
0	15	FR1	Normal	180 kHz	14	10	1	1 ms
1	30	FR1	Normal	360 kHz	14	20	2	0.5 ms
2	60	FR1-2	Normal, Ext	720 kHz	14, 12	40	4	0.25 ms
3	120	FR2	Normal	1.44 MHz	14	80	8	0.125 ms

2.1.3.3. Time domain

As illustrated in Figure 2.11 on page 26 and in Table 2.5 on page 30, a NR-V2X SL **frame** is 10 ms duration fixed like in LTE-V2X. A frame is divided into 10 subframes with the duration of 1 ms each. A **subframe** can have one or many slots, depending on the SCS value.

For example, a **slot** that has a SCS of 15 kHz gets a duration of 1 ms, which is the same as the duration of a subframe. When the SCS value is increased to 30 kHz, the duration of the slot is reduced by half to 0.5 ms, and each subframe consists of two slots. The duration of each slot decreases to 0.25 ms in a 60 kHz SCS, and one subframe contains four slots.

The Cyclic Prefix - Orthogonal Frequency Division Multiplexing (CP-OFDM) **symbol** is smaller than a slot and is the smallest in the entire time domain. Recall that for Normal CP, there are 14 symbols in each slot, and for Extended CP, there are 12 symbols. In this thesis, we assume that we only use Normal CP, therefore whenever we refer to a slot, we mean 14 symbols.

The minimum unit for SL resource scheduling in the time domain is a slot. Figure 2.11 shows the relationship of frame, subframe and slot.

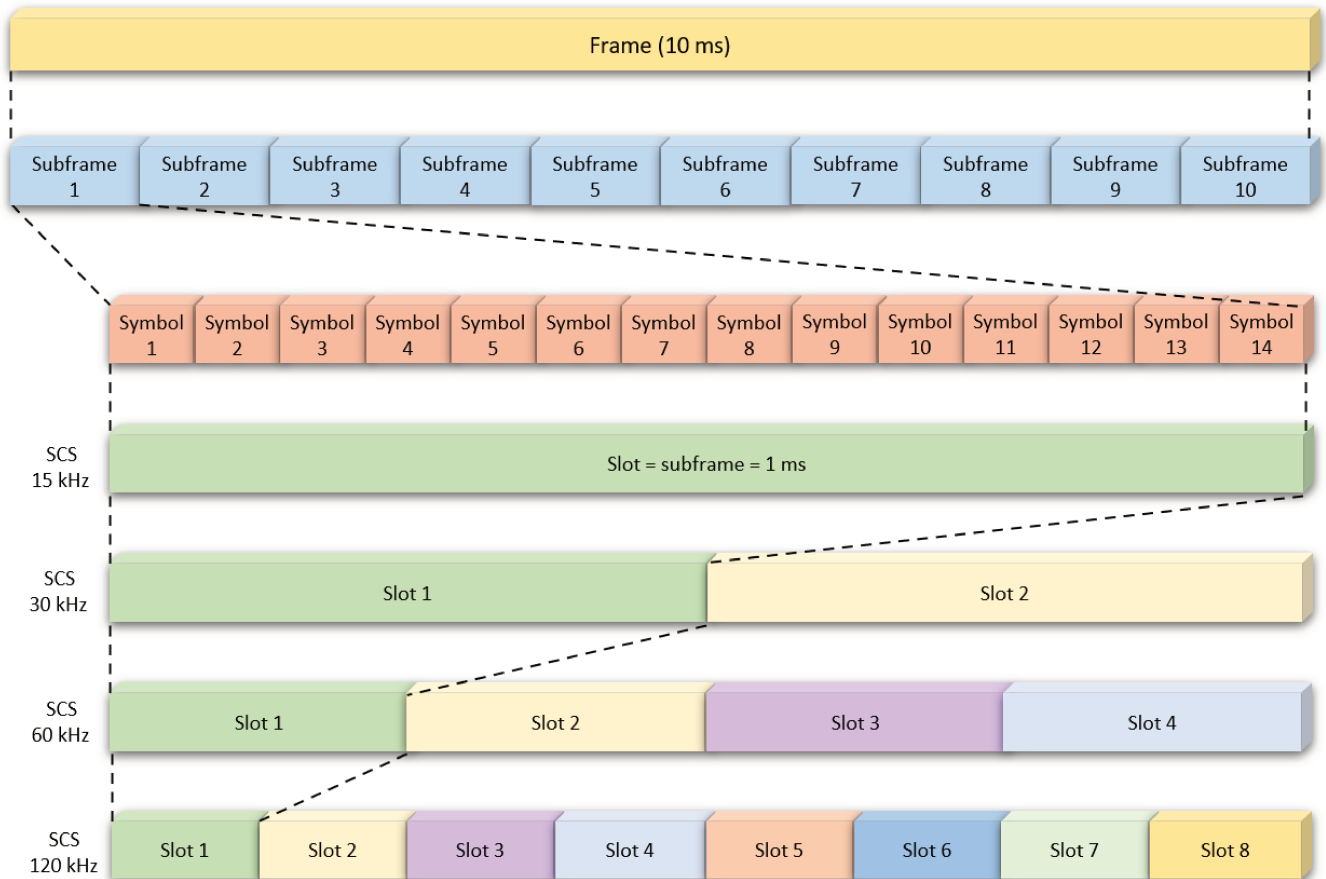


Figure 2.11 – Frame - Subframe - Slot

2.1.3.4. Frequency domain

Bandwidth (BW) and Bandwidth Part (BWP) : In the frequency domain for NR, a carrier BW can go up to 100 MHz in FR1 or 400 MHz in FR2. This large BW leads to a problem that is difficult for UE to handle that whole BW. Thus, the concept of BWP is defined in 5G and this concept is also used in NR-V2X. We must note that, in the 3GPP R16 for NR-V2X, only one SL BWP is configured for NR SL communication in a point of time. All UEs must use the same SL BWP for SL transmissions and receptions. Figure 2.12 shows an example relationship of BW, BWP and subchannel in n47 band. We will describe subchannel

right below.

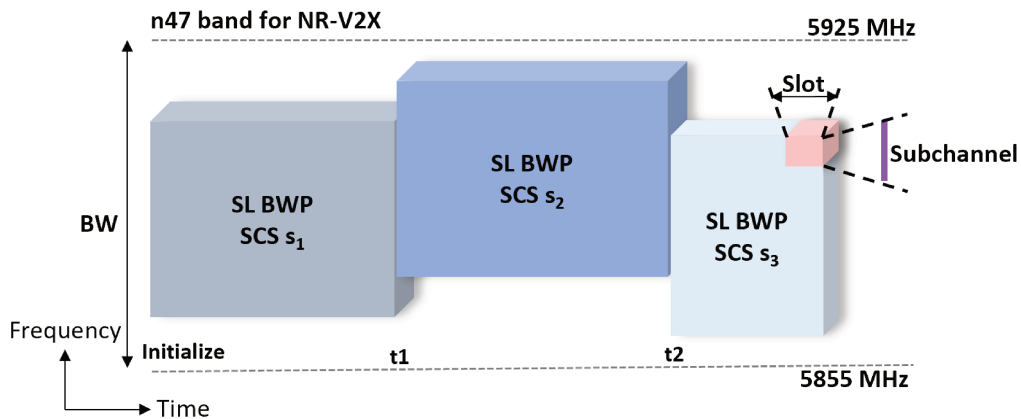


Figure 2.12 – Bandwidth - Bandwidth Part - Subchannel

Subchannel : The SL BWP is divided into smaller parts, called subchannels. A subchannel is a set of 10, 12, 15, 20, 25, 50, 75, or 100 contiguous RBs. All subchannels within SL BWP have the same number of RBs. Subchannel is a minimum unit for SL resource scheduling in frequency domain. We can see briefly an example of subchannel size 10 RBs in Figure 2.14.

Resource Block (RB) : The RB [65] in NR is a little different from LTE where it is defined in both the time and frequency domains, whereas an RB is only defined in the frequency domain as twelve consecutive subcarriers. The sub-carrier is the minimum unit in frequency domain. Consequently, an UE is not expected to receive or transmit in a carrier with more than one numerology for SL.

We must know that, from the definition of RB, there are Common Resource Block (CRB) and Physical Resource Block (PRB) concepts. For a given carrier, CRB is the RBs with the same numerology which are indexed increasingly from the lowest frequency of the carrier (index 0). Similarly, RB related to BWP is called PRB. Resource allocation utilizes only PRB.

Table 2.4 on page 28 provides the maximum number of RBs that can be utilized based on bandwidth and numerology for FR1.

Table 2.4 – Maximum Resource Blocks configuration by bandwidth and numerology for NR-V2X SL [70]

SCS kHz	5 MHz	10 MHz	15 MHz	20 MHz	25 MHz	30 MHz	40 MHz
15	25	52	79	106	133	160	216
30	11	24	38	51	65	78	106
60	N/A	11	18	24	31	38	51

2.1.3.5. Physical resource

Resource Element (RE) : The RE [65] is the smallest resource unit in NR-V2X. RE is one subcarrier in the frequency domain over one CP-OFDM symbol in the time domain. As shown in Figure 2.13, twelve consecutive subcarriers form a RB in the frequency domain, whereas twelve REs are produced by twelve successive subcarriers and one slot time.

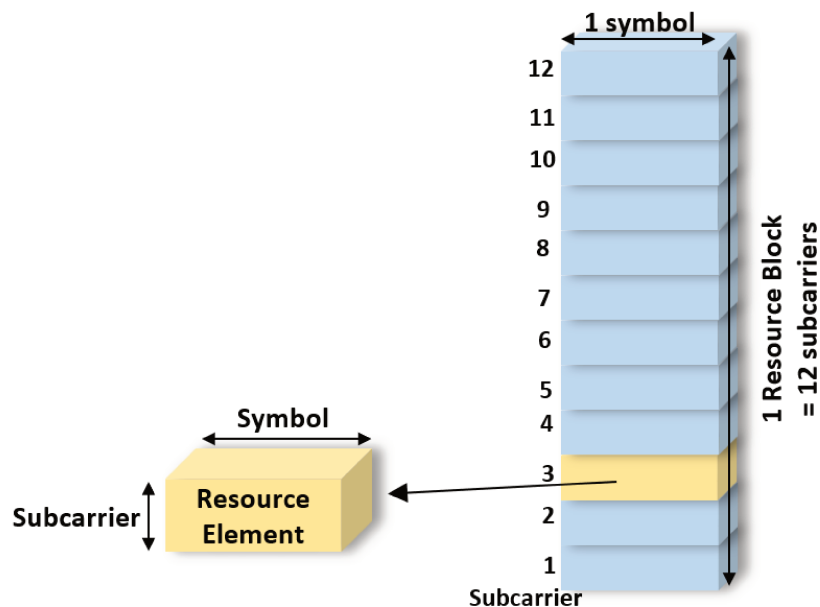


Figure 2.13 – Resource Element - Resource Block - Subcarrier

SL Resource Pool (RP)[71][65][57] : Due to the limitations of UE's capabilities, it is unable to monitor, transmit, or receive across the entire radio bandwidth and time slots of NR radio resources. Hence, this concept is defined and utilized in particular in NR-V2X resource allocation mode 2 for supporting SL

communication, in which a UE will select its own resources based on sensing within the pool. SL RP is a subset of available radio resources configured for SL and must be defined within the SL BWP. In particular, SL RP consists of the subchannels which are consecutively set of minimum 10 RBs. SL RP size in the time domain is less than 10240 ms[68]. We can also note that the PRBs are used in a RP. Physical Sidelink Control Channel (PSCCH) and Physical Sidelink Shared Channel (PSSCH) resources (described in section 2.1.3.6 on page 29) are defined within SL RPs.

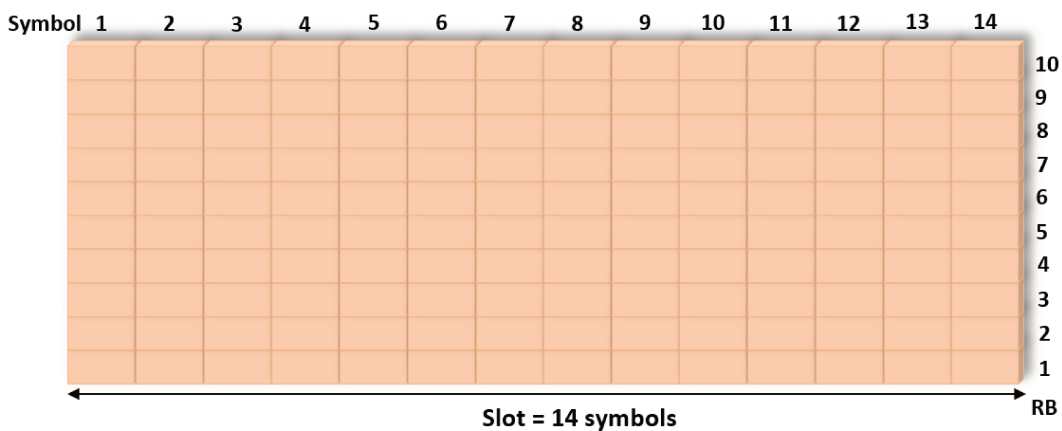


Figure 2.14 – An example of TB with subchannel size 10 RBs

Transport Block (TB) is an additional resource unit with one slot in the time domain and one or more subchannels in the frequency domain. In the context of NR-V2X, the resource assigned for transmitting data in the PHY layer is referred to as TB. It contains the data that is inserted into the PSSCH. We will provide further explanation on the PSSCH information in section 2.1.3.6 on page 29. An example of TB is shown in Figure 2.14. This TB has only one subchannel with size 10 RBs.

Table 2.5 summarizes the elements and their relationship in both time and frequency domain.

2.1.3.6. Transport Block (TB) in detail

a) Physical Sidelink Shared Channel (PSSCH)

PSSCH is used to contain the payload of data for TB and the 2nd-stage SCI. We will explain in detail 2nd-stage SCI below in the same section. PSSCH

Table 2.5 – Physical resource summary

BW → BWP → Subchannel → RB → Subcarrier	
Frequency	BWP = 1 or multiple subchannels
	Subchannel = {10, 12, 15, 20, 25, 50, 75, 100} RBs
	RB = 12 subcarriers with spacing in SCS
	SCS = {15, 30, 60} kHz in FR1 or {60, 120} kHz in FR2
	RE = 1 Subcarrier × 1 Symbol
	TB = 1 Slot × 1 or multiple subchannels
Frame → Subframe → Slot → Symbol	
Time	Frame = 10ms = 10 subframes
	Subframe = 1ms = {1, 2, 4, 8} Slots for {15, 30, 60, 120} kHz respectively
	Slot = 14 symbols

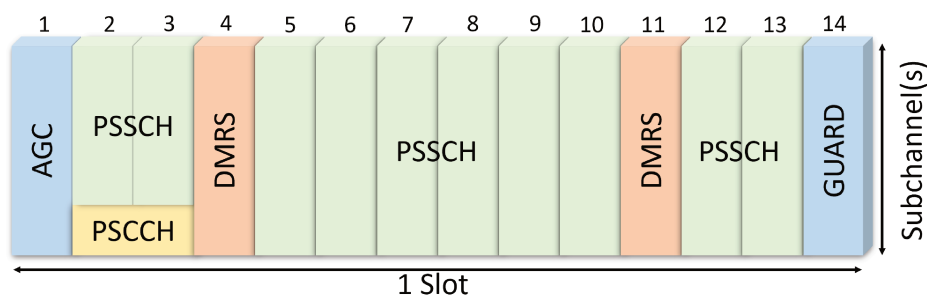


Figure 2.15 – Structure of an example Transport Block with 2-symbol PSSCH, 2-symbol PSSCH-DMRS, without PSFCH

is transmitted from transmitter UE to receiver UE. Modulation scheme for PSSCH data is Quadrature Phase Shift Keying (QPSK), 16 Quadrature Amplitude Modulation (QAM), 64QAM, or 256QAM with Low-Density Parity-Check (LDPC) coding. Meanwhile, QPSK and Polar is used for 2nd-stage SCI. The available slots for PSSCH transmission can accommodate between 7 to 14 symbols that are specifically allocated for SL operation. Within these symbols, PSSCH can be transmitted in a range of 5 to 12 symbols.

b) Physical Sidelink Control Channel (PSCCH)

PSCCH stores the 1st-stage SCI associate to a PSSCH that contains information for a receiver UE identify resource allocation of the PSSCH in which contains the data. Without 1st-stage SCI information, receiver cannot decode

the radio signal and receive the data that was put on PSSCH. PSCCH is only modulated by using QPSK, combined with Polar coding scheme. PSCCH can consume 2 or 3 symbols from the 2nd symbol of the slot in time domain and 10, 12, 15, 20 or 25 consecutively RBs in frequency domain. Unfortunately, the frequency length of PSCCH must be less than subchannel's length. Therefore, PSCCH is always located on only one subchannel. In Figure 2.15, PSCCH consumes only 2 symbols (the second and third symbol of the slot), and 3 symbols (second, third and fourth symbol of the slot) in Figure 2.16.

c) Physical Sidelink Feedback Channel (PSFCH)

PSFCH is a PHY channel that is utilized for transmitting feedback information from the receiver to the transmitter. It plays a crucial role in facilitating reliable and efficient communication in NR-V2X. This PHY channel applies only for Unicast and Groupcast mode communication. It comprises three symbols, from 11th to 13th symbol (as an example shown in Figure 2.16).

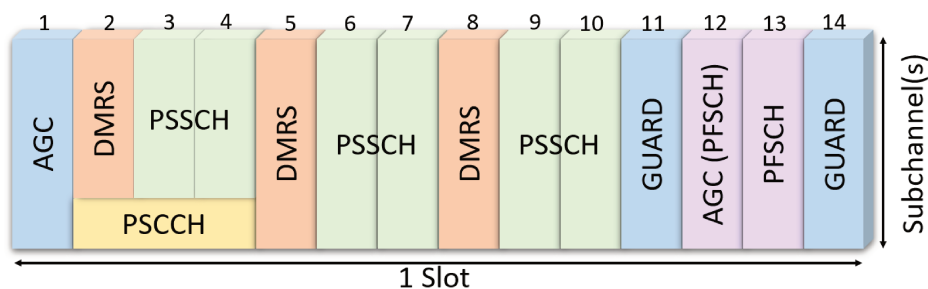


Figure 2.16 – Structure of an example Transport Block with 3-symbol PSCCH, 3-symbol PSSCH-DMRS, and PSFCH

d) Physical Sidelink Broadcast Channel (PSBCH)

PSBCH (Figure 2.17) contains Sidelink Primary Synchronization Signal (S-PSS) and Sidelink Secondary Synchronization Signals (S-SSS). PSBCH with MIB for SL (MasterInformationBlockSidelink [57] from RRC layer) is sent in Sidelink Synchronization Signal Block (S-SSB) periodically 160 ms, uses 132 sub-carriers and QPSK as modulation scheme. The MIB SL contains parameters such as slot index, inside/outside network coverage that are necessary for UEs to synchronize and access the V2X network.



Figure 2.17 – Structure of PSBCH

e) Demodulation Reference Signal (DMRS)

The NR-V2X ecosystem allows for vehicle speeds of up to 500 km/h. In high speeds scenarios, the Doppler effect becomes harder. The higher speed causes larger frequency shifts and phase variations in the received signal due to the relative motion between the transmitter and receiver.

As an reference signal in the transmitted signal, DMRS plays a crucial role in solving for the Doppler effect. By incorporating DMRS into the transmitted signal, the receiver is able to estimate and monitor channel conditions, including frequency shifts and phase variations caused by the Doppler effect. Thus, even at high speeds, DMRS facilitates reliable and robust communication.

DMRS associated with PSSCH, PSCCH or PSBCH help UE to handle Doppler effect [72] and decode in receiver. For DMRS associated with PSSCH, DMRS can take 2, 3 or 4 symbols. Their position depend on the number of symbols used for PSCCH and PSSCH. Table 2.6 shows briefly their position rules. These positions depend on assumption that first symbol is index 1, not 0.

An example is shown in Figure 2.15. DMRS is on 4th and 11th symbol, because this TB has 2 symbols for DMRS, and with the 2-symbol PSCCH and 14 symbols for PSSCH. If this TB had 3 symbols for DMRS, they will be on 2nd, 7th and 12th symbol.

f) Physical signals

In Release 16 for NR-V2X, there are some physical signals specified. First, DMRS associated with PSSCH, PSCCH or PSBCH. Next, SL Channel State In-

Table 2.6 – DMRS position [65]

Number of PSSCH symbols	DM-RS position					
	PSSCH duration 2 symbols			PSSCH duration 3 symbols		
	Number of PSSCH DM-RS			Number of PSSCH DM-RS		
	2	3	4	2	3	4
6	2, 6	-	-	2, 6	-	-
7	2, 6	-	-	2, 6	-	-
8	2, 6	-	-	2, 6	-	-
9	4, 9	2, 5, 8	-	5, 9	2, 5, 8	-
10	4, 9	2, 5, 8	-	5, 9	2, 5, 8	-
11	4, 11	2, 6, 10	2, 5, 8, 11	5, 11	2, 6, 10	2, 5, 8, 11
12	4, 11	2, 6, 10	2, 5, 8, 11	5, 11	2, 6, 10	2, 5, 8, 11
13	4, 11	2, 7, 12	2, 5, 8, 11	5, 11	2, 7, 12	2, 5, 8, 11

formation Reference Signal (CSI-RS) is specified and send from receiver UE in order that transmitter UE can calibrate the Channel State Information (CSI) estimation at the receiver for Unicast transmission. Phase-Tracking Reference Signal (PT-RS) is used only in FR2 for minimizing the effect of the oscillator phase noise. Finally, S-PSS and S-SSS is used to synchronize between UEs.

g) Sidelink Control Information (SCI)

In NR-V2X, SCI is divided into two stages different.

1st-stage SCI (or SCI format 1-A) is carried on PSCCH. Due to the size of 1st-stage SCI, PSCCH can consume symbols of the slot in time domain (2 or 3 symbols) and RBs in frequency domain (only on first subchannel). The first 3 bits is the priority of the associated PSSCH and this priority is taken from the priority of the LC on the MAC layer where this data comes from. Secondly, there are some bits indicating the subchannel of the current transmission PSSCH as well as up to two resource reservations for retransmission. It also takes 5 or 9 bits for the time slot for the resource reservations. The next field for the resource reservation period may be empty or up to 4 bits. SCI format 1-A also indicates which format for the 2nd-stage SCI, DMRS pattern, MCS in-

dex value and thanks for that information the receiver UE can decode data payload on PSSCH. Figure 2.18 describes all fields of 1st-stage SCI and their size in Bit.

In the NR-V2X ecosystem and also in the scope of this thesis, this SCI plays a crucial role in determining the size and structure of the PHY TB. Therefore, the resource allocation scheduler is able to assign an appropriate resource to the UE based on the information provided. Furthermore, it contributes the receiver in correctly decoding the data in the TB.

The detail of all 1st-stage SCI fields are listed in Appendix F on page 143.

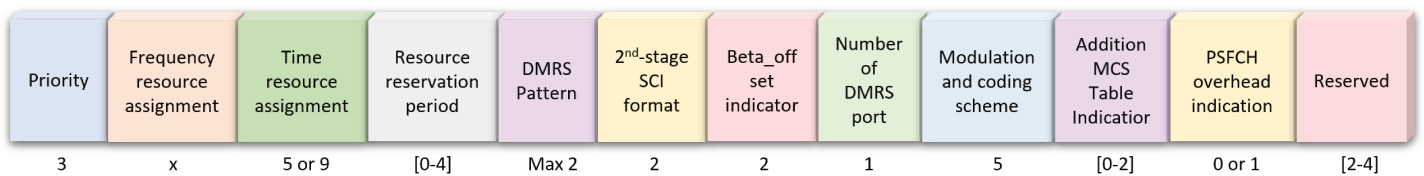


Figure 2.18 – 1st-stage SCI format

2nd-stage SCI is packaged in PSSCH along with data payload. 5 to 12 symbols in the slot associated with PSSCH are used for PSSCH. Although 1st-stage SCI's size is variable, the 2nd-stage SCI's size is fixed. There are two formats for 2nd-stage SCI : SCI format 2-A (35 bits) and SCI format 2-B (48 bits). Figure 2.19 describes all fields of 2nd-stage SCI.

Among the fields of 2nd-stage SCI, Hybrid automatic repeat request (HARQ) Process Number is the first field of 2nd-stage SCI which is 4 bits and uses to identify TB. 1-bit New Data Indicator indicates the TB, which this 2nd-stage SCI associated, is new transmission or retransmission. 2-bit Redundancy Version is the index of the retransmission. To illustrate retransmission, a receiver UE detects New Data Indicator is retransmission, receiver knows this retransmission is for which TB thanks to HARQ Process Number, and index of retransmission thanks to Redundancy Version value. The 2nd-stage SCI also contains the Source and Destination Id. Moreover, the SCI format 2-A includes Cast Type Indicator field with value 0 for Broadcast, 2 for Unicast and 1 or 3 for Groupcast. On the contrary, the SCI format 2-B contains 12-bit Zone Id field, and 4-bit Communication Range with 16 possible value for the range from 20m to 1000m.

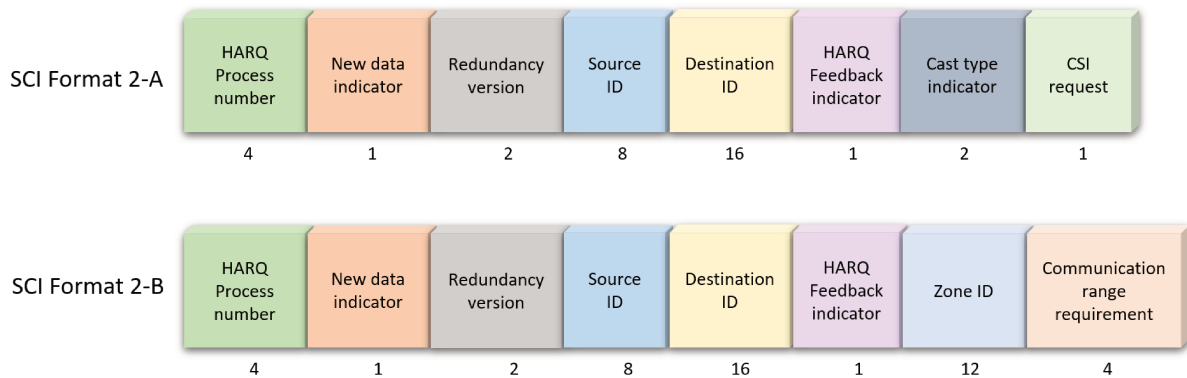


Figure 2.19 – 2nd-stage SCI format

2.1.3.7. Link Adaptation : the Channel-state information (CSI)

The CSI-RS combined with Adaptive Modulation and Coding enables link adaptation in 3GPP 5G NR and in Unicast communication of NR-V2X SL to increase efficiency and reliability. First, a transmitter sends the SL CSI-RS in the PSSCH to a receiver. The latter measures the SL channel and extracts the Channel Quality Indicator (CQI) that indicates the highest modulation and coding scheme the receiver can support. This is done by mapping the radio quality to CQI index from a CQI table associated to the configured MCS table for a PSSCH [68]. Then, the receiver sends the estimated channel state back to the transmitter. Figure 2.20 visualizes the SL CSI and the delay expectation of transmitter.

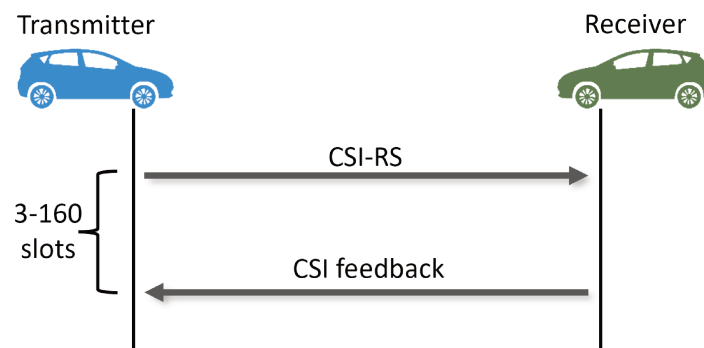


Figure 2.20 – Sidelink Channel State Information

3GPP NR-V2X R16 also provides 3 CQI tables, as you can find in the Appendix Table D.1 , Table D.2 and Table D.3 on page 137. The table is used among these three CQI tables depends on which MCS Table C.1, Table C.2 or Table C.3 on page 134 is used respectively.

2.1.4 . Transport Block Size (TBS) determination

Figure 2.16 on page 31 provides an illustration of a TB. Knowing the structure of the TB allows us to calculate the TBS required to contain the MAC-PDU in MAC layer. This information is essential for assisting the scheduler in identifying a suitable PHY resource for MAC-PDU on the transmitter. Therefore, we will now explain the process of determining the TBS.

Step 1 : Determine the number of REs allocated for PSSCH within a PRB :

$$N'_{RE}$$

$$N'_{RE} = N_{sc}^{RB} \times (N_{symbol}^{sh} - N_{symbol}^{PFSCCH}) - N_{oh}^{PRB} - N_{RE}^{DMRS} \quad (2.1)$$

Where :

- N_{sc}^{RB} is the number of subcarriers in a RB, and equal to 12.
- N_{symbol}^{sh} is the number of SL symbols within the slot provided parameter sl-LengthSymbols in RRC layer, normally from 7 to 14 symbols, excludes two symbols (the first and the last symbol in a slot cannot be used).
- N_{symbol}^{PFSCCH} is 0 or 3 symbols.
- N_{oh}^{PRB} given by higher layer parameter sl-X-Overhead, with value is 0, 3, 6 or 9. xOverhead represents sets the resource allocation overhead used for CSI-RS and the CORESET TBS.
- N_{RE}^{DMRS} : by parameter sl-PSSCH-DMRS-TimePattern from RRC and table, we can determine this value using Table 2.7

Step 2 : determines the total number of REs allocated for PSSCH : N_{RE}

$$N_{RE} = N'_{RE} \times n_{PRB} - N_{RE}^{SCI,1} - N_{RE}^{SCI,2} \quad (2.2)$$

Where :

- n_{PRB} is the number of RBs for the TB, equal to number of subchannel \times subchannel size.
- $N_{RE}^{SCI,1}$ is the number of REs used for PSCCH.
- $N_{RE}^{SCI,2}$ is the number of REs used for the 2nd-stage SCI.

Table 2.7 – N_{RE}^{DMRS} according DMRS Time Pattern [68]

Index	DMRS Time Pattern	N_{RE}^{DMRS}
1	{2}	12
2	{3}	18
3	{4}	24
4	{2}{3}	15
5	{2}{4}	18
6	{3}{4}	21
7	{2}{3}{4}	18

Step 3 : determines the N_{info}

$$N_{info} = N_{RE} \times R \times Q_m \times v \quad (2.3)$$

Where :

- R is Code Rate and Q_m is Modulation Order.
- v is the MIMO layer. In NR-V2X SL, v can be 1 or 2.

If $N_{info} \leq 3824$ we move to **Step 4a**, otherwise we move to **Step 4b**.

Step 4a : When $N_{info} \leq 3824$, determines the N'_{info} then TBS

$$N'_{info} = Max \left(24, 2^n \times \lfloor \frac{N_{info}}{2^n} \rfloor \right) \quad (2.4)$$

Where :

$$n = Max(3, \lfloor \log_2(N_{info}) \rfloor - 6) \quad (2.5)$$

Then, find the TBS which is smallest but bigger then N'_{info} in the Table G.1 on page 145.

Step 4b : When $N_{info} > 3824$, determines the N'_{info} then TBS

$$N'_{info} = Max \left(3840, 2^n \times round \left(\frac{N_{info} - 24}{2^n} \right) \right) \quad (2.6)$$

Where :

$$n = \lfloor \log_2(N_{info} - 24) \rfloor \quad (2.7)$$

• If $R \leq 1/4$ then

$$TBS = 8 \times C \times \lceil \frac{N'_{info} + 24}{8 \times C} \rceil - 24 \quad (2.8)$$

Where :

$$C = \lceil \frac{N'_{info} + 24}{3816} \rceil \quad (2.9)$$

• If $R > 1/4$ and $N'_{info} > 8424$

$$TBS = 8 \times C \times \lceil \frac{N'_{info} + 24}{8 \times C} \rceil - 24 \quad (2.10)$$

Where :

$$C = \lceil \frac{N'_{info} + 24}{8424} \rceil \quad (2.11)$$

• Otherwise $R > 1/4$ and $N'_{info} \leq 8424$

$$TBS = 8 \times \lceil \frac{N'_{info} + 24}{8} \rceil - 24 \quad (2.12)$$

2.1.5 . Service requirements and use cases for NR-V2X

2.1.5.1 . LTE-V2X

Generally, LTE-V2X in Release 14 is designed for basic safety for vehicular. It used mainly BSM, CAM which are periodic messages, and DENM which is aperiodic message.

In V2X communication, BSM and CAM communications facilitate the exchange of safety-related information. They provide data on the vehicle's location, speed, direction, acceleration, and other factors. BSM messages provide basic vehicle-related data and are periodically broadcast to surrounding vehicles. In contrast, CAM messages provide more comprehensive situational awareness information and enable direct communication between nearby vehicles. CAM messages enable advanced cooperative safety applications by facilitating direct cooperation and localized situational awareness between nearby vehicles. These messages are classified as non-real-time services.

On the other hand, DENM is an event-triggered (or aperiodic) message type used in V2X communication to provide critical real-time information about road hazards or unusual traffic conditions. It facilitates decentralized communication and notification of various environmental incidents, such as sudden braking, road construction, traffic congestion, weather conditions, and parking availability. The DENM message offers comprehensive event details such as type, location, levels of severity, duration, and instructions. By distributing this information between vehicles and infrastructure units, DENM messages improve situational awareness and facilitate well-informed decision-making for drivers and traffic management authorities. They contribute to enhanced traffic efficiency, safety, and comfort by facilitating quick reactions and adaptations to a dynamic V2X environment.

LTE-V2X in Release 14 by 3GPP has some constraints :

- The periodic broadcast messages carry payloads ranging from 50 to 300 bytes.
- The aperiodic messages can have payload up to 1200 bytes.
- Transmit up to 10 messages per second.
- The maximum allowable latency for V2V and V2P is 100 ms. For V2V pre-crash sensing, the maximum allowable latency is 20 ms.
- The latency for V2I communication is a maximum of 100 ms.

- The maximum latency of V2N is 1s.
- The maximum allowable relative speed between vehicles is 500 km/h. In addition, the absolute maximum speed for both V2V and V2P is 250 km/h, as is the case for the UE and RSU.
- Requirements relating to security, integrity, authorization, and privacy.

2.1.5.2. NR-V2X

Developed from LTE-V2X, NR-V2X R16 is designed for advanced safety [73] [74] [71]. It has higher throughput, higher reliability, wide-band ranging, and lower latency requirements compared to LTE-V2X.

The requirements depend on each use case, which is categorized into four use case groups : platooning, extended sensors, advanced driving, and remote driving.

a) Vehicles Platooning gives vehicles a chance to dynamically join together and travel as a group. In order to coordinate platoon operations, the leading vehicle periodically transmits data to all other vehicles within the platoon. Thus, the distance between vehicles will be significantly reduced. Platooning applications can support autonomous driving for member vehicles of the platoon. Table E.1 of Appendix E on page 140 shows the requirements of the scenarios for Vehicles Platooning use case.

b) Advanced Driving facilitates the operation of vehicles with either semi-automated or fully-automated capabilities. The advantages of utilizing this particular use case group include enhanced safety during travel, avoidance of collisions, and increased efficiency of traffic. It is considered that there will be a longer distance between vehicles. Every individual vehicle or RSU has the capability to share data that it has gathered from its own local sensors with other nearby vehicles. This enables the vehicles to coordinate their trajectories or maneuvers in order to work together. Furthermore, every automobile shares its driving intentions with other vehicles in its vicinity. We can find the requirements of the scenarios for Advanced Driving use case in Table E.2 of Appendix E on page 141.

c) Extended Sensors use case group facilitates the sharing of either raw or processed data that has been collected through local sensors or live video data. This sharing is between various entities such as vehicles, RSUs, devices

used by pedestrians, and V2X ASs. The act of sharing helps vehicles increase their perception of their surroundings beyond the capabilities of their own sensors, resulting in a more comprehensive understanding of their current surroundings. The requirements of this use case are shown in Table E.3 of Appendix E on page 142.

d) Remote Driving facilitates the operation of a vehicle situated in hazardous surroundings or for drivers who are unable to drive themselves. This is achieved through the use of a remote driver or a V2X application, which enables the remote control of the vehicle. In situations where variation is limited and routes can be predicted, such as in public transportation, it is feasible to employ cloud computing for driving purposes. Furthermore, it may consider the utilization of a cloud-based back-end service platform for this particular use case group. Table E.4 of Appendix E on page 142 illustrates the requirements of this use case.

Table 2.8 shows briefly the requirement ranges for all use case groups in summary. In general, SL range is maybe up to 1000 m, maximum throughput is 1 Gbps, shortest latency is 3 ms, maximum transmission rate is 100 messages per second, and maximum reliability is 99.999%.

Moreover, the 3GPP NR-V2X system needs to support relative lateral position accuracy of 0.1 m between vehicles and support high connection density for congested traffic.

Finally, the International's Standard J3016 [75] from Society of Automotive Engineers (SAE) defines six categories of automation and is commonly used by 3GPP to categorize these Levels of Automation (LoA).

- 0 – No Automation : At this level, no automation is present within the system. Human drivers perform all driving tasks, including V2X communication, without any assistance or automation.
- 1 – Driver Assistance : This level consists of fundamental driver assistance systems that provide particular functions to help drivers such as lane-keeping assistance or blind-spot monitoring in the context of NR-V2X. V2X communication can enhance these functions by offering extra knowledge about nearby vehicles, road conditions, or hazards.
- 2 – Partial Automation : Level 2 includes systems that can simultaneously control different aspects of the driving task, such as advanced

Table 2.8 – Summary requirement use case group

Use case group	Payload (Bytes)	Tx rate (Message/Sec)	Max end-to-end latency (ms)	Reliability (%)	Data rate (Mbps)	Min required communication range (meters) (130km/h relative speed)
Vehicles Platooning	50-6000	2-50	10-500	90-99.99	65	80-350
Advanced Driving	UL :450 SL :300-12000	UL :50 SL :10-100	3-100	90-99.999	UL :0.25-10 DL :50 SL :10-50	360-700
Extended sensors	1600	10	3-100	90-99.999	10-1000	50-1000
Remote Driving	-	-	5	99.999	UL :25 DL :1	-

driver assistance systems. However, the level's ability to react to external events is limited. The human driver must observe and react to certain external events and conditions by taking over control.

- 3 – Conditional Automation : At this level, the system is capable of handling the majority of driving activities under certain circumstances; however, the driver must be available to take control when necessary. Level 3 automation allows the driver to cease actively observing their surroundings, but it still necessitates that they be ready to take control when the system indicates so. In NR-V2X, this can include coordinated vehicle movement within certain circumstances, including platooning or cooperative merging.
- 4 – High Automation : Level 4 automation allows the system to carry out the majority of driving tasks and control the vehicle in specific situations without any requirement for the driver to be present. Nonetheless, a human driver has the ability to take charge if necessary. In the context of NR-V2X, level 4 automation may include advanced cooperative driving.

- 5 – Full Automation : The system can perform all driving tasks in all conditions without human interference in this level. It consists of completely autonomous vehicles that are capable of operating in any environment or transportation scenario, including urban settings.

2.1.6 . Resource allocation modes

In R16 NR-V2X, two new modes are defined : Mode 1 (in coverage) and Mode 2 (in or out of coverage) [71], as illustrated in the Figure 2.21. The latter support Unicast, Groupcast and Broadcast communication on NR-PC5 interface. Note that these two modes are not the same as Mode 1 and Mode 2 in Release 12 proposed for D2D.

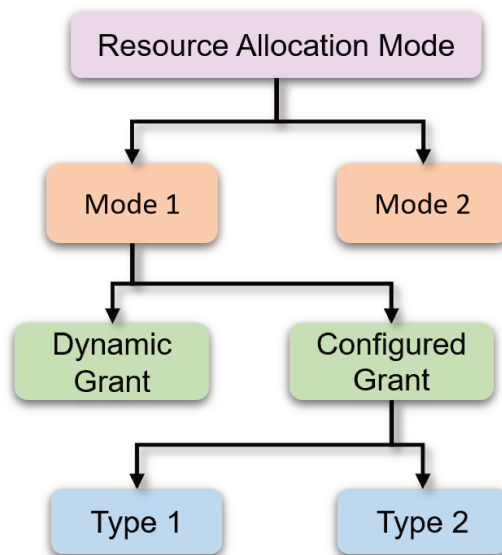


Figure 2.21 – Resource Allocation mode

2.1.6.1 . Mode 1

In Mode 1 of NR-V2X, the gNB is responsible for managing the allocation of wireless resources when UEs and vehicles are present within the macrocell coverage area. Mode 1 provides two sub-modes, namely Dynamic Grant (DG) and Configured Grant (CG), for dealing with aperiodic and periodic message types.

a) Dynamic Grant (DG)

DG is suitable for aperiodic message type. To do that, UE sends a Scheduling Request (SR) to the gNB using Physical Uplink Control Channel (PUCCH) whenever it has data to transmit. SR is processed at the MAC layer. The gNB analyzes SR and responds with Downlink Control Information (DCI) format 3_0 over Physical Downlink Control Channel (PDCCH). DCI contains time/frequency resource assignment and some other information for one and up to two re-transmissions of a TB (if HARQ is enabled).

b) Configured Grant (CG)

In DG, UE needs to request the resource from gNB for each TB, leading to degradation of delay and overload of signaling which consumes resources and energy. Thus, CG is designed to solve these issues. The gNB has the ability to allocate a set of SL resources to a UE for transmitting several TBs. Therefore, CG is suitable for periodic traffic.

CG proceeds as follows : First, the UE sends over the Uplink (UL) interface to gNB station a UEAssistanceInformation[57] message containing the size, time, periodicity and QoS requirement of the TB. Then, gNB uses this SL Traffic Pattern to calculate the CG, sends to the UE via DCI format 3_0 on PDCCH.

Note that maximum 8 CG profiles for an UE can be defined for provision for different services, traffic types. CG supports periodicity from 1 to 1000 ms and maximum 3 SL resources for only one new TB and retransmission.

CG is divided into two types : CG Type 1 and CG Type 2. The difference between them consists in using immediately or not the resources once a UE receives the grant from the gNB. The UE can utilize the CG Type 1 right after receiving it. On the contrary, UE needs to receive activation or deactivation signaling from gNB via DCI format 3_0 before using or ending a CG Type 2. The resources assigned by a CG Type 1 are exclusively reserved for one UE. However, the resources assigned for a non-active CG Type 2 can be assigned to other UEs. Hence, the signaling traffic in CG Type 2 is higher compared to Type 1.

2.1.6.2. Mode 2

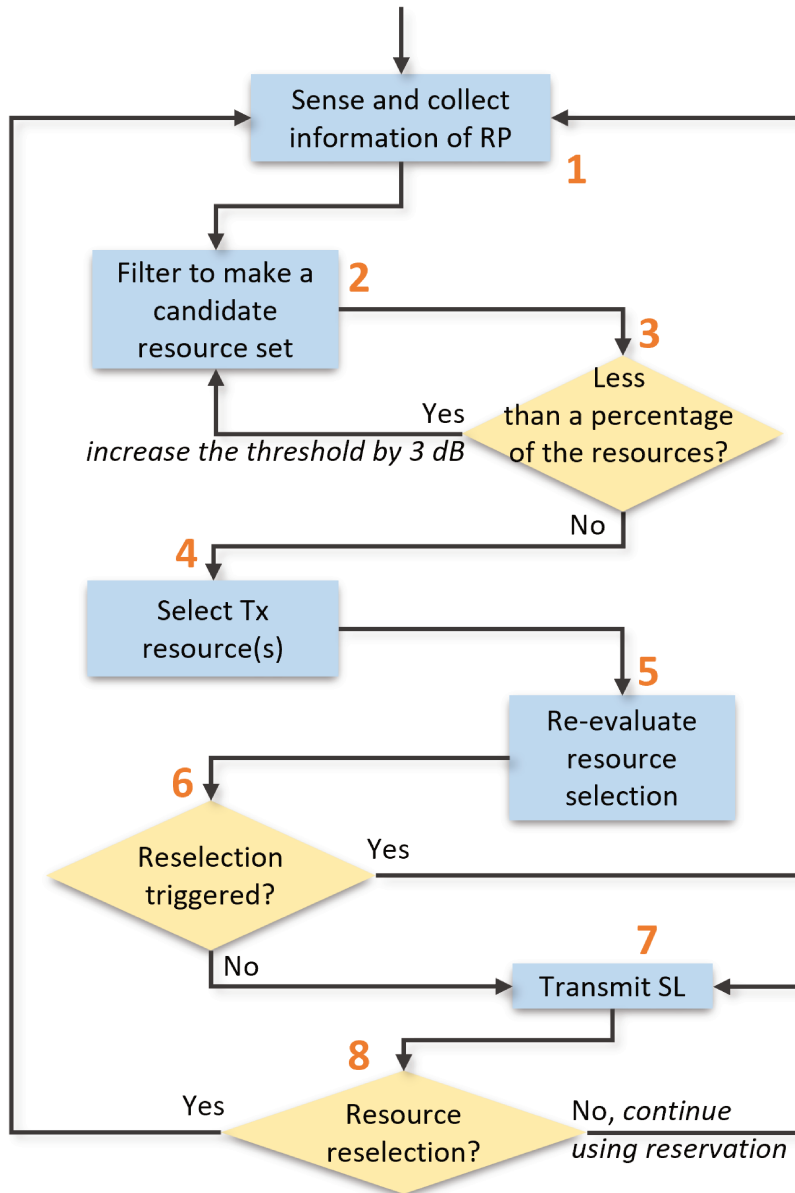


Figure 2.22 – Procedure of Mode 2 resource allocation

Mode 2 [71][62][68][57] can be considered as Autonomous resource selection. This mode can be used in or out of gNB macrocell that UEs need to monitor themselves the RP to find one or more suitable resources for its SL transmission(s). Figure 2.22 describes how Mode 2 works.

For example, in Figure 2.23, at time n , a UE is triggered about having packets to be transmitted (step 1 in Figure 2.22). The UE has already monitored the RP in the Sensing Window duration. This Sensing Window is calculated by $T_0 - T_{proc,0}$.

Note that duration $T_0 = 100$ ms (recommended for aperiodic traffic) or 1100 ms (recommended for periodic traffic), and duration $T_{proc,0}$ is 1, 1, 2, or 4 slot time for a SCS of 15, 30, 60 or 120 kHz respectively before time n (see sl-SensingWindow in [57]).

To be more precise, this Sensing Window lasts from [1100ms or 100ms] to [1ms or 0.5ms] before time n . This period is called Sensing Window in which a UE listened, decoded 1st-stage SCI from every transmitter UE around. In doing so, a UE can identify the occupied resources by its neighbors. Moreover, a UE can also detect and measure the SL-Reference Signal Received Power (RSRP) of either PSSCH-RSRP or PSCCH-RSRP in this period (see sl-RS-ForSensing [57]).

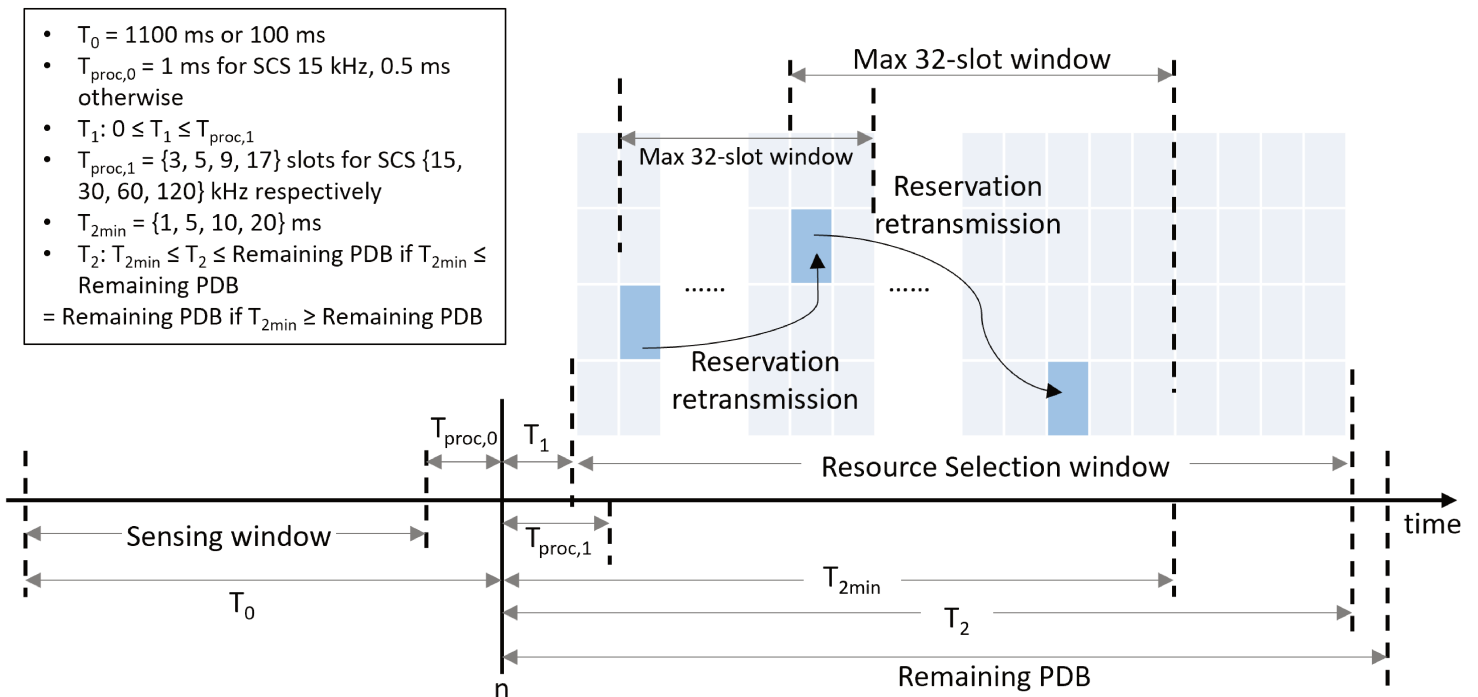


Figure 2.23 – Example of timeline of sensing and resource selection procedure triggered at time n .

Thus, the sensing UE gets M_{total} candidate resources within a Resource Selection Window. The latter starts at $n + T_1$ and ends at $n + T_2$. T_1 is between 0 and $T_{proc,1}$. The duration $T_{proc,1}$ is determined as 3, 5, 9 or 17 slots for a SCS of 15, 30, 60 or 120 kHz respectively. T_2 is between $T_{2min} \leq T_2 \leq RemainingPDB$ (in slots). In case $T_{2min} > RemainingPDB$, T_2 is equal to Remaining Packet Delay Budget (PDB). Additionally, T_{2min} is set to 1 ms, 5 ms, 10 ms, or 20 ms. Consequently, mode 2 can guarantee 1 ms minimum latency compared to 10 ms in LTE-V2X mode 4.

Next, the UE then selects resources from M_{total} candidates located in the Resource Selection Window. Resources that have not been monitored in the Sensing Window period are excluded due to the HD, sensing is not possible. In addition, all resources reserved by other transmitting UEs are excluded also.

The sensing UE also filters resources in the M_{total} with SL-RSRP above a threshold, which is determined by the priorities of the traffic of the sensing and transmitting UEs (step 2 in Figure 2.22). The remaining candidate resources if less than a percentage of the M_{total} which has possible value 20%, 35% or 50% depend on the traffic priority, the sensing UE increases the RSRP by 3 dB and filters the resources in the M_{total} again (step 3 in Figure 2.22).

Finally, the sensing UE randomly selects a resource in the remaining candidate resources (step 4 in Figure 2.22). If HARQ is enabled, the UE can select up to two more resources in the window of maximum 32 slots between two successive retransmissions within the remaining candidate resources, as illustrated in the Figure 2.23.

Furthermore, if UE transmits this TB periodically, the resources can be allocated periodically each Resource Reservation Interval. It lasts [0 :99], 100, 200, 300, 400 500, 600, 700, 800, 900, 1000 ms, and must be bigger than PDB. UE also uses the Resource Reservation Interval to get the Re-selection Counter as follows : in case Resource Reservation Interval \geq 100 ms, this counter is randomly set within the interval [5, 15]. If not, set within the interval $[5 \times R, 15 \times R]$ where :

$$R = \frac{100}{\max(20, \text{Resource Reservation Interval})}$$

Once the Sensing Window duration is over, maybe there are late-arriving SCIs due to an aperiodic higher-priority service from a transmitter. For this reason, sensing UE can decide whether to repeat the sensing step to check if the selected resource is still available during a period x (step 5-6 in Figure 2.22). This stage is called Re-evaluation, as illustrated in the Figure 2.24, and is left to UE implementation. If we consider time m is the slot time of the first reserved resource, sensing UE senses more until the time maximum $m - T_3$. The duration T_3 is equal to $T_{proc,1}$, and x is the period that sensing UE can select again candidate resources. In the Figure 2.24, z is the point of time sensing UE to do the re-evaluation to find other resources.

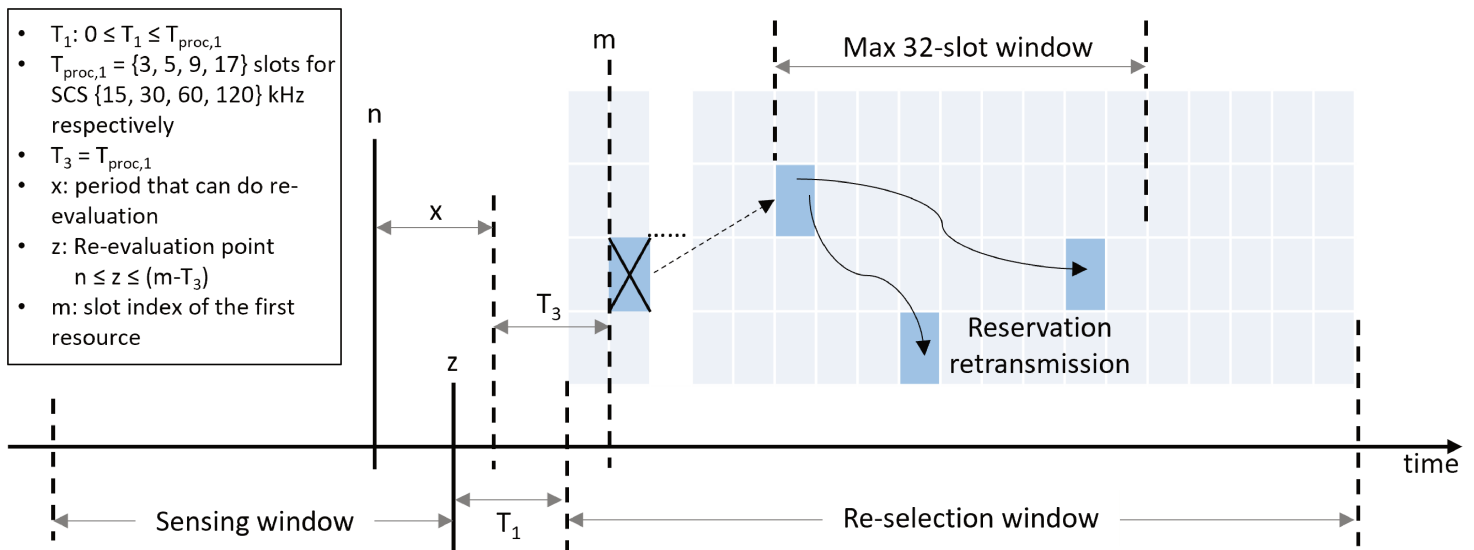


Figure 2.24 – Example of timeline of sensing and resource selection procedure triggered at time n , with re-evaluation at time z before $(m - T_3)$.

An important novel feature in mode 2 NR-V2X compared to mode 4 in LTE-V2X is preemption which is useful for aperiodic traffic. A UE re-selects (step 6-8 in Figure 2.22) the resources already reserved if another transmitter UE with higher priority traffic and the SL-RSRP is above the exclusion threshold wants to transmit in any of them. A UE does not proceed preemption later than time T_3 .

2.1.7 . QoS NR-PC5

The UE can be set with default PC5 QoS parameters (shown in Figure 2.25) to handle V2X communication over NR-PC5. Table 2.9 defines a standardized set of PC5 5G QoS Indicators, also known as (PQI). The Per-flow QoS model should be used for NR-based communication in unicast, groupcast, and broadcast modes over PC5. An example mapping of Per-flow QoS model for NR-PC5 is given in Figure 2.26.

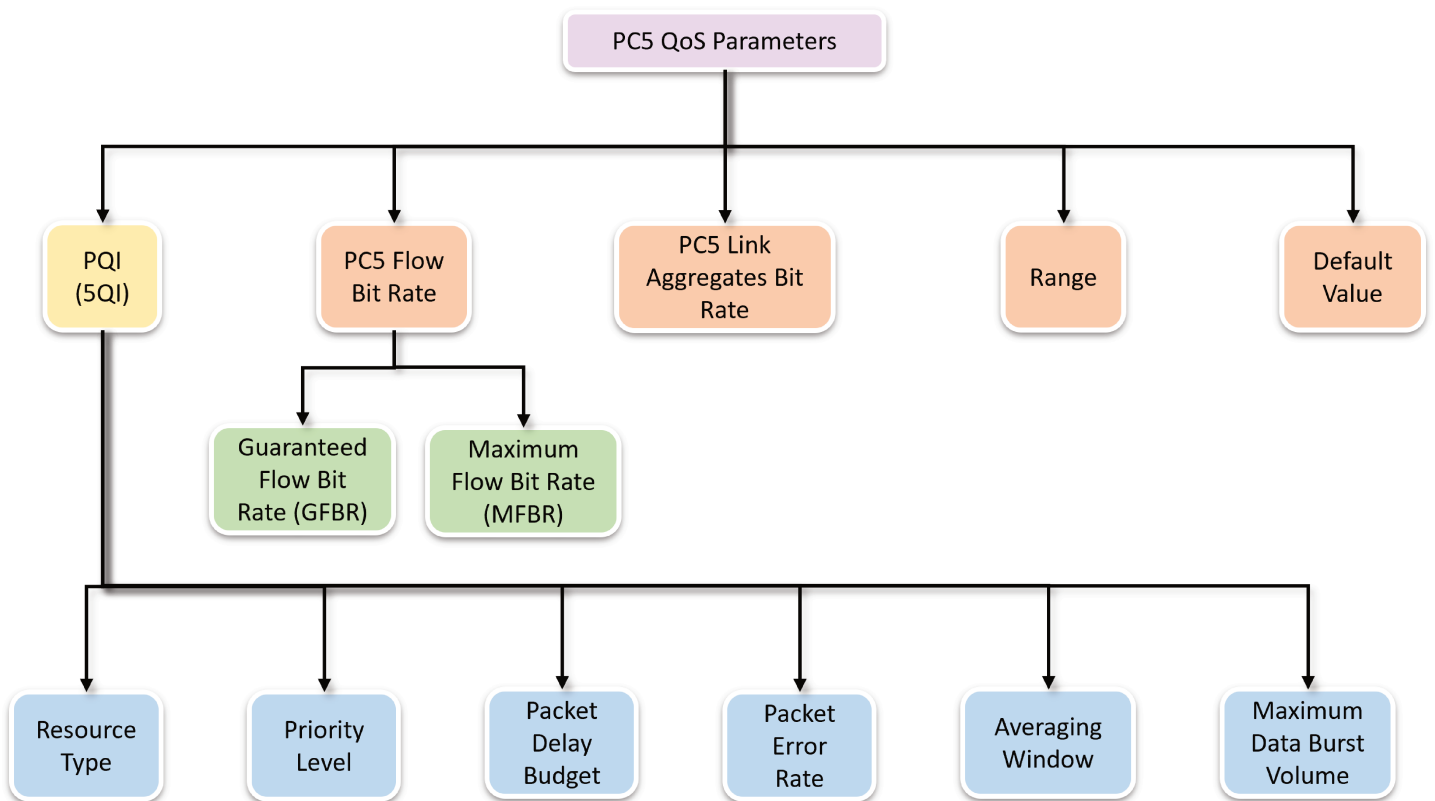


Figure 2.25 – NR-PC5 QoS parameters and characteristic

2.1.7.1 . PC5 QoS parameters

- PC5 5G QoS Identifier (PQI) : is a special 5G QoS Identifier (5QI) used for SL. PQI is used as a reference to PC5 QoS characteristics which is presented in Table 2.9. For example, PQI value 21 corresponds to Priority 3, PDB 20 ms, etc.
- PC5 Flow Bit Rates : is only apply for Guaranteed Bit Rate (GBR) Flows. It is used for bit rate control on PC5 reference point over the Averaging

Time Window. The bit rates need above the Guaranteed Flow Bit Rate (GFBR) value and up to the Maximum Flow Bit Rate (MFBR) value.

- PC5 Link Aggregates Bit Rate : is only used for unicast communication and apply on non-GBR flows. Each PC5 unicast link is associated with Per Link Aggregate Maximum Bit Rate (PC5 LINK-AMBR) that limits the aggregate bit rate that can be expected to be provided across all Non-GBR QoS Flows.
- Range : is only used for groupcast communication. When the receiving UEs are not within the Range specified distance from the transmitting UE, the communication is best effort. The UE is configured with the maximum Range value it can use for a particular V2X service. A V2X service may request a different range value but cannot exceed the maximum Range value.
- Default Value : will be used if the corresponding PC5 QoS parameter is not provided.

2.1.7.2 . PC5 QoS characteristics

PC5 QoS characteristics together with PQI given by upper layer can override the standardized.

- Resource type : It consists three resource types : Guaranteed Bit Rate (GBR), Delay Critical - Guaranteed Bit Rate (DC-GBR) and Non-GBR.
- Priority Level : eight possible values (from 1 to 8) and lower number meaning higher priority.
- Packet Delay Budget (PDB) : it is an upper bound of time that a packet may be delayed between the UEs.
- Packet Error Rate (PER) : Define an upper bound for packet losses.
- Averaging Window : Represents the duration over which the GFBR and MFBR shall be calculated. Each DC-GBR and GBR resource type is mapped to an Averaging window.
- Maximum Data Burst Volume (MDBV) : is the largest amount of data that the PC5 reference point is required to serve within a period of PDB of the PQI. This value is only applied on DC-GBR.

Table 2.9 – Standardized PQI to QoS characteristics mapping

PQI value	Resource Type	Priority	PDB	PER	MDBV	Average Window
21	GBR *	3	20 ms	10^{-4}	N/A	2000 ms
22		4	50 ms	10^{-2}	N/A	2000 ms
23		3	100 ms	10^{-4}	N/A	2000 ms
55	Non-GBR	3	10 ms	10^{-4}	N/A	N/A
56		6	20 ms	10^{-1}	N/A	N/A
57		5	25 ms	10^{-1}	N/A	N/A
58		4	100 ms	10^{-2}	N/A	N/A
59		6	500 ms	10^{-1}	N/A	N/A
90	DC-GBR *	3	10 ms	10^{-4}	2000 bytes	2000 ms
91		2	3 ms	10^{-5}	2000 bytes	2000 ms

* : GBR and DC-GBR PQIs can only be used for unicast PC5

2.1.7.3 . PC5 QoS Flow

For the NR-V2X PC5, a PC5 QoS Flow identified by different PC5 QoS Flow Identifiers (PFI)s is associated with a PC5 QoS Rule and the PC5 QoS parameters. The UE may be configured with a set of default PC5 QoS parameters to use for the V2X service types.

When a service data packet or request from the V2X application layer is received, the UE determines if there is any existing PC5 QoS Flow matching the service data packet or request, i.e. based on the PC5 QoS Rules for the existing PC5 QoS Flow(s).

If there is no PC5 QoS Flow matching the service data packet or request, the V2X layer determines the PC5 QoS parameters based on the V2X service type or V2X Application Requirements (e.g. priority requirement, reliability requirement, delay requirement, range requirement). Then, UE check among existing PC5 QoS Flow, is there any adapt that PC5 QoS parameters or not. If

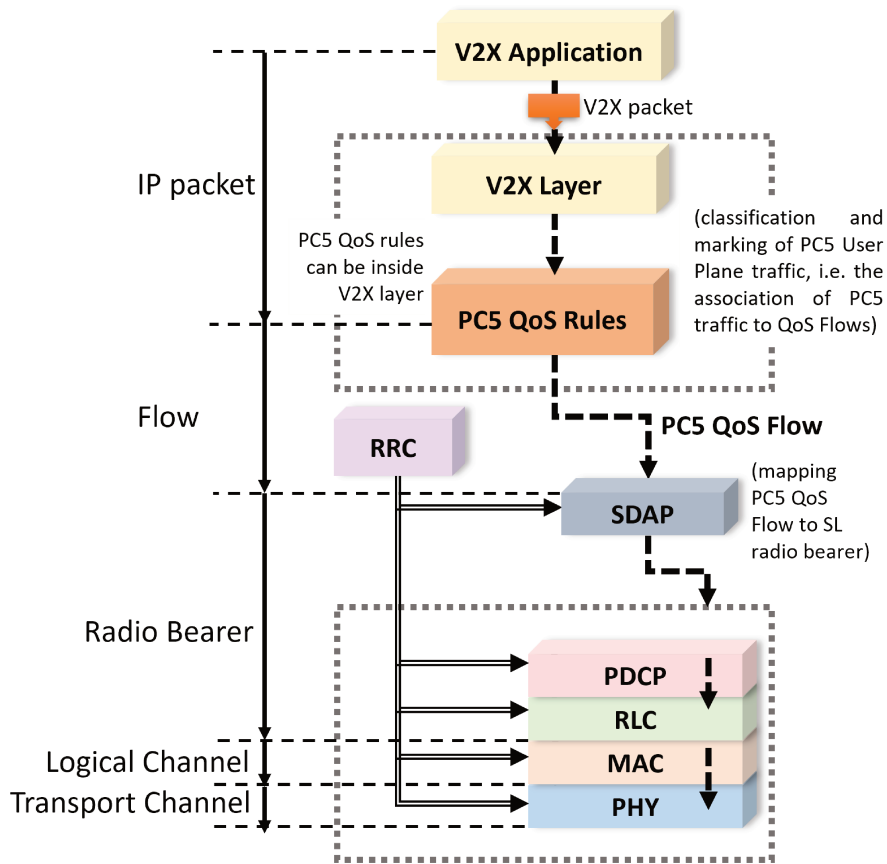


Figure 2.26 – NR-PC5 Per-Flow QoS Model

not, the UE creates a new PC5 QoS Flow for that PC5 QoS parameters, assigns a PFI and other information. Otherwise, UE updates the PC5 QoS Flow which fit for that that PC5 QoS parameters.

We must note that the PC5 QoS Flow is the finest granularity of QoS differentiation in the same destination. User Plane traffic with the same PFI receives the same traffic forwarding treatment and the PFI is unique within a same destination.

In Figure 2.26, IP Packets from V2X Application are categorized into different QoS Flow depend on their constraints, requirements from their V2X service where they came from. A UE can have maximum 2048 QoS Flows for NR-V2X SL communication. In SDAP sublayer 2, different flows are map to different SL-DRBs. Multiple PC5 QoS Flows can be mapped into one SL-DRB. The SL-DRB serves for User Plane. Another type of Radio Bearer served for Control Plane is called SL-SRB. The SL-SRB0 is utilized to send the PC5 signa-

ling message during unicast PC5-RRC connections, before the establishment of the signaling security procedure. The SL-SRB1 is sent for transmitting messages to establish security. After establishing security, the SL-SRB2 is utilized for transmitting signaling messages. Finally, the SL-SRB3 is used for transmitting the PC5-RRC signaling, which is protected and sent only once security is established. The SL-SRB has higher priority compare with SL-DRB, and the SL-SRB0 has the highest priority among SL-SRBs. In MAC sublayer, Radio Bearers are mapped to LC then TC in PHY layer to put into TB for sending to the receiver(s).

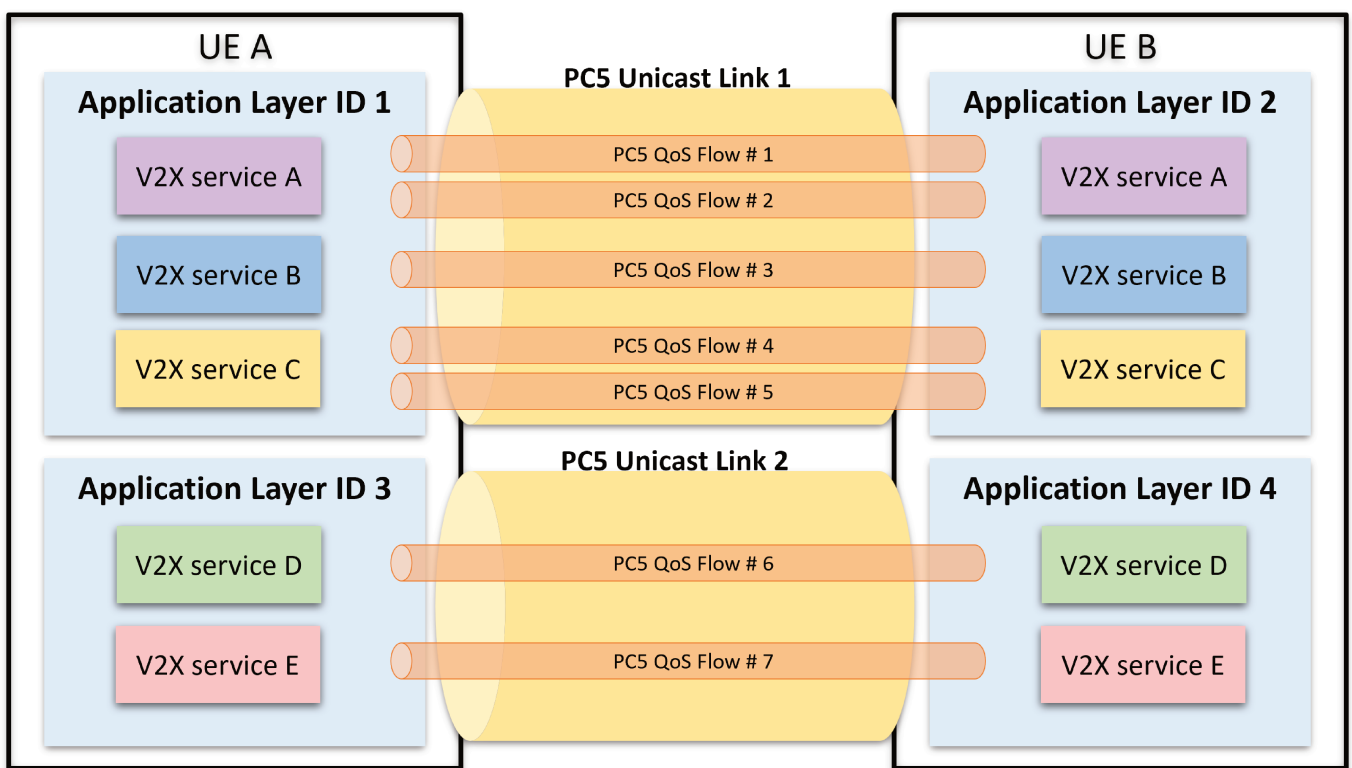


Figure 2.27 – PC5 QoS Flow in V2X Application Layer point of view

In Figure 2.26, we demonstrate the vertical transformation from IP Packets at the V2X Application layer to TB at the PHY layer. Next, the horizontal flows and Unicast Link between vehicles in SL are illustrated in Figure 2.27. On each vehicle, there are multiple V2X applications, and each has its own Application Layer ID. One or more V2X services may be used by a V2X application. Through one or more PC5 QoS Flows, a V2X service in one vehicle connects to the same service type in another vehicle. One and only one PC5 Unicast Link is used

to connect a V2X application on one vehicle to a V2X application on another vehicle. One vehicle can have multiple PC5 Unicast Links to another vehicle (same destination).

2.2 . NR-V2X resource allocation (RA) problematic and approaches

While NR-V2X is the most advanced technology for C-ITS, resource allocation issues still exist. Due to the dynamic nature of the communication environment and the restricted resources available, the resource allocation in NR-V2X faces a number of issues. The following are some issues of NR-V2X's resource allocation :

- **Power** : The transmission and reception of data in NR-V2X communication require energy resources. Power consumption problems are caused by this, particularly for equipment with limited resources like sensors, moving cars, or cellphones carried by pedestrians with low battery capacity. Efficient resource allocation must take power impacts into account to maximize device lifespan and minimize vehicle or infrastructure energy consumption.
- **Security and privacy** : V2X systems communicate and share private data, such as communication messages, location information, and vehicle identification. In order to ensure security, resource allocation systems must take into account issues such as authentication, data integrity, and confidentiality to prevent unauthorized access, spoofing, or data leaks.
- **Interference and congestion** : In V2X communication, several vehicles and infrastructure components are simultaneously sending and receiving data, which may cause interference and congestion. A high-density scenario is another example that can also lead to this issue. In order to minimize interference, maximize the utilization of the available bandwidth, as well as ensure reliable and efficient communication, effective resource allocation is necessary.
- **Scalability** : As the number of connected vehicles and infrastructure components increases, the resource allocation becomes more com-

plex. Managing scalability can be difficult when the system must handle numerous communication requests, effectively allocate resources, and manage interference. Creating resource allocation algorithms that can handle the increasing number of V2X devices while keeping performance is a big challenge.

- **Coexistence** : NR-V2X communication must coexist with other wireless technologies that operate in the same spectrum, such as DSRC and LTE-V2X. Effective resource allocation strategies are necessary to manage interference and ensure stable communication in an existence of other wireless systems, while also ensuring fair and efficient spectrum sharing.
- **Dynamic network topology** : Traffic network is changed due to the movement of vehicles in and out of communication range. The density of vehicles may also vary across different areas and times. With the goal to ensure efficient use of resources and reliable communication when dealing with unpredictable network topology, it is necessary for resource allocation to adapt to the dynamic environment.
- **Out-of-coverage** : The term "out-of-coverage" mode refers to cases when a device, such as a vehicle or infrastructure device, faces an absence of connectivity with the cellular network. The allocation of resources faces a big challenge due to the necessity for decentralized decision-making, cooperative behavior among devices, and efficient utilization of limited resources in a distributed manner.
- **QoS requirements** : V2X applications have various QoS requirements based on their characteristics. Applications that are safety-critical, such as collision warnings, require communication that is highly-reliability and low-latency. However, non-safety applications, such as traffic information services, can have higher latency and lower reliability. Assigning resources to fulfill the varied QoS demands of various applications can be difficult, which requires effective scheduling and prioritization methods.

Efforts in research and development are ongoing to address problematic aspects in NR-V2X communication systems. These efforts focus on developing efficient resource allocation algorithms, optimizing power consumption, en-

ensuring security and privacy, promoting interoperability, and addressing scalability etc.

Since the standardization of NR-V2X by the 3GPP, there have been limited research studies in the literature on resource allocation in NR-V2X technology. The papers [76], [77], [78] and [79] concentrate on an energy approach to decrease energy usage of devices. Meanwhile, studies from [80], [81], [82], [83], [84] and [85] examine the autonomous resource allocation mode (mode 2). Further research, as in [86] and [87], is being done on mmWave technology, which is expected to be standardized in the future. Recently, several studies have utilized deep learning or reinforcement learning to enhance resource allocation efficiency. These studies can be found in [88], [89], [90], [91], [76] and [92]. Scalability issue is studied by Lucas-Estañ et al. [93] [94]. In addition, V2X services such as DENM or CAM messages, basic safety services, URLLC services, aperiodic and periodic can be considered as another option. For example, [81] and [95] work on aperiodic services, Yan et Härrri [96] focus on URLLC service. Romeo et al. [95] [97] [98] investigate on DENM message. Several papers perform an inspection on NR-V2X resource allocation or comparison with LTE-V2X resource allocation, such as [83] and [99]. Ali et al. [83] evaluate the impact of the primary parameters of the Semi-Persistent Scheduling (SPS) algorithm on the overall system performance. The authors consider various parameters, including NR flexible numerologies, maximum resources per reservation, MCS, and resource selection window in this study. Sehla et al. [99] offer a thorough explanation and survey of Resource Allocation in LTE-V2X (modes 3 and 4) and NR-V2X (modes 1 and 2) technologies. These studies offer information and metrics to the research community for proposing their proposals.

Unfortunately, there is limited study on the impact of numerologies on V2X use cases. The 5G NR-V2X technology is designed to accommodate a changing environment where factors such as traffic network topology, V2X services, density, and radio state etc, change over time. Hence, it is very important to select the suitable numerology, taking into account the surrounding environmental conditions, before starting the radio resource allocation process. Selecting a suitable numerology for a particular V2X use case is still an open issue. State-of-the-art on numerology in NR-V2X will be described in the following section.

2.3 . State-of-the-art on numerology in NR-V2X

Regarding the literature, there are few research works on 5G NR numerology (e.g. [100][101][102][103][104]) and even fewer on its impact on V2X use cases.

The research of Khabaz et al. [105] aims to analyze the impact of 5G numerologies on V2X communications. The study specifically examines the performance of V2X applications (safety V2V and infotainment) and the PHY layer. The paper offers suggestions for choosing an appropriate numerology based on the scenario by applying simulations (using Simu5G, SUMO, and the 5G Vienna Link Level Simulator) and analysis. The authors observed that choosing a suitable numerology depends on V2X requirements and is a trade-off between the stringent requirements of V2X applications, the Inter-Carrier Interference (ICI) problem, and the Inter-Symbol Interference (ISI) problem. The work addresses the open issue of selecting a suitable numerology for V2X communications and provides significant perspectives on the domain. However, Khabaz et al. [105] test only with bandwidth 5 MHz (3GPP supports maximum 40 MHz for n47), without consider different subchannel size.

Wang et al. [106] provide a comparison of physical layer performance between LTE-V2X and NR-V2X using Block Error Rate (BLER) and Signal to Noise Ratio (SNR) values. Furthermore, the author examined the effect of numerologies on the PHY layer of NR-V2X. Only BLER and SNR are taken into account, while other factors are not referenced. Therefore, the outcome is weak in demonstrating the worth of 5G NR technology.

Autonomous resource allocation mode in NR-V2X (mode 2) is addressed by Ali et al. [107]. The study analyzes the impact of numerology on throughput, inter-packet reception delay, and packet reception ratio in a highway scenario using the NS3 simulator. Furthermore, the authors investigate the impact of communication range, transmit power, and packet size. Nevertheless, the authors did not take NR-V2X application requirements into account. They only study only basic safety periodic traffic on PHY layer without various subchannel size.

This autonomous resource allocation approach is also addressed by Todisco et al. [80]. The WiLabV2Xsim simulator is introduced by the authors as an ex-

tension of LTEV2Vsim. The author investigates the performance of 5G NR-V2X Mode 2 in a highway setting with varying density and data traffic patterns. The research highlights the impact of 5G NR-V2X's new features, including NR's flexible SCS. Nevertheless, the study only focuses on periodic safety services, limited bandwidth as in LTE-V2X. Meanwhile, the 5G NR-V2X technology is designed for different scenarios, including advanced driving, platooning, extended sensors, and remote driving. The advantage is a larger bandwidth of 40 MHz and various subchannel sizes.

Another two researches on Mode 2 is done by Valgas et al. [108] and Campolo et al. [109]. The study evaluates the impact of NR numerology with varying speeds in [108]. However, the simulations rely on LTE-V2X parameters. The authors of [109] examine the utilization of NR numerology in a highway context, where periodic CAM messages are sent by varying vehicle speeds. Unfortunately, The simulations are performed using LTEV2Vsim, a simulator specifically designed for LTE-V2X. [108] and [109] have both reached the conclusion that a higher numerology results in a shorter Transmission Time Intervals (TTI) length, which is important for enhancing reception ratio and delay performance. That conclusion has been confirmed in [110]. Ali et al. [110] deploy the 5G-LENA simulator, which respects to the 3GPP 5G NR standard, for investigating periodic services in platooning on highways.

Lucas-Estañ et al. [93] utilize a different approach. The authors investigate how numerology impacts the performance of the Radio Access Network (RAN). One vehicle will transmit UL data to the gNB, which will then send it Downlink (DL) to other vehicles. This process is known as Vehicle-to-Network-to-Vehicle (V2N2V). The research analyzes the latency, reliability, and spectrum efficiency achievable at the RAN for a cooperative lane change service in a highway scenario. Nonetheless, vehicles have the capability to transmit data directly through V2V (sidelink) communication, which can help to reduce the overhead of the system.

An interesting algorithm namely Priority and Satisfaction-based Resource Allocation algorithm with Mixed Numerology, can be called PSRA-MN, is proposed by Khabaz et al. [111]. There is insufficient research that addresses the allocation of resources, taking into account the varying requirements and categorizations of different V2X applications. Therefore, the authors propose PSRA-MN. The algorithm is divided into two phases. The first phase is to de-

side the suitable numerology based on the application requirements, channel conditions, and vehicle speed. In the second phase, safety traffic is prioritized through resource scheduling. The resources that are left after allocating for safety are distributed in the most efficient way for non-safety services in order to maximize the average satisfaction rate. Nevertheless, the author studied periodic safety traffic. It will be more interesting if the NR-V2X use case scenarios are taken into account, especially the URLLC aperiodic service.

Summary State-of-the-art of numerology in NR-V2X is shown in Table 2.10.

Table 2.10 – State-of-the-art of numerology in NR-V2X

Paper	Scenario	Approach	Simulator	Performance Metrics
[105]	Rural, Urban	Impact of 5G numerologies on PHY and application layer	Simu5G, SUMO, 5GVLL	Latency, Throughput, BER
[106]	N/A	Compare PHY LTE-V2X and NR-V2X	N/A	BLER, SNR
[107]	Highway - Mode 2	Investigate the performance of the NR V2X network under different network settings	NS-3	Packet Reception Ratio, Packet Inter-reception time, Throughput
[80]	Highway - Mode 2	Analyze 5G-V2X Mode 2	WiLabV2Xsim	Packet reception ratio, end-to-end delay, packet inter-reception
[108]	Highway - Mode 2	Analyze the performance of DENM co-existing with CAM traffic over the 5G-V2X mode 2	LTEV2Vsim	Reliability, average packet reception ratio
[109]	Mode 2	study the performance of the LTE-V2X Mode 4 augmented with the NR flexible numerology	LTEV2Vsim	Packet reception ratio, update delay
[110]	Highway, Platoon, Mode 2	study the impact of the numerology and the size of the resource selection window in mode 2	NS-3 5G-LENA	Packet Inter-reception Delay, Cumulative Density Function
[111]	Urban Macrocell, Mode 1	Propose PSRA-MN that can choose SCS, prioritize safety traffic in RA	Simu5G and SUMO	Average allocation rate, average satisfaction rate, average end-to-end delay

2.4 . Conclusion

This chapter present the context of our research, from overview of 5G 3GPP NR-V2X to the state-of-the-art on numerology.

Regarding to the literature review on the numerology of NR-V2X, we concluded that most of the research in the literature focus on studying the impact of the numerology on the system's performance, particularly at the PHY layer. In addition, there is limited research on resource allocation for various vehicular applications. There are various types of traffic, scenarios, and services with different requirements. The scheduler allocates a PHY resource to transmit data for a transmitter vehicle. This resource is determined by a slot and subchannel(s). Numerology impacts the duration of a slot and the size of the subchannel's bandwidth. Selecting a numerology and subchannel size in PHY is a very challenging task. Then, in order to efficiently allocate resources to vehicles, a resource allocation algorithm considers factors such as service requirements, density, radio condition, scenarios, and V2X service pattern.

Table 2.11 shows briefly the number of PHY resources in terms of SCS, BW, and subchannel size. Note that this PHY resource is one slot and one subchannel. It is shown as a pair value. When $SCS = 15$ kHz, $BW = 10$ MHz, and subchannel = 10 RBs, for example, the pair (5, 2) shows that we have 5 resources but lose 2 RBs that we cannot use.

There is a possibility that resource allocation cannot adjust to the V2X requirements due to the dynamic nature of the vehicular environment. At that point, changing the subchannel size and numerology can make the resource allocation better meet the requirements of V2X. This is the main issue that we will address in the first contribution in the following chapter.

Table 2.11 – Number of subchannels related to SCS and subchannel size for n47

SCS	BW	Available PRBs	Subchannel size (PRBs)							
			10	12	15	20	25	50	75	100
Number of subchannels, the remaining PRBs										
15	10	52	5, 2	4, 4	3, 7	2, 12	2, 2	1, 2	-	-
	20	106	10, 6	8, 10	7, 1	5, 6	4, 6	2, 6	1, 31	1, 6
	30	160	16, 0	13, 4	10, 10	8, 0	6, 10	3, 10	2, 10	1, 60
	40	216	21, 6	18, 0	14, 6	10, 16	8, 16	4, 16	2, 66	2, 16
30	10	24	2, 4	2, 0	1, 9	1, 4	-	-	-	-
	20	51	5, 1	4, 3	3, 6	2, 11	2, 1	1, 1	-	-
	30	78	7, 8	6, 6	5, 3	3, 18	3, 3	1, 28	1, 3	-
	40	106	10, 6	8, 10	7, 1	5, 6	4, 6	2, 6	1, 31	1, 6
60	10	11	1, 1	-	-	-	-	-	-	-
	20	24	2, 4	2, 0	1, 9	1, 4	-	-	-	-
	30	38	3, 8	3, 2	2, 8	1, 18	1, 13	-	-	-
	40	51	5, 1	4, 3	3, 6	2, 11	2, 1	1, 1	-	-

3 - A FLEXIBLE NUMEROLOGY CONFIGURATION FOR EFFICIENT RESOURCE ALLOCATION IN 3GPP V2X 5G NEW RADIO

Contents

3.1	Introduction	63
3.2	Problem formulation	64
3.2.1	System description	64
3.2.2	V2X application and traffic model	64
3.2.3	PHY layer	65
3.2.4	Mobility environment	66
3.2.5	Problem formulation	68
3.2.6	Performance evaluation parameters	70
3.3	Proposal	72
3.3.1	Adaptive PHY layer Configuration (APC)	73
3.3.2	Resource Allocation Scheduler	75
3.4	Performance Evaluation	79
3.5	Conclusion	83

3.1 . Introduction

The preceding chapter provided a brief description of the literature review on NR-V2X and numerology. In this chapter, we will present the Adaptive PHY Layer Configuration (APC) algorithm as our first contribution. The objective of our proposal is to optimize the ETP. This APC enables the telecommunications operator to adjust the PHY layer configuration to manage radio resources more efficiently in a 5G NR-based system. The scheduler, with the help of the Adaptive Expected Serving Packet Rate (AESPR) algorithm (in order to avoid starvation issue) and pre-emption mechanism, will assign TBs to V2X packets. If the scheduler fails to adapt to the V2X requirement due to factors such as high mobility, density, radio channel state, or enabling/disabling of V2X services, APC will be triggered to seek out a new PHY Layer configuration.

This chapter is organized as follows. Next section 3.2 briefly explains system description and problem formulation. Relying on 3GPP NR-V2X compliant design, a robust RA scheme using a dynamic numerology is proposed in section 3.3. Section 3.4 presents our methodology and the obtained simulations results. Finally, section 3.5 concludes this chapter.

3.2 . Problem formulation

3.2.1 . System description

We consider a single 3GPP R16 5G NR cell. The latter serves a set of transmitter vehicles denoted v . We assume that all vehicles operate in mode 1 DG, broadcast mode communication, and scheduled by gNB.

3.2.2 . V2X application and traffic model

The system supports three types of V2X applications denoted by A_1 , A_2 , and A_3 .

- Service A_1 refers to Emergency Trajectory Alignment service (EmerTA). This type of service is time-critical constrained.
- Service A_2 corresponds to Cooperative Collision Avoidance service (CoCA). It is less critical than those of service A_1 but still has a delay time constraints.
- Service A_3 consists of Sensor Information Sharing (SensIS) and has the lowest priority.

The arrival packet time t_{avp} is periodic for service A_2 and service A_3 and is aperiodic for service A_1 .

Besides, as described in Table 3.1, these applications are mapped to three LCs, each one is associated with a packet queue. These packets are denoted by $p_c^{(v,rx)}$ where c is the service class, v the transmitter vehicle sending the packets, and rx the receiver vehicles that receiving the packet, that means all neighbors of v in broadcast mode communication. c is the service class and also represents for the priority of the service class, where c has a smaller value gets higher priority. Thus c equals to 1 is the highest priority service class.

We assume that the packet size of each MAC-PDU $p_c^{(v,rx)}$ for service A_c , $c \in \{1, 2, 3\}$ is equal to $RS_{p_c}^{(v,rx)}$ bits corresponding to the requested bits of v .

Table 3.1 – An example of User Cases V2X QoS requirement

Use case group	Communication scenario	Service	MAC layer	Priority	Payload (Bytes)	Tx rate (Message/Sec)	Max end-to-end latency(ms)	Reliability (%)	Data rate (Mbps)
Advanced Driving	EmerTA	A ₁	LC 1	1	2000	-	3	99.999	30
Advanced Driving	CoCA	A ₂	LC 2	2	2000	100	10	99.99	10
Extended sensors	SensIS	A ₃	LC 3	3	1600	10	100	99	-

3.2.3 . PHY layer

In this contribution, we assume a 3GPP 5G NR-V2X SL architecture and we consider that the system parameters correspond to those defined in 3GPP standard R16 as illustrated in Table 3.2.

As illustrated in Figure 3.1, we assume that our system supports in the frequency domain one SL BWP denoted by $SL-BWP$. The bandwidth offered by this later is defined as follows : $SL-BWP=(k+1) \times W$, where $k \in \mathbb{N}$, and W is the subchannel size which is a set of contiguous RBs defined by $W = \{10, 12, 15, 20, 25, 50, 75, 100\}$ RBs.

Let us index the frequency with a **subcarrier index** s . Recall that each RB corresponds to 12 subcarriers. This is later defined by a subchannel with index j as following : $s = j \times 12 \times W = Z \times j$, where Z is number of subcarriers in one subchannel and $Z = 12 \times W$. For example , if the subchannel index $j = 0$ that means subchannel index by 0 includes subcarriers from index 0 to $12 \times W - 1$, if $j = 1$ this means that this subchannel includes subcarrier $12 \times W$ to $12 \times 2 \times W - 1$ etc.

In order to transmit MAC-PDU $p_c^{(v,rx)}$ of vehicle v , the **minimum RU** that can be assigned in the PHY layer is tb_{ij} , where i is the slot index in time domain, and j is the subchannel index in frequency domain. Note that the minimum RU is equal to 1 slot \times 1 subchannel. However, RU defined by i and j must belong to the group of selected RUs (subset of $I_{p_{v,c}} \times J_{p_{v,c}}$) for packet $p_c^{(v,rx)}$

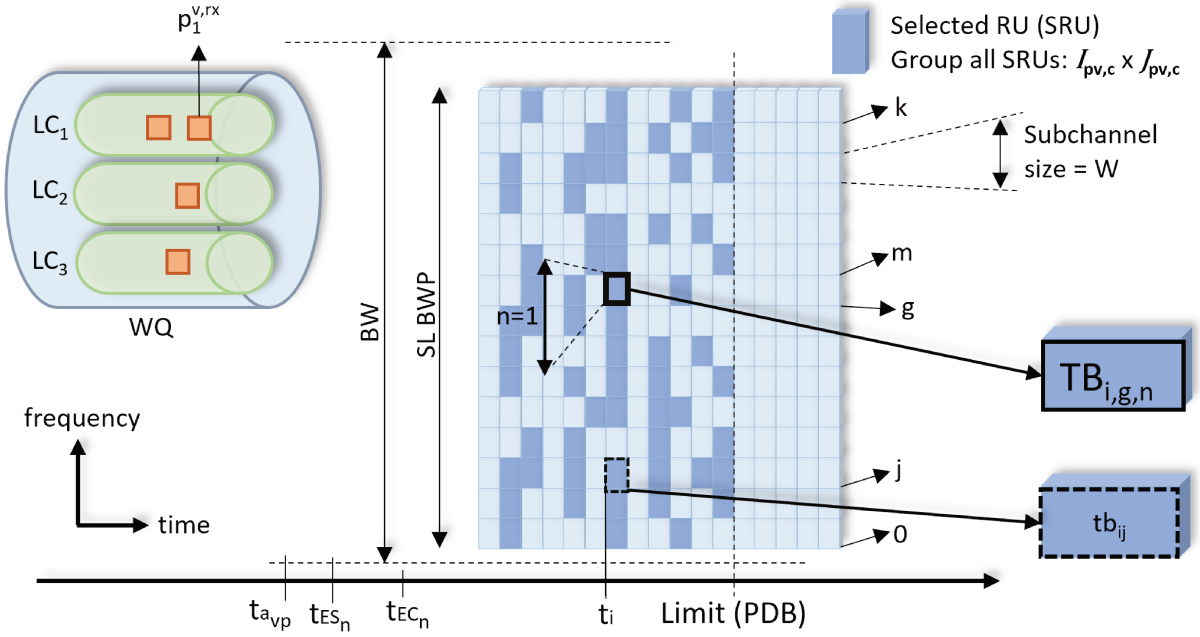


Figure 3.1 – System description

such that $tb_{ij} \in I_{p_{v,c}} \times J_{p_{v,c}}$, where $I_{p_{v,c}} = \{t\}_{t \in \mathbf{N}}$ and $J_{p_{v,c}} = [0, Z \times k]$, with $0 \leq j \leq k$.

Consequently, as previously described in section 2.1.3.5, the **Transport Block (TB)** assigned to a given packet $p_c^{(v,rx)}$, denoted by $TB_{i,j,n}^{p_c^{(v,rx)}}$ corresponds to a set of n contiguous tb_{ij} from index j such that $(i, j) \in I_{p_{v,c}} \times J_{p_{v,c}}$ and $n = m - g$, $g \leq j \leq m - 1$. In fact, in this contribution, we assume that TB is one slot and one subchannel. Thus, the **TB** assigned to a given packet $p_c^{(v,rx)}$, denoted as $TB_{i,j,n}^{p_c^{(v,rx)}}$, is equal to the **minimum RU** tb_{ij} , where $n=1$, i is the slot index in time domain, and j is the subchannel index in frequency domain, i and j must belong to the group of selected RUs for packet $p_c^{(v,rx)}$ such that $tb_{ij} \in I_{p_{v,c}} \times J_{p_{v,c}}$.

3.2.4 . Mobility environment

Since we consider a wireless vehicular network which is a particular mobile radio environment, the system capacity varies with radio channel conditions.

Thus, each transport block $TB_{i,j,n}^{p_c^{(v,rx)}}$ will correspond to a total number of bits equal to b_{ij} depending on the channel conditions (i.e., interference, ve-

Table 3.2 – 3GPP 5G NR-V2X SL parameters

Symbol(s)	Meaning
v	The ID of the transmitter vehicle
rx	The ID of the receiver vehicle
T	The slot duration
i	The slot index in the time domain
j	The subchannel's index in SL BWP
W	Subchannel's size in {10, 12, 15, 20, 25, 50, 75, 100} RBs
Z	Number of subcarriers in one subchannel
k	Last subchannel's index in SL BWP
$p_c^{(v,rx)}$	The MAC-PDU packet with service c from v to rx
$x_{ij}^{p_v}$	0-1 variable deciding whether tb_{ij} is allocated to $p_c^{(v,rx)}$
$I_{p_c^{(v,rx)}}$	Set of the slot's indexes selected for the packet $p_c^{(v,rx)}$
$J_{p_c^{(v,rx)}}$	Set of subchannel's indexes selected for the packet $p_c^{(v,rx)}$
tb_{ij}	A RU defined by slot i and one subchannel from index j
$TB_{i,j,n}^{p_c^{(v,rx)}}$	Transport block, at slot i from subchannel $j \dots j + n$ for $p_c^{(v,rx)}$
b_{ij}	The number of bits carried by tb_{ij}
$RS_{p_c^{(v,rx)}}$	Requested payload of $p_c^{(v,rx)}$
$S_{i,s,v}$	Signal power over SCS s in time slot i for vehicle v
$\bar{S}_{i,v}$	Average Signal power
N	Noise power
$SINR_{i,j}^{(v,rx)}$	Signal to Interference Plus Noise Ratio (SINR) over RU j in time slot i by v to V_{rx}
μ	Bandwidth of a SCS
t_{avp}	Time packet p of vehicle v arrived
t_{ES_n}	Time scheduler n is activated
t_{EC_n}	Time scheduler n finishes the calculating
$t_{interest}$	Interest window time

hicle position, velocity etc.).

The channel state sensed by each vehicle corresponds to the Signal to Interference plus Noise Ratio (SINR) and is reported to the base station gNB.

We denote $SINR_{i,j}^{(v,rx)}$ the channel state of the transmission between v

and rx for subchannel j in a slot i .

3.2.5 . Problem formulation

Following Shannon theorem, for a given subcarrier index s in a time slot t_i , the capacity of a subchannel from s is given by (3.1) :

$$C_{i,s}^v = \sum_s^{s+Z-1} \mu \times \log_2 \left(1 + \frac{S_{i,s,v}}{N} \right) \quad (3.1)$$

Where $S_{i,s,v}$ is the signal power over subcarrier index s at time slot t_i of vehicle v , and μ is the bandwidth of SCS.

Consequently, the number of bits $b_{i,s}^v$ carried by one RU $tb_{i,s}$ is defined in (3.2) below :

$$b_{i,s}^v = T \times C_{i,s}^v = T \times \sum_s^{s+Z-1} \mu \times \log_2 \left(1 + \frac{S_{i,s,v}}{N} \right) \quad (3.2)$$

Where T is the time duration of a slot which is constant.

As described before, the transport block $TB_{i,j,n}^{p_c^{(v,rx)}}$ assigned to vehicle v and packet $p_c^{(v,rx)}$ is a minimum RU $tb_{i,j}$ where $(i, j) \in I_{p_v,c} \times J_{p_v,c}$. Then, we compute the total bit that $TB_{i,g,n}^{p_c^{(v,rx)}}$ can transport to adapt the requested payload of $p_c^{(v,rx)}$ (3.14).

$$TB_{i,j,n}^{p_c^{(v,rx)}} = \sum_{j=Z \times g}^{Z \times (m-1)} b_{i,j}^v \quad (3.3)$$

$$= T \sum_{j=Z \times g}^{Z \times (m-1)} \sum_{s=j}^{j+Z-1} \mu \times \log_2 \left(1 + \frac{S_{i,s,v}}{N} \right) \quad (3.4)$$

$$= T \sum_{s=Z \times g}^{(Z \times m - Z + Z - 1)} \mu \times \log_2 \left(1 + \frac{S_{i,s,v}}{N} \right) \quad (3.5)$$

$$= T \sum_{s=Z \times g}^{(Z \times m - 1)} \mu \times \log_2 \left(1 + \frac{S_{i,s,v}}{N} \right) \quad (3.6)$$

$$\approx T \times Z \times (m - g) \times \mu \times \log_2 \left(1 + \frac{\bar{S}_{i,v}}{N} \right) \quad (3.7)$$

$$\approx T \times Z \times \mu \times \log_2 \left(1 + \frac{\bar{S}_{i,v}}{N} \right) \quad (3.8)$$

Where :

$$\bar{S}_{i,v} = \frac{\sum_{s=Z \times g}^{Z \times m - 1} S_{i,s,v}}{Z \times n} \quad (3.9)$$

$$n = m - g = 1 \quad (3.10)$$

$$Z = 12 \times W \quad (3.11)$$

The total bit of $TB_{i,j,n}^{p_c^{(v,rx)}}$ needs to adapt the requested payload of packet $p_c^{(v,rx)}$, called $RS_{p_c^{(v,rx)}}$

$$\Rightarrow TB_{i,j,n}^{p_c^{(v,rx)}} \geq RS_{p_c^{(v,rx)}} \quad (3.12)$$

In order to optimize the PHY resource, we assume that $TB_{i,j,n}^{p_c^{(v,rx)}}$ is equal to $RS_{p_c^{(v,rx)}}$

$$\Rightarrow TB_{i,j,n}^{p_c^{(v,rx)}} = RS_{p_c^{(v,rx)}} \quad (3.13)$$

Using formula (3.8) we obtain :

$$\Rightarrow RS_{p_c^{(v,rx)}} = T \times Z \times \mu \times \log_2 \left(1 + \frac{\bar{S}_{i,v}}{N} \right) \quad (3.14)$$

On the other side we also have data rate calculation method, denoted by A , from 3GPP [112] for SL in one slot

$$A = L_{\text{layer}} \times f \times Q_m \times R \times \frac{N_{\text{RB}} \times 12}{T_{\text{symbol}}} \times (1 - OH) \quad (3.15)$$

Where :

$$N_{\text{RB}} = W \quad (3.16)$$

$$T_{\text{symbol}} = \frac{T}{14} \quad (3.17)$$

f is the scaling factor and in [1, 0.8, 0.75, 0.4].

OH is overhead, equals to 0.23 for FR1 and 0.25 for FR2.

Table 3.3 – CQI/SINR mapping [113]

CQI	SINR	CQI	SINR
1	-1.889	9	13.32
2	-0.817	10	14.68
3	0.954	11	16.62
4	2.948	12	18.91
5	4.899	13	21.58
6	7.39	14	24.88
7	8.898	15	29.32
8	11.02	-	-

By replacing N_{RB} and T_{symbol} in (3.15) we obtain :

$$\Rightarrow A = L_{layer} \times f \times Q_m \times R \times \frac{Z}{T/14} \times (1 - OH) \quad (3.18)$$

And it must also adapt the requested payload $RS_{p_c}^{(v,rx)}$

$$\Rightarrow RS_{p_c}^{(v,rx)} = A \times T \quad (3.19)$$

Using formula (3.14), (3.18) and (3.19), we obtain a relationship between the modulation coding scheme MCS and the SINR

$$Q_m \times R = \frac{T \times \mu \times \log_2(1 + \bar{S}_{i,v}/N)}{L_{layer} \times f \times (1 - OH) \times 14} \quad (3.20)$$

In our system we adapt the modulation scheme order Q_m and the coding rate R to the instantaneous quality of the radio link $SINR_{i,j}^{(v,rx)}$

3.2.6 . Performance evaluation parameters

3.2.6.1 . Throughput

For a given vehicle v , the **throughput** of the service class c is the total bit transported by all TB allocated for c within v (3.21), where x_{ij}^{pv} is a 0-1 variable deciding whether tb_{ij} is allocated to the vehicle transmitting $p_c^{(v,rx)}$.

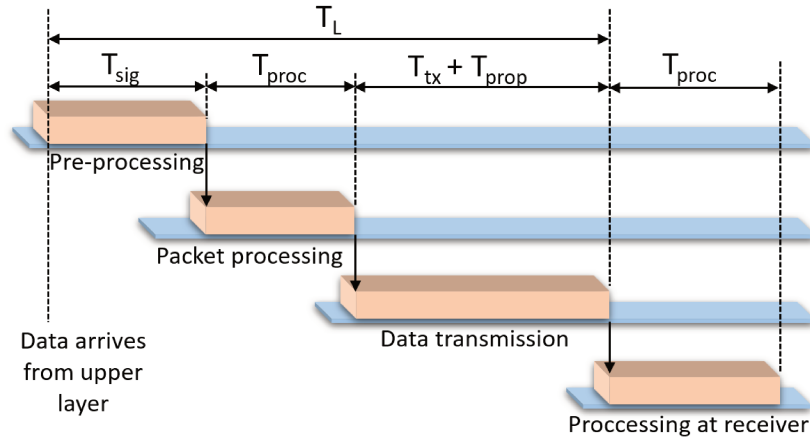


Figure 3.2 – Latency components in PHY layer

$$th_{v,c} = \frac{1}{T} \sum_{(i,j) \in I_{pv,c} \times J_{pv,c}} x_{ij}^{pv,c} b_{ij} \quad (3.21)$$

3.2.6.2. Latency

PHY layer **latency** [114], as illustrated in Figure 3.2 is divided into four components as follows :

$$TL = T_{tx} + T_{prop} + T_{proc} + T_{sig} \quad (3.22)$$

Where :

- T_{tx} is the transmission time of a packet.
- T_{prop} is the propagation delay of the signal from transmitter to receiver.
- T_{proc} is the time needed to perform encoding and decoding, as well as channel estimation in the initial transmission.
- T_{sig} is the pre-processing delay for the exchange of signals such as connection request, scheduling, channel training and feedback, and queuing delay.

3.2.6.3. Reliability

Reliability is the probability that a data of size D is successfully delivered within a time period T from source to destination. For broadcast, unicast or

groupcast transmission, a Transmitter (TX) vehicle sends packet to neighbor Receiver (RX) vehicles around. Among the received packets N_r , the receiver may fail to decode some packets.

The reliability parameter R is computed as follows :

$$R = \frac{N_s}{N_r} \quad (3.23)$$

where N_s is the number of packets decoded successfully and N_r is the number of packets received.

3.2.6.4 . *Effective Transmitted Packet (ETP)*

Let's define a new performance metric denoted by ETP. It is computed as follows :

$$ETP = N * R \quad (3.24)$$

where N is the number of packets received RU to send on transmitter and R is the reliability on receiver.

Thus, the ETP estimates the number of transmitted packets that could be effectively received and decoded by the receiving vehicle.

3.3 . **Proposal**

The most challenging problem in the V2X ecosystem is how to handle the dynamic nature of the vehicular environment, where traffic networks, V2X services, density, radio conditions, etc. vary over time. Even if only V2X services are considered, there are numerous traffic types, scenarios, and services with varying requirements. In NR-V2X, some use cases have stringent QoS requirements, especially in advanced applications that include URLLC V2X services. To serve data traffic from V2X services, the scheduler assigns a PHY resource to the transmitter vehicle. This resource is determined by a slot and one or more subchannels. Due to the dynamic nature of the vehicular environment, it is possible that RA cannot adapt to V2X specifications. The 5G NR-V2X technology is designed to tackle this issue.

In order to achieve the V2X QoS requirements, we have to consider this dynamic environmental factor. In this context, we propose to adjust the PHY

layer configuration SCS μ and subchannel size W with respect to the QoS triggers : latency, reliability, and throughput. As illustrated in Figure 3.3, our proposal consists of two main stages :

1. Radio Resource Allocation (RA) : Our scheduler handles this feature to identify the suitable RU.
2. Adaptive PHY layer Configuration (APC) : This algorithm selects the best pair of configuration (μ, W) in order to maximize ETP defined in Section 3.2.6.4.

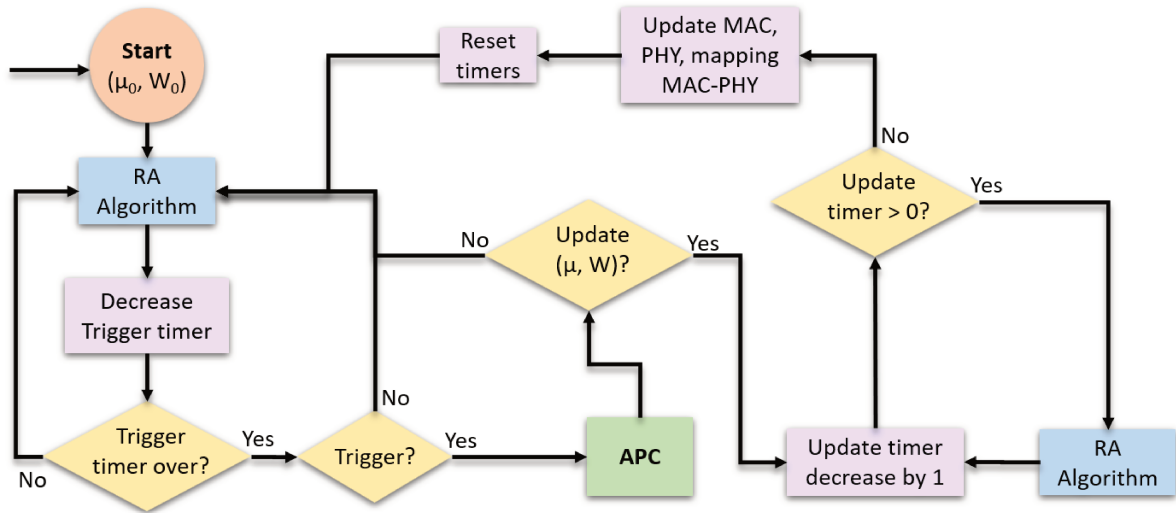


Figure 3.3 – Interact between APC and RA

3.3.1 . Adaptive PHY layer Configuration (APC)

Our proposal takes advantage of the flexible numerology offered by the PHY layer 5G NR and adapts the value of μ and the size of the subchannel W when the performance of radio RA algorithm is not as expected.

These performances are indicated by three parameters defined in Section 3.2.6 : latency, reliability, and data rate. When one of these three constraints is violated, the related trigger is activated, and the system applies APC to update the PHY layer configuration.

These configuration consists of selecting the pair :

$$(\mu, W) \in \{15, 30, 60\} \times \{10, 12, 15, 20, 25, 50, 75, 100\}, \quad (3.25)$$

Table 3.4 – Number of RUs by SCS μ - Subchannel size W in n47 band - 40MHz bandwidth

$\mu \setminus W$	10	12	15	20	25	50	75	100
15	21	18	14	10	8	4	2	2
30	10	8	7	5	4	2	1	1
60	5	4	3	2	2	1	-	-

Table 3.5 – State index by SCS μ - Subchannel size W

$\mu \setminus W$	10	12	15	20	25	50	75	100
15	1	2	3	4	5	6	7	8
30	9	10	11	12	13	14	15	16
60	17	18	19	20	21	22	-	-

where μ in kHz and W in number of contiguous RBs.

The PHY layer represents these pairs (μ, W) with an index number. In this thesis, the index is referred to as "**State**" as displayed in Table 3.5. For example, state index 3 corresponds to the configuration pair of SCS $\mu = 15$ kHz and subchannel size $W = 15$ RBs. These pairs also show the total number of RUs for the entire BWP within the slot time, as presented in Table 3.4. The same example of the configuration pair of SCS $\mu = 15$ kHz and subchannel size $W = 15$ RBs with state index 3 in Table 3.5 offers 14 RUs in Table 3.4. Table 3.4 summarizes the pairs of combinations in the PHY layer for 40MHz bandwidth, which were extracted from Table 2.11 on page 62. Choosing one of these values is similar to the process of handover.

We have to switch the configuration of (μ, W) from one pair to another depending on the trigger. By observation, in Table 3.4, if we increase the SCS then throughput increases. In term of subchannel size, if we decrease the subchannel size, the number of RUs is increased so more vehicles can be served (in case of high density). Unfortunately, assume that the payload does not

change, this case will make the MCS value increase and reliability decrease. Thus, the ETP, defined in Section 3.2.6.4 on page 72, is decreased due to reduced reliability. This is the trade off between the reliability and the number of RUs.

For example, if the PHY layer is in state 5, this indicates that the subchannel size is 25 RBs. One modulation and coding rate can be used to pack a data payload into a TB. Then, the PHY layer is modified to state 3, the subchannel size is changed to 15 RBs. Consequently, the TB size in this state is less than that of state 5. The data payload must be loaded into the TB in state 3 using a greater modulation and coding rate. The radio state remains unchanged, while MCS increases. In this case, it will be more difficult for the receiver to decode the signal, which will reduce reliability and also ETP.

Depending on the environment, the scheduler's performance may vary due to factors such as radio environment, density, or data traffic. This can result in a degradation of latency, reliability, and throughput. In this scenario, the triggers are activated. Then, a configuration update is performed at the PHY layer in order to find a new state that can adapt to latency, reliability, and throughput.

As described in Section 3.2.2 on page 64, LC_1 has the highest priority. First, APC will shift to other states with different SCS. This state must provide a minimum throughput that is greater than the throughput constraint of the highest priority LC. Our objective is to meet the QoS requirement of the highest priority currently in the system. Then, APC will change the subchannel size in order to maximize ETP. The state that has the maximum ETP is called **Balance State (BS)**.

3.3.2 . Resource Allocation Scheduler

RA Scheduler, as illustrated in Figure 3.4, acts as a distributor of RUs for packets in the Waiting Queue (WQ). Recall that RU is a PHY resource combined by one subchannel in the frequency domain and 1 slot in the time domain. The scheduler will serve packets ordered by AESPR algorithm which is described below.

The scheduler will consider each RU in time domain that does not exceed the appropriate PDB and in frequency domain of SL BWP from the lowest to the highest subchannel index for each slot. Then scheduler checks slot by

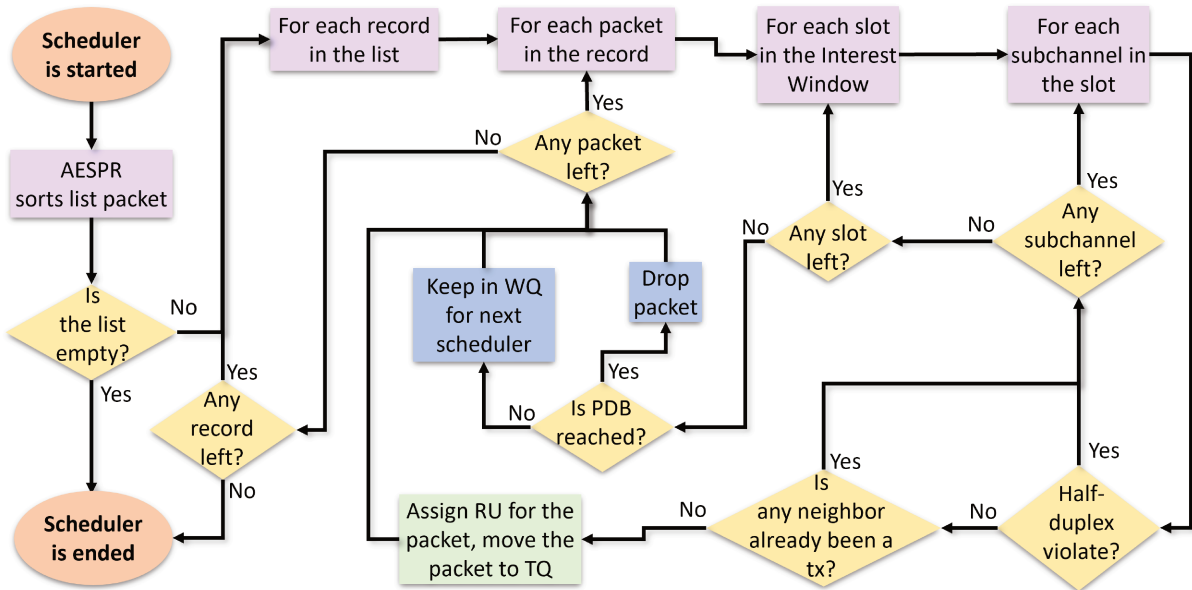


Figure 3.4 – RA step by step

slot until the end. We must note that a vehicle in one slot can only send only one TB. We assume in this contribution that TB is equal to RU. The first RU satisfying both of the following constraints will be chosen by the scheduler to transmit the packet :

- No other RU in this slot time has been assigned to that vehicle before
- Not being used by any neighbor vehicle.

After a packet receives RU, it will be moved to the Transmission Queue (TQ). Otherwise, the packet will remain in the WQ or be discarded upon reaching the PDB. Algorithm 1 summarizes our proposal RA Scheduler.

Note that in literature as described in Section 2.2 on page 54, a lot of RAs are listed. However, it is not our purpose in this thesis.

3.3.2.1 . Pre-emption method

The pre-emption is when scheduler allocates a RU already assigned to another packet. Since we cannot predict the aperiodic packet arrival in high-priority LCs to make an “early” reservation for them, the packets will take over RU that has been already assigned to another packet in the lower priority LC.

We create a time window named Interest Window (denoted as $t_{interest}$) dedicated to the scheduler. It selects only the RU present in this window to

Algorithm 1: Resource Allocation Scheduler

Data: $t_{a_{vp}}$ time packet p of vehicle v arrive t_{ES_n} time execution scheduler n is enabled t_{Ec_n} time execution scheduler n finished t_i time slot i $t_{interest}$ interest window time j index of the subchannel j WQ \leftarrow AESPR**for** all $p_{v,c}$ in the WQ **do**

```
    while  $\left\{ \begin{array}{l} \cdot t_i - t_{a_{vp}} < PDB \\ \cdot t_i < t_{Ec_n} + t_{interest} \\ \cdot t_i > t_{Ec_n} > t_{ES_n} > t_{a_{vp}} \end{array} \right.$  do
         $a \leftarrow$  is any  $tb_{i-}$  in slot  $i$  assigned to  $v$  before?
        if  $a$  is false then
            for  $j$  from 0 to  $k$  subchannel in the BWP do
                 $b \leftarrow$  is  $tb_{ij}$  assigned to any neighbor of  $v$ ?
                if  $b$  is false then select  $tb_{ij}$ ;
            end
        end
    end
    if  $p_{v,c}$  doesn't have any RU  $tb_{i,j}$  assigned then
        if  $t_i = PDB$  then Drop  $p_{v,c}$ ;
    end
end
```

serve the packets in the WQ.

Packets that are not picked by the scheduler remain in WQ and wait for a processing opportunity of the following scheduling period. The system will discard those that PDB has been reached. This window must be smaller than the smallest value of all PDBs. The RUs candidate to be selected by the scheduler must occur in this window.

3.3.2.2 . Adaptive Expected Serving Packet Rate (AESPR)

Another issue is the starvation phenomenon of packets belonging to LCs of low priority. Since the scheduler prioritizes LCs with high priorities, those with lower priorities will spend a lengthy time in the WQ before being dropped after they have exceeded the PDB. A certain percentage of packets must always be handled by the scheduler, regardless of the priority of its LCs, in order to address a more equal use of resources.

Depending on the priority of LC_c , we define a rate value, denoted $Rate_{Exp_c}$. This rate represents the expectation that the scheduler can serve the lowest ratio of packets related to the priority. The bigger $Rate_{Exp_c}$ value is, the more packets can have change to be assigned a RU. This value is from 100 for LC of highest priority that we need to serve all packets, to a rate 50 for LC of lowest priority.

Let's define an observation window w_o corresponding of a number of time slot.

First, we can predict, N_{tot}^p , the number of the packets able to be assigned RUs within the current time slot, by averaging over the past observation window.

$$N_{tot}^p = \frac{\sum_{t=1}^{w_o} N_t}{w_o} \quad (3.26)$$

Where N_t is the packet at time t within queue.

Then, we can compute the expected number of packets in each LC_c queue as follows :

$$N_{Exp}^{LC_c} = Rate_{Exp_c} \times N_c \quad (3.27)$$

We deduce the total number of expected packets :

$$N_{tot}^{Exp} = \sum_{c=1}^3 N_{Exp}^{LC_c} \quad (3.28)$$

The expected processing rate $Rate_{LC_c}$ for each LC_c is :

$$Rate_{LC_c} = \frac{N_{Exp}^{LC_c}}{N_{tot}^{Exp}} \quad (3.29)$$

Finally, we determine $N_{ser}^{LC_c}$, number of packets that scheduler must process first in each LC_c , we expect that a majority of these packets will be assigned a RU for transmission.

$$N_{ser}^{LC_c} = Rate_{LC_c} \times N_{tot}^p \quad (3.30)$$

Next, the scheduler processes the remaining packets in WQ to maximize sending capacity of the system, even if the probability that these packets receive RU for transmission can be low.

By following this approach, we can prevent the occurrence of starvation and ensure that the scheduler processes at least a minimum number of packets from each LC.

3.4 . Performance Evaluation

We evaluate the performance using a self-developed simulator implementing 3GPP R16 NR-V2X standard, built upon the LTEV2Vsim v3.5 simulator [115]. Table 3.6 illustrates the simulation parameters.

In this scenario, we simulate the vehicles' movements in a Urban road of length 4000 meters, composed of 3 lanes 3.5 meters width in each direction. The average speed is set to 57 km/h and a standard deviation of 12.65 km/h. Simulations were conducted for 400 vehicles in the road, which means 100 vehicles/km density.

We simulate the three NR-V2X services A_c of three user cases [73] that map to three logical channels $LC_c c \in \{1, 2, 3\}$. We assume that the packet size of these applications is constant. We set $R_1 = R_2 = 2000$ bytes for A_1 and A_2 , and , $R_1 = 1600$ bytes for A_3 . The arrival time is set as follows : $t_{a-vp_2} = 10\text{ms}$; $t_{a-vp_3} = 100\text{ms}$. Since A_1 is non periodic traffic, we simulate a uniform random arrival time distribution. The application A_2 starts with the simulation, after 800 ms A_3 appears in LC_3 . Finally, A_1 begins from 1100 ms to 1300 ms. In short, Table 3.1 lists the mapping rules and requirements for these NR-V2X services.

We run for each scenario 20 simulations and we show hereafter the average.

Table 3.6 – Simulation parameters

Name	Value
Size of map	4000m length \times 21m width
Lanes	6 both directions
Frequency band	n47
Bandwidth	40 MHz
Velocity of vehicles	60 km/h
Density	100 vehicles/km
Mode scheduling	Mode 1 Dynamic Grant
HARQ retransmissions	No
MIMO	No
DMRS pattern	2 symbols DMRS
Transmission power	23 dBm
Transmitter antenna gain	3 dB
Receiver antenna gain	3 dB
Noise figure	9 dB
Channel Model	3GPP 3-D mm-Wave [116]
Duplex Mode	Half-duplex
Mode communication	Broadcast
Initial SCS - Subchannel size	30 kHz - 100 RBs
Transport Block	1 slot \times 1 subchannel
Symbol PSSCH per slot	14
Symbol for PSCCH	2
SCI 2 nd -stage type	SCI format 2-A

First, we consider a density of 100 vehicles/km neither using the APC algorithm to search for the BS (defined in Section 3.3.1 on page 73 nor the algorithm AESPR. We see that, as shown in Figure 3.5 (a), the packets of LC_3 are not at all served by the scheduler due to its low priority, thus LC_3 did not receive any RU for transmission and suffers from starvation.

Next, in Figure 3.5 (b), by applying the algorithm AESPR, we see that a certain ratio of packets of LC_3 are served via the line of LC_3 appears. AESPR is efficient in avoiding the starvation issue. Finally, Figure 3.7 shows the results

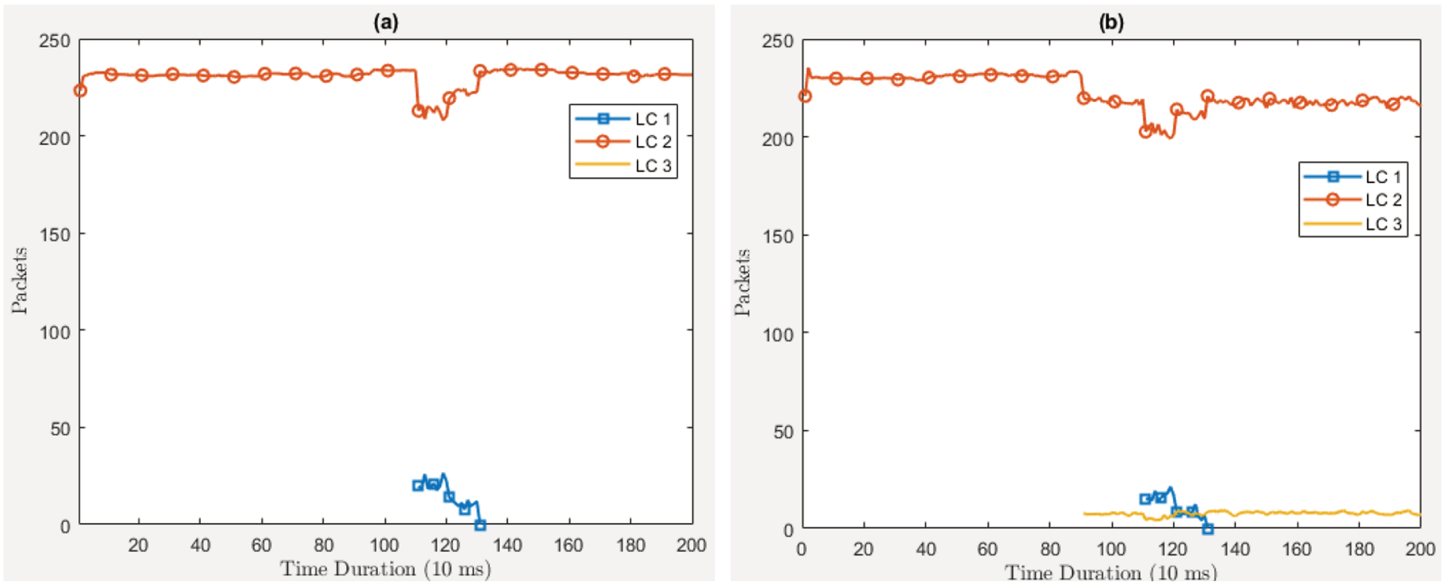


Figure 3.5 – Packet Sent (a) : without APC + without AESPR, (b) : without APC + with AESPR

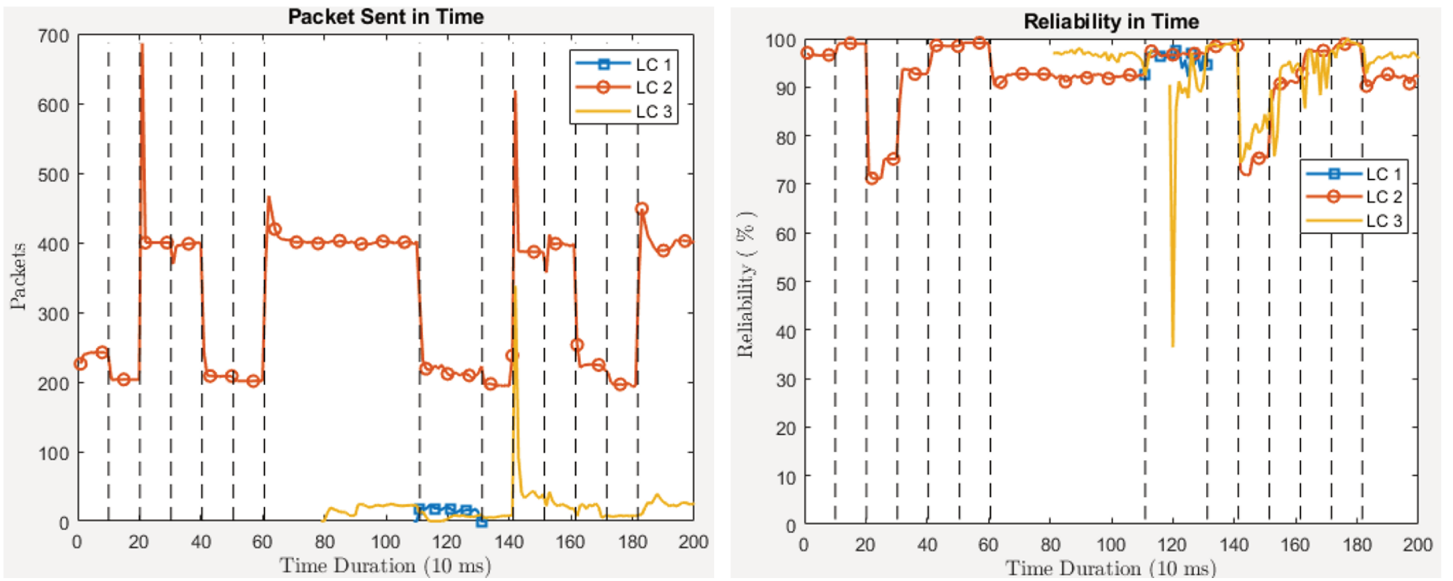


Figure 3.6 – Trade-off between Packet Sent and Reliability by APC

obtained when the APC algorithm that searches for the BS and the algorithm AESPR are deployed. The dashed vertical lines represent the moments where the PHY layer changes the value of SCS and subchannel size by the APC algorithm. In 3GPP R16, the PHY layer can be configured rapidly prior to the performance evaluation phase. At 600 ms, the PHY layer converges toward

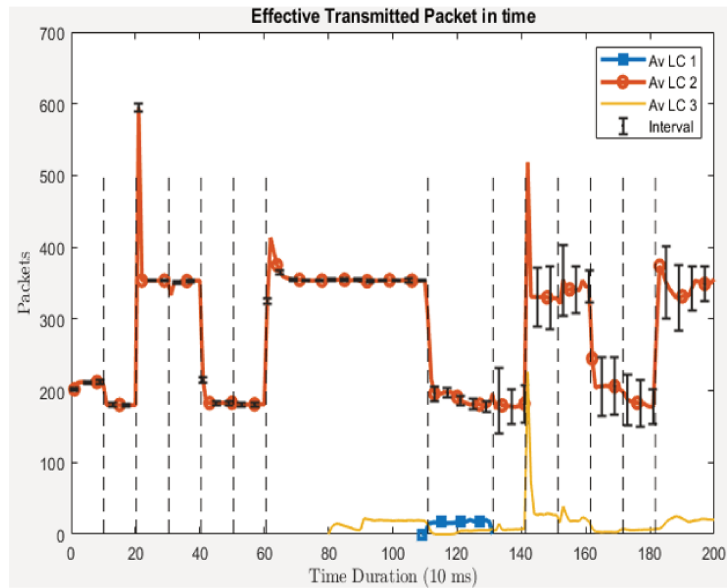


Figure 3.7 – ETP by APC

the equilibrium where the trade-off between the reliability and the number of served and effectively transmitted packets is the most balanced. At 1100 ms, packets from LC_1 arrive. As a consequence, the configuration at the PHY layer changes to serve better LC_1 . When no more packet arrives from LC_1 , the system returns to the equilibrium point at 1800 ms.

Figure 3.6 illustrates the trade-off between Packet Sent and reliability. From 400 ms to 500 ms, In Table 3.5, the PHY layer configuration shifts from state 6 to 7, which results in a larger W subchannel size and fewer RUs. When there are less RU available, the number of packets sent will drop. However, the subchannel size W gets larger, thereby improving the reliability due to the decrease in MCS value. Considering another case, from 200 ms to 300 ms, the configuration in PHY layer is changed from state 8 to 5, which results in a smaller W subchannel size and more RUs. When the subchannel size W gets smaller, thereby reducing the reliability. In this case, the number of Packet Sent is very high but reliability is low. In both cases, ETP values are not optimized. Finally, at 600 ms, the configuration in PHY is state 6 and achieves the maximum ETP, meaning that the number of packets successfully decoded at the receiver is highest.

We calculate the 98% Confidence Interval, as illustrated in the third plot of Figure 3.7.

3.5 . Conclusion

Low latency and high-reliability communications for applications' flows is one of the main 5G cellular network objective, which is especially relevant for connected autonomous vehicles.

However, efficient wireless resource allocation is complicated. To address this problem, we propose to adapt the PHY layer numerology configuration by fine-tuning it with APC algorithm in aim to maximize the ETP.

Besides, we propose an adaptive scheme AESPR to maximize the expected packet serving rate while avoiding the starvation phenomenon of low priority LC.

Based on extensive simulations, results show that our proposal achieves good performance in terms of ETP maximization and starvation minimization of low priority LCs.

In next chapter, we will take advantage of 5G NR-V2X mode communication that does not exist in LTE-V2X : Unicast.

4 - A NOVEL RADIO-AWARE AND ADAPTIVE NUMEROLOGY CONFIGURATION IN V2X 5G NR COMMUNICATIONS

Contents

4.1	Introduction	85
4.2	Problem formulation	86
4.2.1	System description	86
4.2.2	V2X application and traffic model	86
4.2.3	PHY layer	87
4.2.4	Mobility environment	88
4.2.5	Problem formulation	88
4.2.6	Performance evaluation parameters	91
4.3	Proposal	91
4.3.1	Radio-Aware Adaptive PHY layer Configuration (RA-APC)	92
4.3.2	Resource Management Algorithm	93
4.4	Performance Evaluation	97
4.5	Conclusion	100

4.1 . Introduction

The preceding chapter 3 provided a concise explanation of the APC algorithm's functionality in broadcast mode communication, using one slot and one subchannel TB for RA algorithm. The RA scheduler operates without considering CSI channel condition. The SINR metric is solely utilized by the receiver to determine if a packet was received successfully. We aim to monitor the network's behavior through the utilize of APC.

Currently, 5G NR-V2X R16 offers three communication modes for different scenarios : unicast, groupcast, and broadcast. Therefore, we introduce the RA-APC algorithm in this chapter for addressing unicast mode communication.

TB can now have vary in size with regards to the quantity of subchannels. Furthermore, the RA scheduler considers CSI as a parameter while searching for PHY resources. Finally, we observe the behavior of the system in considering all of the combination of numerology and subchannel size.

This chapter is organized as follows. Next section briefly presents related work. Section 4.2 explains system description and problem formulation. Relaying on 3GPP NR-V2X compliant design, a robust RA scheme using a dynamic numerology is proposed in Section 4.3. Section 4.4 presents our methodology and the obtained simulation results. Finally, Section 4.5 concludes this chapter.

4.2 . Problem formulation

We will outline the problem statement. The problem formulation in this contribution is based on the previous one described in section 3.2 and is very similar. We generated it for adaptation to Unicast mode communication and other requirements. This means that certain information and formulas are utilized again.

4.2.1 . System description

We are examining a single 5G NR cell from 3GPP R16. It serves for a set of TX vehicles identified as v . It is assumed that all vehicles operate in mode 1 DG, Unicast mode communication, and are scheduled by gNB.

4.2.2 . V2X application and traffic model

We consider three types of V2X applications denoted by A_1 , A_2 , and A_3 .

- Service A_1 is for EmerTA. It is the most time-critical constrained service.
- Service A_2 refers to CoCA.
- service A_3 corresponds to SensIS and has the lowest priority.

For services A_2 and A_3 , the arrival packet time t_{avp} is periodic, nonetheless for service A_1 , it is aperiodic.

These applications are mapped to three LCs, as shown in Table 3.1, each one is associated with a packet queue. These packets are denoted by $p_c^{(v,rx)}$ where c is the service class, v is the vehicle that sends the packets to one rx

such that $tb_{ij} \in I_{p_{v,c}} \times J_{p_{v,c}}$.

As a consequence, the **TB** assigned to a given packet $p_c^{(v,rx)}$, denoted by $TB_{i,j,n}^{p_c^{(v,rx)}}$ corresponds to a set of $n=m-g$ contiguous tb_{ij} from index j such that $(i,j) \in I_{p_{v,c}} \times J_{p_{v,c}}$ and $g \leq j \leq m-1$. Thus, the maximum size of the TB, $TB_{i,g,n}^{p_c^{(v,rx)}}$ in time and frequency domain is 1 slot \times $(k+1)$ subchannels which corresponds setting $g=j=0$ and $m=k+1$, where k is the highest subchannel index and $k+1$ is the number of subchannels assigned to the given MAC-PDU $p_c^{(v,rx)}$. Note that the TB in our first contribution is one slot and one subchannel.

4.2.4 . Mobility environment

The capacity of the system and the number of bits b_{ij} per TB are affected by mobility such as channel conditions, interference and velocity in a wireless vehicular network operating in a radio environment.

Each vehicle senses the channel state, which corresponds to the signal-to-interference plus noise ratio (SINR), and reports it to the gNB.

The channel state of the transmission between v and rx for subchannel j in slot i is referred to as $SINR_{i,j}^{(v,rx)}$.

4.2.5 . Problem formulation

We develop a scheduling algorithm to identify which MAC-PDUs to be transmitted and a PHY resource assignment strategy to select the best TB satisfying the requested QoS constraints of the MAC-PDU in the LC. We focus solely on SL communication in mode 1 DG . Configuring the PHY layer involves choosing the coupling SCS and subchannel size (μ, W) according to the system conditions.

Hereafter, we describe the system specification and the QoS performance parameters impacting the choice of the optimal PHY layer configuration and TB allocation.

Following Shannon theorem, for a subcarrier index s in a time slot t_i , the capacity of a subchannel from s is given by Equation(4.1) where $S_{i,s,v}$ is the signal power over subcarrier index s at time slot t_i for the vehicle v .

$$C_{i,s}^v = \sum_s^{s+Z-1} \mu \times \log_2 \left(1 + \frac{S_{i,s,v}}{N} \right) \quad (4.1)$$

Where $S_{i,s,v}$ is the signal power over subcarrier index s at time slot t_i of vehicle v .

Thus, a RU $tb_{i,s}$ can carry the number of bits $b_{i,s}^v$ defined in (4.2) where T is the constant duration of a slot.

$$b_{i,s}^v = T \times C_{i,s}^v = T \times \sum_{j=s}^{s+Z-1} \mu \times \log_2 \left(1 + \frac{S_{i,j,v}}{N} \right) \quad (4.2)$$

As described before, the transport block $TB_{i,j,n}^{p_c^{(v,rx)}}$ assigned to vehicle v and packet $p_c^{(v,rx)}$ is a set of $n=m-g$ contiguous tb_{ij} from index j where $(i, j) \in I_{p_v,c} \times J_{p_v,c}$. Then, we compute the total bit that $TB_{i,g,n}^{p_c^{(v,rx)}}$ can transport to adapt the requested payload of $p_c^{(v,rx)}$ (4.8).

$$TB_{i,j,n}^{p_c^{(v,rx)}} = \sum_{j=Z \times g}^{Z \times (m-1)} b_{i,j}^v \quad (4.3)$$

$$= T \sum_{j=Z \times g}^{Z \times (m-1)} \sum_{s=j}^{j+Z-1} \mu \times \log_2 \left(1 + \frac{S_{i,s,v}}{N} \right) \quad (4.4)$$

$$= T \sum_{s=Z \times g}^{(Z \times m - Z + Z - 1)} \mu \times \log_2 \left(1 + \frac{S_{i,s,v}}{N} \right) \quad (4.5)$$

$$= T \sum_{s=Z \times g}^{(Z \times m - 1)} \mu \times \log_2 \left(1 + \frac{S_{i,s,v}}{N} \right) \quad (4.6)$$

$$\approx T \times Z \times (m - g) \times \mu \times \log_2 \left(1 + \frac{\bar{S}_{i,v}}{N} \right) \quad (4.7)$$

$$\approx T \times Z \times n \times \mu \times \log_2 \left(1 + \frac{\bar{S}_{i,v}}{N} \right) \quad (4.8)$$

Where :

$$\bar{S}_{i,v} = \frac{\sum_{s=Z \times g}^{Z \times m - 1} S_{i,s,v}}{Z \times n} \quad (4.9)$$

$$n = m - g \quad (4.10)$$

$$Z = 12 \times W \quad (4.11)$$

$TB_{i,j,n}^{p_c^{(v,rx)}}$ need adapt the requested payload of p , called $RS_{p_c^{(v,rx)}}$

$$\Rightarrow TB_{i,j,n}^{p_c^{(v,rx)}} \geq RS_{p_c^{(v,rx)}} \quad (4.12)$$

In order to optimize the PHY resource, we assume that $TB_{i,j,n}^{p_c^{(v,rx)}}$ is equal to $RS_{p_c^{(v,rx)}}$

$$\Rightarrow TB_{i,j,n}^{p_c^{(v,rx)}} = RS_{p_c^{(v,rx)}} \quad (4.13)$$

$$\Rightarrow RS_{p_c^{(v,rx)}} = T \times Z \times n \times \mu \times \log_2 \left(1 + \frac{\bar{S}_{i,v}}{N} \right) \quad (4.14)$$

On the other side we also have data rate calculation method from 3GPP [112] for SL

$$A = L_{\text{layer}} \times f \times Q_m \times R \times \frac{N_{\text{RB}} \times 12}{T_{\text{symbol}}} \times (1 - OH) \quad (4.15)$$

Where :

$$N_{\text{RB}} = W \times n \quad (4.16)$$

$$T_{\text{symbol}} = \frac{T}{14} \quad (4.17)$$

f is the scaling factor and in [1, 0.8, 0.75, 0.4]

OH is overhead, equals to 0.23 for FR1 and 0.25 for FR2

$$\Rightarrow A = L_{\text{layer}} \times f \times Q_m \times R \times \frac{Z \times n}{T/14} \times (1 - OH) \quad (4.18)$$

And it must also adapt the requested payload $RS_{p_c^{(v,rx)}}$

$$\Rightarrow RS_{p_c^{(v,rx)}} = A \times T \quad (4.19)$$

Using formula (4.14), (4.18) and (4.19), we obtain (4.20)

$$Q_m \times R = \frac{T \times \mu \times \log_2 \left(1 + \frac{\bar{S}_{i,v}}{N} \right)}{L_{\text{layer}} \times f \times (1 - OH) \times 14} \quad (4.20)$$

Q_m and R are mapped to MCS_{tx} index value [68].

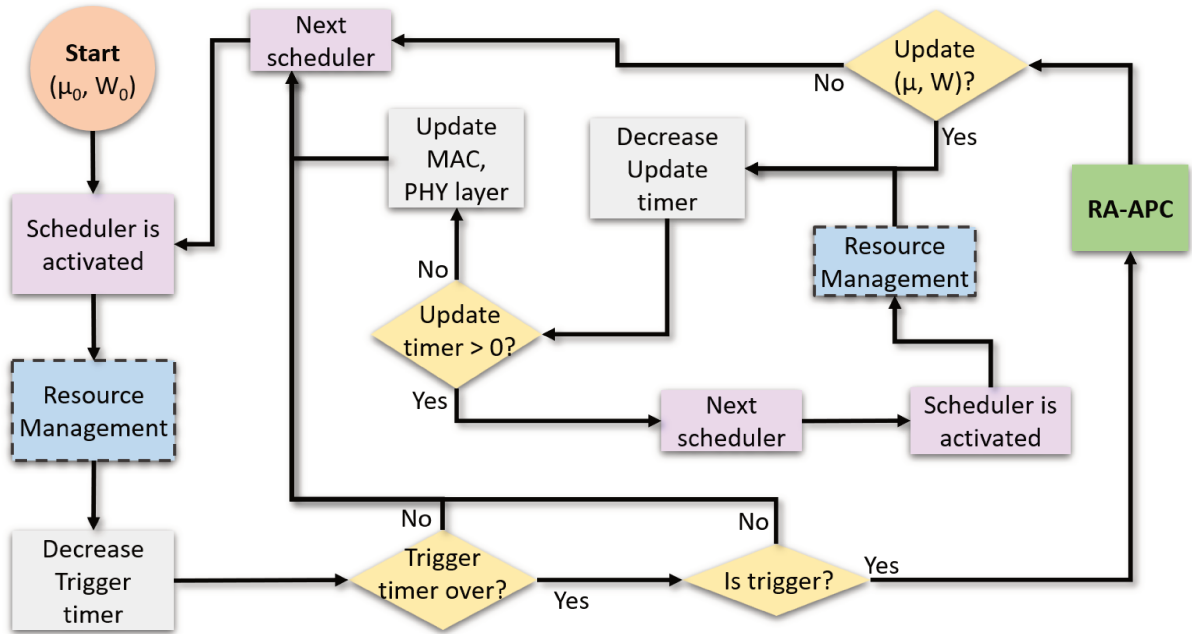


Figure 4.2 – Interaction between RM and RA-APC.

On the receiver, let $\min SINR_{ig,n,v,rx}$ be the minimum SINR with j from g to $g + n - 1$.

SL-CSI maps $SINR_{i,j,v,rx}$ to CQI value, we obtain MCS_{rx} , therefore (4.21) holds. In Unicast mode communication

$$MCS_{tx} \leq MCS_{rx} \quad (4.21)$$

4.2.6 . Performance evaluation parameters

We use again the performance evaluation parameters which are defined in section 3.2.6 : Latency, throughput, reliability, and ETP.

4.3 . Proposal

Our solution is based on two main stages (Figure 4.2). First, the Radio-Aware Adaptive PHY layer Configuration (RA-APC) selects the best pair (μ, W) to maximize the ETP. Then, the RM, handled by our scheduler, identifies the suitable TB for the packet. Note that, the difficulty in this contribution is that one TB is in one slot and multiple subchannels

4.3.1 . Radio-Aware Adaptive PHY layer Configuration (RA-APC)

Our proposal utilizes the adaptable numerology provided by the PHY layer of 5G NR. It adjusts the values of μ and the subchannel size W when the radio RA algorithm's performance is not as expected.

The performances are identified by three parameters specified in section 3.2.6 : latency, reliability, and data rate. If any of the three constraints are broken, the specific trigger is activated, and the system uses RA-APC to update the state.

Please note that the term "**state**", as defined in section 3.3.1, refers to the combination of SCS μ and subchannel size W in the PHY layer configuration, where :

$$(\mu, W) \in \{15, 30, 60\} \times \{10, 12, 15, 20, 25, 50, 75, 100\}, \quad (4.22)$$

μ in kHz and W in number of contiguous RBs.

The state index is available in Table 3.5. The state indicates the total number of RUs for the entire BWP within the slot time, as shown in Table 3.4. For example, state index 2 denotes the configuration pair of subcarrier spacing $\mu = 15$ kHz and subchannel size $W = 15$ RBs, which provides 18 RUs in Table 3.4.

The scheduler's performance can change based on the environment, including factors like radio environment, density, or data traffic. This may lead to a decrease in latency, reliability, and throughput. In this situation, the triggers are activated to update PHY layer configuration to a new state.

In the beginning, RA-APC will move to other states concerning SCS, guaranteeing the minimum throughput is greater than the highest priority LC's throughput constraints. Then, RA-APC will change the subchannel size to maximize ETP. The state with the highest ETP is known as the **BS**.

The RA-APC is an enhancement of APC, as explained in section 3.3.1. RA-APC takes into account the priority of V2X services. In other words, during any given observation time, RA-APC will only respond to the trigger of the highest priority V2X service. For example, a second-priority service might be triggered according to latency, throughput, or reliability. Nonetheless, a higher-priority service existed in the system during the period of observation. Therefore, RA-

APC does not take action even when there is a trigger from the second priority service. In addition, RA-APC eliminates the necessity of moving to states with existing ETP values to save time. An additional enhancement is that if the ETP of the BS reduces by more than 10%, the system will reset all ETP values and activate RA-APC to find a new BS. This enhancement helps RA-APC better respond to the dynamic nature of the V2X environment.

4.3.2 . Resource Management Algorithm

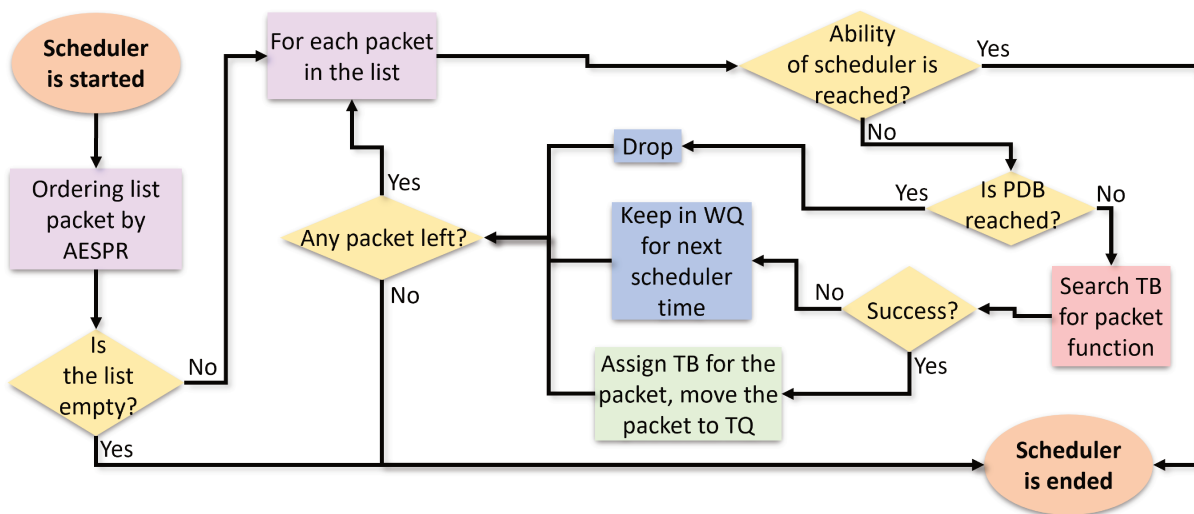


Figure 4.3 – RA step by step

Before introducing the RA scheduler, it is important to note that this scheduler could be replaced with a well-known scheduler from the literature. Since we concentrate on adapting the subchannel size and numerology to improve the system's performance, this is not our main objective.

The RA scheduler, as illustrated in Figure 4.3, acts as a distributor of PHY resources (or TB) for packets in the WQ. Packets in the WQ are ordered by AESPR algorithm into a list of packets. This list of packets helps scheduler know which packet must be served first, or later. In the context of this contribution, TB is one slot and one or multiple subchannels. Thus, the scheduler processes each packet in the list in the time domain that does not exceed the PDB and in the frequency domain from the lowest to highest subchannel index for each slot. The searching process is illustrated in in Figure 4.4. For each slot, The scheduler searches in the frequency domain from the lowest

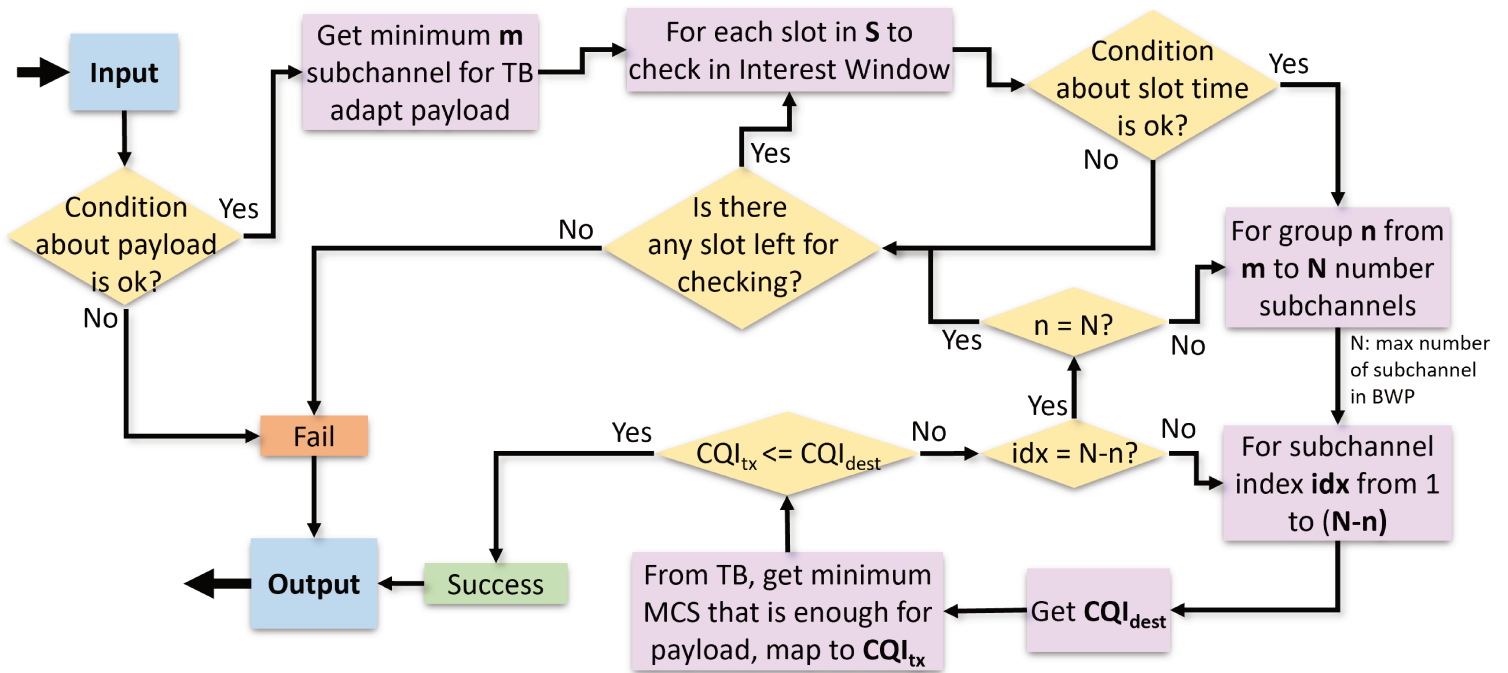


Figure 4.4 – RA step by step (continue)

to highest subchannel index with one subchannel at first, then repeat it with a group of two continuously subchannels until all subchannels in BWP.

There are the constraints for scheduler choose the TB. The first TB satisfying these constraints is chosen by the scheduler to transmit the packet :

- Duplexing mode constraint : Within the chosen slot time, TX cannot act as a RX in another transmission. Moreover, the RX cannot act as TX in another transmission.
- 3GPP standard constraint : One transmitter can only transmit only one TB in a given slot. Thus, if the TX was already assigned a TB in this slot before, scheduler will avoid to assign any TB to that TX in this slot.
- Channel condition constraint : The TB must adapt the CQI feedback from the RX.

We provide further information about the channel condition constraint. In this contribution, the scheduler takes the radio condition into account when assigning PHY resources to the transmitter. When the scheduler identifies a suitable PHY resource candidate, it compares the MCS_{tx} of the transmitter

and the MCS_{rx} of the receiver.

First, for the transmitter, the scheduler determines the minimum modulation and coding rate (MCS_{tx}) that can be used, allowing the TB to store the entire MAC-PDU payload. This MCS_{tx} shows the capability that the transmitter can provide. In order to store the MAC-PDU in the given TB candidature, the scheduler must use MCS_{tx} or larger.

Second, the scheduler determines for the receiver the highest modulation and coding rate (MCS_{rx}) at which the receiver can decode the signal despite interference and noise. This MCS_{rx} indicates the requirement from the receiver's side. The receiver expects the modulation and coding rate to be less than MCS_{rx} ; otherwise, the signal cannot be decoded.

Consequently, if $MCS_{tx} \geq MCS_{rx}$, it indicates that the supply from the transmitter side cannot accommodate the demand from the receiver side. Therefore, it is probably that the receiver will be unable to decode the signal. The channel condition constraint therefore requires that $MCS_{tx} \leq MCS_{rx}$.

After a packet receives TB, it is moved to the TQ. Otherwise, it waits in the WQ or is dropped if it reaches PDB. Algorithm 2 summarizes our proposal.

Algorithm 2: Resource Management Algorithm

Data:

$t_{a_{vp}}$ arrival time of a packet p of vehicle v
 t_{ES_n} starting time of the execution scheduler n
 t_{Ec_n} finish time of the execution scheduler n
 t_i time slot i
 $t_{interest}$ interest window time
 j index of the subchannel j
 k index of the last subchannel in BWP

WQ \leftarrow AESPR;

for all $p_c^{(v,rx)}$ in the WQ **do**

$a \leftarrow$ whether the entire BWP can contain $p_c^{(v,rx)}$ payload ;

if a is false **then**

 Drop $p_c^{(v,rx)}$;

 Check next $p_c^{(v,rx)}$ in WQ;

end

while $\begin{cases} t_i - t_{a_{vp}} < PDB \\ t_i < t_{Ec_n} + t_{interest} \\ t_i > t_{Ec_n} > t_{ES_n} > t_{a_{vp}} \end{cases}$ **do**

$a \leftarrow$ Check slot i violated half-duplex constraint ;

if a is true **then** Check next slot i ;

$minSub \leftarrow$ min #subchannel can contain $p_c^{(v,rx)}$;

for n from $minSub$ to $(k + 1)$ subchannel **do**

for j from 0 to $(k - n - 1)$ subchannel index **do**

$MCS_{tx} \leftarrow$ minimum MSC such that $TB_{ij,n}$ can contain $p_c^{(v,rx)}$;

$MCS_{rx} \leftarrow$ maximum MSC such that V_{rx} can decode $TB_{ij,n}$;

if $MCS_{tx} \leq MCS_{rx}$ **then**

 Select $TB_{ij,n}$;

 Check next $p_c^{(v,rx)}$ in WQ;

end

end

end

end

if $t_i \geq PDB$ **then** Drop $p_c^{(v,rx)}$;

else Keep $p_c^{(v,rx)}$ in WQ;

end

4.4 . Performance Evaluation

We assess the performance of our proposal using a self-developed simulator implementing 3GPP R16 NR-V2X standard, built upon the LTEV2Vsim v3.5 simulator¹. Note that we changed a lot of the coding in Matlab since the proposal is on Unicast. Furthermore, we added a variable radio environment. Finally, we consider a different structure of TB consisting of one slot and one or more subchannels.

Table 4.1 summarizes the main network parameters.

We simulate the vehicles' movements in a 4000-meter urban road, composed of three lanes of 3.5 meters width in each direction, one micro-cell and control by a gNB. The average speed is set to 57 km/h with a standard deviation of 12.65 km/h. Simulations are conducted for 1000 vehicles in the road, which means 250 vehicles/km density.

We simulate three NR-V2X services A_c of three user cases [73], described in Table 3.1, mapped to three logical channels LC_c , $c \in \{1, 2, 3\}$. Assuming a constant packet size for these applications, we set $R_1 = R_2 = 2000$ bytes for A_1 and A_2 , $R_3 = 1600$ bytes for A_3 . The arrival time is $t_{a-vp_2} = 10$ ms and $t_{a-vp_3} = 100$ ms. Since A_1 is non periodic traffic, we simulate a uniform random arrival time distribution. A_2 started with the simulation, after 800 ms A_3 appears in LC_3 . Finally, A_1 is executed from 1100 ms to 1300 ms.

We ran 1100 simulations for 22 states.

First, we compare our proposal RA-APC with the baseline non-aware radio APC algorithm fixing the TB's size to one subchannel in the first contribution described in chapter 3.

Figure 4.5 and Figure 4.6 show the trade-off between Packet Sent and Reliability of APC and our proposal RA-APC (left and right column, respectively). For APC, the density is set to 100 vehicles/km. In Figure 4.5, we see that RA-APC manages the resources much better even if the density is 2.5 times higher. When the density increases, the performance parameters degrade. Consequently, RA-APC adapts the PHY layer configuration to obtain more PHY resources, while also considering the variations in the radio environment.

1. <https://github.com/alessandrobazzi/LTEV2Vsim>

Table 4.1 – Simulation network parameters

Name	Value
Size of map	4000m length × 21m width
Lanes	6 lanes in both directions
Frequency band	n47
Bandwidth	40 MHz
Velocity of vehicles	60 km/h
Density	250 vehicles/km
Mode scheduling	Mode 1 Dynamic Grant
HARQ retransmissions	No
MIMO	No
DMRS pattern	2 symbols DMRS
Transmission power	23 dBm
Transmitter antenna gain	3 dB
Receiver antenna gain	3 dB
Noise figure	9 dB
Channel Model	3GPP 3-D mm-Wave [116]
CSI	Yes
Duplex Mode	Half-duplex
Mode communication	Unicast
Initial SCS - Subchannel size	All 22 states
Transport Block	1 slot × 1 or multiple subchannels
Symbol PSSCH per slot	14
Symbol for PSCCH	2
SCI 2 nd -stage type	SCI format 2-A
MCS	Table MCS 1
CQI	Table CQI 1

We also achieved a better reliability $\approx 99.75\%$ (Figure 4.6). This can be explained thanks to RA-APC which can detect the variations in the radio state, and hence successfully decodes more packets than APC.

In Figure 4.7, RA-APC always achieved the maximum ETP, whereas APC only reached it after 600 ms within a 98% confidence interval for all LCs.

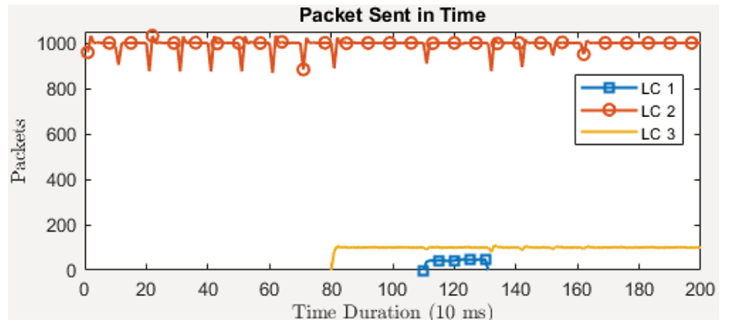
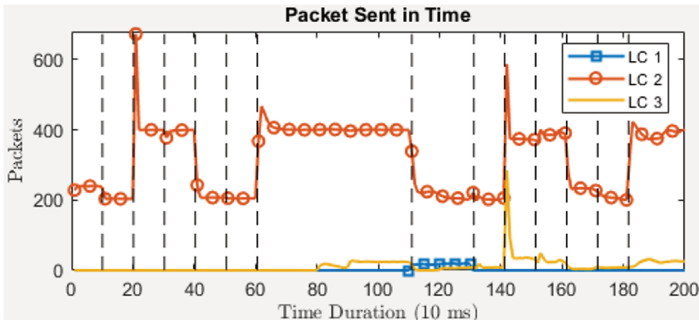


Figure 4.5 – Packet sent +/- Radio awareness,

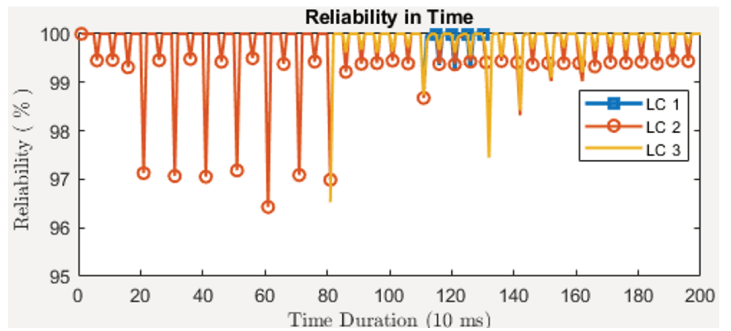
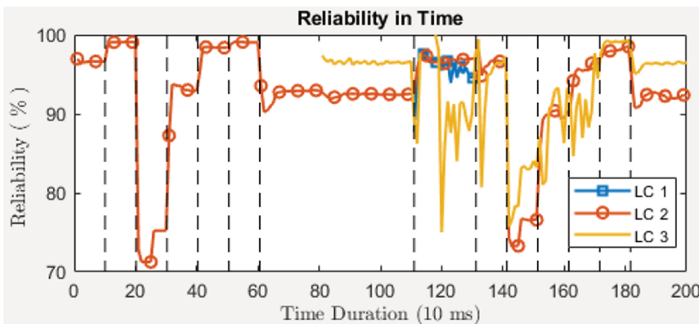


Figure 4.6 – Reliability +/- Radio awareness

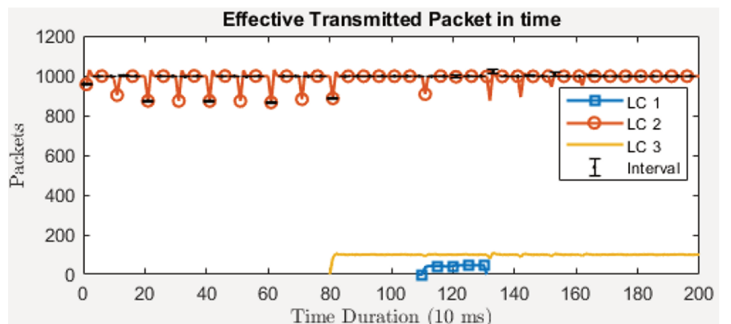
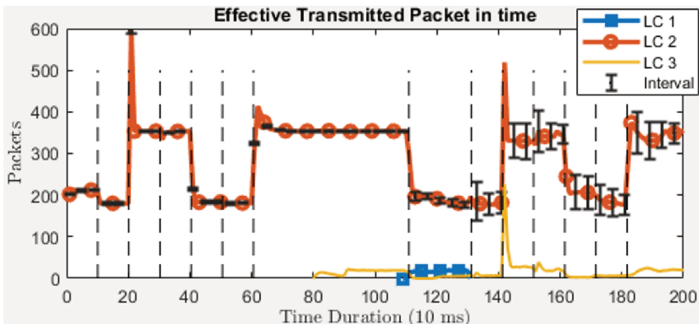


Figure 4.7 – ETP +/- Radio awareness

Furthermore, we also observe the system in terms of all 22 states. Figure 4.8 on the left presents the balance point corresponding to the best configuration for each starting state and for every SCS. Figure 4.8 in the middle demonstrates a good performance in terms of ETP for each state and each application A_c . Finally, Figure 4.8 on the right visualizes the Packet Drop Rate (PDR) of LC_1 , which has the most stringent requirements, while varying (μ, W) . The worst case is when $PDR = 0.025$ that is very low and matches with the constraints of a contingent application like A_1 .

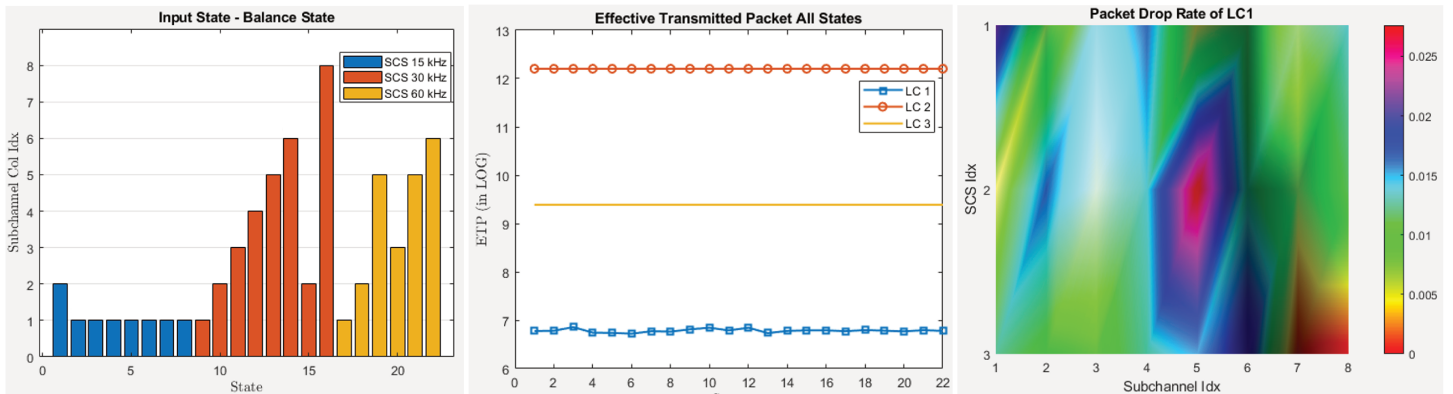


Figure 4.8 – Balance state, ETP, and Packet Drop of all States

4.5 . Conclusion

As the main goal of connected autonomous vehicles' communications is to enhance traffic safety and save lives, any design of a resource allocation scheme must consider the stringent requirements of these applications in terms of latency and reliability in a dynamic environment. For this reason, 5G networks are appropriate for addressing these challenges.

The proposal in the preceding chapter consisted of allowing the telco operator to adapt the PHY layer configuration for efficient radio resource management in a 5G NR-based system. The APC algorithm was introduced for maximizing the value of ETP.

Based on that concept, we propose to adjust the PHY layer configuration by fine-tuning it using the RA-APC algorithm and interact with RA management in a dynamic environment.

The originality of our contribution is threefold :

- Consider the radio channel state when determining the PHY resource for the transmission.
- Study unicast communication rather than broadcast communication.
- Utilize multiple subchannels for the TB

Our proposal, RA-APC, has been extensively simulated and has shown significant improvements in ETP, reliability, and latency. It has also taken into account safety and non-safety traffic scenarios.

This algorithm serves as the foundation for the upcoming contribution, which we will explain on in the following chapter.

5 - DETRAP : A NOVEL AI/ML V2X 5G NR ADAPTIVE PHYSICAL LAYER CONFIGURATION

Contents

5.1	Introduction	103
5.2	Machine learning preliminaries	104
5.2.1	Machine learning	104
5.2.2	Decision tree learning	106
5.3	Problem formulation	107
5.3.1	System description	107
5.3.2	Problem formulation and performance parameters	109
5.4	Proposal : Decision Tree Adaptive Physical layer Configuration (DeTrAP)	110
5.5	Performance Evaluation	114
5.6	Conclusion	118

5.1 . Introduction

The preceding chapter 4 explained how the RA-APC algorithm works in unicast mode communication. In addition, the second contribution's RA scheduler takes into account CSI as a parameter when searching for PHY resources. It considers one slot with multiple subchannel transport blocks. Nevertheless, the duration required to attain the Balance state (BS) is high. Such delay does not fit for emergency V2X services, for which the system must switch to the BS as fast as possible. In a dynamic V2X service environment, particularly with URLLC services, it is necessary to decrease this convergence time.

What is the method to accomplish this goal? Providing the available data, how can be applied to analyze past behavior and make predictions for the future? To amend this limitation of RA-APC, we present the DeTrAP algorithm as our third contribution which relies on a heuristical search strategy to avoid exhaustive iterations and to reduce the search time in this chapter. DeTrAP also limits the frequency of changes done to the PHY layer configuration. The

DeTrAP algorithm relies on machine learning techniques and utilizes data generated from the second contribution. Furthermore, in this submission, we also examine the density and services dynamics.

This chapter is organized as follows. We provide a brief overview of Machine Learning (ML) and Decision Tree (DT) learning in the following section 5.2. Section 5.3 formulates the problem statement. In Section 5.4, we dive into the details of DeTrAP. Section 5.5 presents the simulation results of our proposed approach. Finally, in Section 5.6, we conclude our work.

5.2 . Machine learning preliminaries

This section starts with a brief overview of ML, and discusses how a DT is built on observational data. Then, we consider previous works, if any, on NR-V2X PHY configuration using ML to position our work in the literature body.

5.2.1 . Machine learning

Machine learning (ML) is a methodology that “teaches” a model to perform an intended task based on a set of observational data [117]. The multiplication of data-generating IoT devices coupled with the improvement of computing hardware has fueled the rapid development of ML. Being versatile, ML has been widely applied in a variety of domains. In this study, we wish to leverage the strength of ML to optimize the PHY layer configuration for efficient resource allocation.

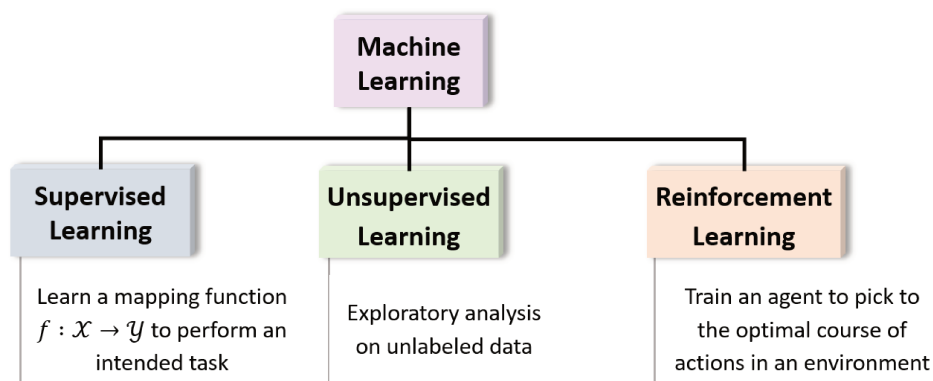


Figure 5.1 – Three paradigms of machine learning

ML has three primary paradigms : supervised learning, unsupervised learning, and reinforcement learning [118] (Figure 5.1).

- Supervised learning learns a mapping function from the input space to the output space, thus learning to perform a predefined task such as classification if the output is discrete or regression if the output is continuous.
- Unsupervised learning only deals with an input space and is mainly used for exploratory data analysis, clustering data, or anomaly detection.
- Reinforcement learning differs significantly from the other two because it is agent-based learning : given an environment and an objective, reinforcement learning teaches an agent to navigate such environment to attain the objective by picking a sequence of best “actions” that maximizes the final reward. It is based on the Markov Decision Process (MDP) theory [119][120].

Among the three learning paradigms, supervised learning has been thoroughly studied and constantly improved by the ML community, which motivates our choice of a supervised approach for our study. There is a plenitude of supervised learning algorithms : DT, support vector machines, logistic regression, and neural networks. Each method is suitable for specific scenarios. For instance, logistic regression and support vector machines handle binary classification, although the latter can be extended for multiclass classification but is generally more time consuming than the former. Decision trees (DT) can work on data of diverse value ranges and are easily interpretable. Neural networks are by far the most powerful learner that can approximate an extensive range of functions, but are also computationally expensive and demand sophisticated fine-tuning to reach an acceptable accuracy. It is thus not suitable for real-time application constraints.

Having considered the strengths and weaknesses of these supervised methods, we deem DT the most suitable to our study because DT are efficient, does not require time-consuming fine-tuning nor complicated data preprocessing, and can be explained easily by visualizing the resulting trees [121]. Our goal is to obtain a baseline result with DT to demonstrate the applicability of ML for NR-V2X, from which we can experiment with other learning

algorithms in the future.

5.2.2 . Decision tree learning

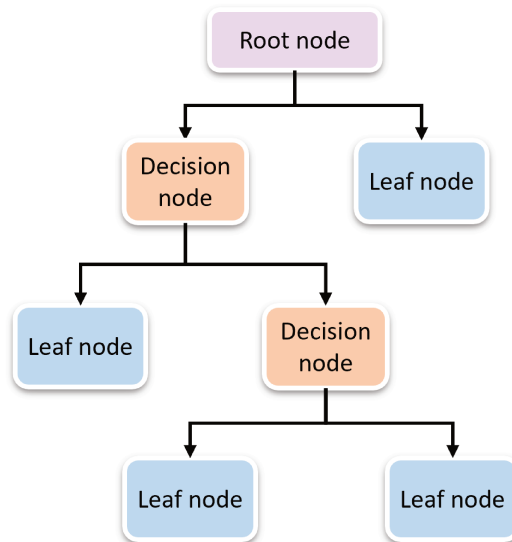


Figure 5.2 – A decision tree

As shown in Figure 5.2, a DT is a binary tree in which root node and internal nodes (Decision node) are an attribute (also called *variables* or *features*) that halve a data space, and leaf nodes contains a sub-sample from the original data set with mixed class labels. Training and prediction with a DT proceed as follows.

5.2.2.1 . Training

Given a data set $\mathcal{D} = \{(x^{(i)}, y^{(i)})\}_{1 \leq i \leq N}$ of N data examples, where $x^{(i)} \in \mathbb{R}^d$ denotes the i^{th} example containing d attributes and $y^{(i)} \in \mathcal{L}$ the associated label, where \mathcal{L} is a set of discrete class values. To train a DT on \mathcal{D} , we start by computing a “score” for each attribute (such as information gain or Gini index [122]) and select the attribute with the highest score as the splitting node : the intuition is to halve the data space, such that each subtree contains a purer sub-sample of the original data, and that a leaf node should contain a sub-sample as pure as possible. The purity of a sub-sample is determined via the ratio of examples from different classes : A sample is pure if it contains the data examples from only one class. Splitting the tree is done recursively at each node. The training stops when all the leaves are pure or a maximum

depth has been reached. The time complexity of building a DT is $O(Nd \log N)$ [123].

5.2.2.2 . Prediction

To predict the class of an unseen example, it is necessary to navigate in the tree according to its value of an attribute at a splitting node until it falls into a leaf node. The class with the significant count in this leaf will be returned as the predicted label for this example. The time complexity of issuing a prediction for an example is $O(\log N)$.

5.3 . Problem formulation

In this section, we first give a description of the system in which NR-V2X RA operates (Section 5.3.1). Then, we formally state our problem (Section 5.3.2).

5.3.1 . System description

Let v be a transmitter (TX) vehicle that uses 3GPP R16 NR-V2X mode 1 DG, scheduled by gNB within one cell.

5.3.1.1 . V2X application and traffic model

As in the contribution one and two, we consider that the system offers three V2X applications for three user cases as detailed in [73], namely A_1 , A_2 , A_3 , which communicate in unicast mode at the PHY layer. A_1 is the aperiodic EmerTA service working under time-critical constraint, A_2 is the periodic CoCA service and is less critical than A_1 but is still under delay constraint, and A_3 is the periodic SensIS service with the lowest priority (Table 3.1). These applications are associated with three LC, each of which has a packet queue. These packets are denoted by $p_c^{(v,rx)}$ where c is the service class, v the TX sending the packets, and rx the receiver (RX) vehicle in unicast mode.

5.3.1.2 . PHY layer

We set the system parameters according to the 3GPP R16 standard for NR-V2X SL (Table 5.1). The frequency domain supports one **SL BWP**. All PHY layer parameters are detailed in section 4.2.3.

Let tb_{ij} be the **RU** in the PHY layer to transmit MAC-PDU $p_c^{(v,rx)}$ from v to rx , such that i and j are respectively the slot index in the time domain and

Table 5.1 – 3GPP 5G NR-V2X SL parameters

Symbol(s)	Meaning
v	The ID of the transmitter vehicle
rx	The ID of the receiver vehicle
T	The slot duration
i	The slot index in the time domain
j	The subchannel's index in SL BWP
W	Subchannel's size in {10, 12, 15, 20, 25, 50, 75, 100} RBs
k	Last subchannel's index in SL BWP
$p_c^{(v,rx)}$	The MAC-PDU packet with service c from v to rx
$x_{ij}^{p_v}$	0-1 variable deciding whether tb_{ij} is allocated to $p_c^{(v,rx)}$
$I_{p_c}^{(v,rx)}$	Set of the slot's indexes selected for the packet $p_c^{(v,rx)}$
$J_{p_c}^{(v,rx)}$	Set of subchannel's indexes selected for the packet $p_c^{(v,rx)}$
tb_{ij}	A RU defined by slot i and one subchannel from index j
$TB_{i,j,n}^{p_c^{(v,rx)}}$	Transport block, at slot i from subchannel $j \dots j + n$ for $p_c^{(v,rx)}$
b_{ij}	The number of bits carried by tb_{ij}
$RS_{p_c}^{(v,rx)}$	Requested payload of $p_c^{(v,rx)}$
$SINR_{i,j}^{(v,rx)}$	SINR over RU j in time slot i by v to V_{rx}
μ	Bandwidth of a SCS
$t_{a_{vp}}$	Time packet p of vehicle v arrived
t_{ES_n}	Time scheduler n is activated
t_{EC_n}	Time scheduler n finishes the calculating

the subchannel index in the frequency domain, tb_{ij} is therefore equal to one slot \times one subchannel, such that $tb_{ij} \in I_{p_v,c} \times J_{p_v,c}$ is the RUs selected for the packet $p_c^{(v,rx)}$.

As illustrated in Figure 4.1, the **Transport Block** $TB_{i,j,n}^{p_c^{(v,rx)}}$ assigned to a packet $p_c^{(v,rx)}$ is a set of $n = m - g$ contiguous tb_{ij} such that $(i, j) \in I_{p_v,c} \times J_{p_v,c}$ and $g \leq j \leq m - 1$. Thus, the maximum size of the TB, $TB_{i,g,n}^{p_c^{(v,rx)}}$ in time and frequency domain is 1 slot \times $(k + 1)$ subchannels which corresponds setting $g = j = 0$ and $m = k + 1$, k the highest subchannel index and $k + 1$ the number of subchannels assigned to the $p_c^{(v,rx)}$.

Channel conditions such as interference and vehicle position within a ra-

dio environment have an impact on the system capacity of a wireless vehicular network, which consequently affects the total number of bits b_{ij} of each TB. Each vehicle senses the channel state in terms of Signal to Interference plus Noise Ratio (SINR), which is then transmitted to the base station gNB. The channel state of the transmission between v and rx for subchannel j in a slot i is represented by $SINR_{i,j}^{(v,rx)}$ which is detailed in section 4.2.

5.3.2 . Problem formulation and performance parameters

We focus solely on SL communication in mode 1 DG. Configuring the PHY layer involves choosing the coupling SCS and subchannel size (μ, W) according to the system conditions. The full system specification and the QoS performance parameters impacting the choice of the optimal PHY layer configuration and TB allocation are detailed in chapter 4. We compute the following performance evaluation parameters for every LC based on the problem formulation described in section 4.2.5.

- For a vehicle v , the **throughput** of the service c is the total bit transported by all TBs allocated for c within v (5.1), where x_{ij}^{pv} is a 0-1 variable deciding whether tb_{ij} is allocated to the vehicle transmitting $p_c^{(v,rx)}$.

$$th_{v,c} = \frac{1}{T} \sum_{(i,j) \in I_{pv,c} \times J_{pv,c}} x_{ij}^{pv,c} b_{ij} \quad (5.1)$$

where $b_{i,j}$ is the number of bits carried by one RU tb_{ij} .

- **Latency** is the sum of four components : i) transmission time, ii) the signal propagation delay from TX to RX, iii) the time required to perform encoding, decoding and channel estimation in the initial transmission, and iv) the preprocessing delay for the signal exchange such as connection request, scheduling, and queuing delay.
- **Reliability** is the probability that a data of size D is successfully delivered within a time period T from source to destination. For broadcast, unicast or groupcast transmission, a TX vehicle sends packet to neighbor RX vehicles around. Among the received packets N_r , the receiver may fail to decode some packets. The reliability parameter R is ratio between the number of packets decoded successfully N_s and the number of packets received by RX vehicles :

$$R = \frac{N_s}{N_r} \quad (5.2)$$

- **RateETP** is our performance parameter computing the rate of effectively transmitted packets among N_{TB} , the number of packets that have obtained the TB using the RA algorithm :

$$rateETP = \frac{N_{TB} \times R}{P} \quad (5.3)$$

where P is the number of packets that go to the WQ of each LC. WQ is the queue in which the RA scheduler distributes the TBs for the packets.

We modify ETP from the first and second contributions to rateETP in order to highlight the efficacy of the system, where a higher rateETP indicates that a greater percentage of packets on the transmitter's side are successfully decoded on the receiver's side.

5.4 . Proposal : Decision Tree Adaptive Physical layer Configuration (DeTrAP)

DeTrAP leverages historical data captured by the system to avoid exhaustively iterating through all states. These data contain information about the environments in which the system has been and which the **balance state BS** is chosen for each environment. Our solution has two primary steps, as illustrated in Figure 5.3 :

1. Building data set and
2. Applying DeTrAP to predict the PHY layer configuration.

First, we use RA-APC to select the best pair (μ, W) (the BS) and record all information in three data sources, namely **TabA**, **TabB**, and **TabC**. Then, DeTrAP uses these data sources to find a **Good State (GS)** within a shorter investigating time. A GS is a state that is likely to be a BS (defined in Section 3.3.1 on page 73), for it can raise the network performance to nearly the same extent as the BS. The uncertainty comes from the lack of data that would be required to confirm that this approximate state indeed has the highest rateETP as if it is a BS. We will give an example of the data saved in each data source for specific case 1 with a density of 100 vehicles/km and the input state 1. As

illustrated in Table 5.6, **case** is the index of a combination status of $[LC_1, LC_2, LC_3]$. For example, case 1 is means that all LC_1, LC_2 and LC_3 are activated and have packets to send.

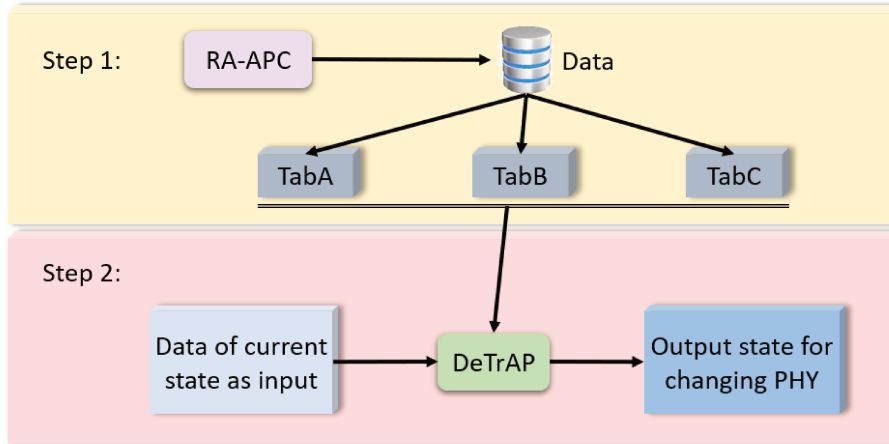


Figure 5.3 – Two-step process

Table 5.2 (**TabA**) corresponds to the data set \mathcal{D} as defined in section 5.2.2. It contains the information about the inputs (features, $x^{(i)}$) and the associated BS, (output state or label, $y^{(i)}$) of each input, which are used to train the DT. The features include : case, density, current state, rateETP of current state, average vehicle neighbors, average vehicle neighbors that are transmitters, maximum neighbor, maximum neighbors that are transmitters, packet kept rate, packet dropped rate, packet sent rate, reliability, and state output (the BS). These rates are computed over the total number of packets in the WQ.

TabB stores the data mapped to a combination of [case, density, state input]. Example Table 5.3 is for case 1 (LC_1, LC_2 and LC_3 are activated) in a density 100 vehicles/km and state input 1 ($\mu = 15$ kHz and $W = 10$ RBs). For each combination, after repeated runs, TabB saves the list of BSs in which the combination has been in, alongside the number of times it is chosen, the maximum, minimum, average, and standard deviation of rateETP.

Table 5.4 (TabC) organizes the states chosen as the BS for each combination of [case, density, state input]. These states are sorted by the number of times a BS is chosen in the past in the descending order.

These three tables are used for the second step (Figure 5.5) to assist De-

Table 5.2 – TabA for case 1

Density	Input State	Rate ETP	Features								Labels
			Avg Neig	Avg Neig Tx	Max Neig	Max Neig Tx	rate Kept	rate Drop-ped	rate Sent	reliability	Output State
100	1	0.9925	47	1	80	4	0.01	0	1	0.9925	4
100	1	0.9925	47	0	88	3	0.005	0	1	0.992	4
100	1	0.995	48	0	89	2	0.01	0	1	0.995	5
100	1	0.9925	47	0	86	3	0.0075	0	1	0.9925	1
..

Table 5.3 – TabB for [case 1, density 100, input state 1]

BS	1	2	3	4	5	6	7	8
Accuracy	12	3	7	4	9	8	4	3
Max	1	1	0.9975	0.9975	1	1	0.9975	1
Min	0.9925	0.9925	0.99	0.9925	0.99	0.9925	0.99	0.995
Average	0.9948	0.9967	0.9943	0.999	0.9964	0.9969	0.995	0.9975
StDev	0.0023	0.0038	0.0024	0.002	0.0031	0.0026	0.0035	0.0025

Table 5.4 – TabC for [case 1, density 100, input state 1]

Order	1	2	3	4	5	6	7	8
BS	1	5	6	3	4	7	2	8
Accuracy	12	9	8	7	4	4	3	3

TrAP in finding to which state to change the SCS and subchannel size of the PHY layer. Figure 5.4 illustrates the interaction between RA and DeTrAP. RA selects the TB for the packets in the WQ. When the requirements of the V2X services are not met, RA will evoke DeTrAP to select the pair (μ, W) that may better address such requirements.

DeTrAP alternates between two phases (Figure 5.5). DeTrAP always starts

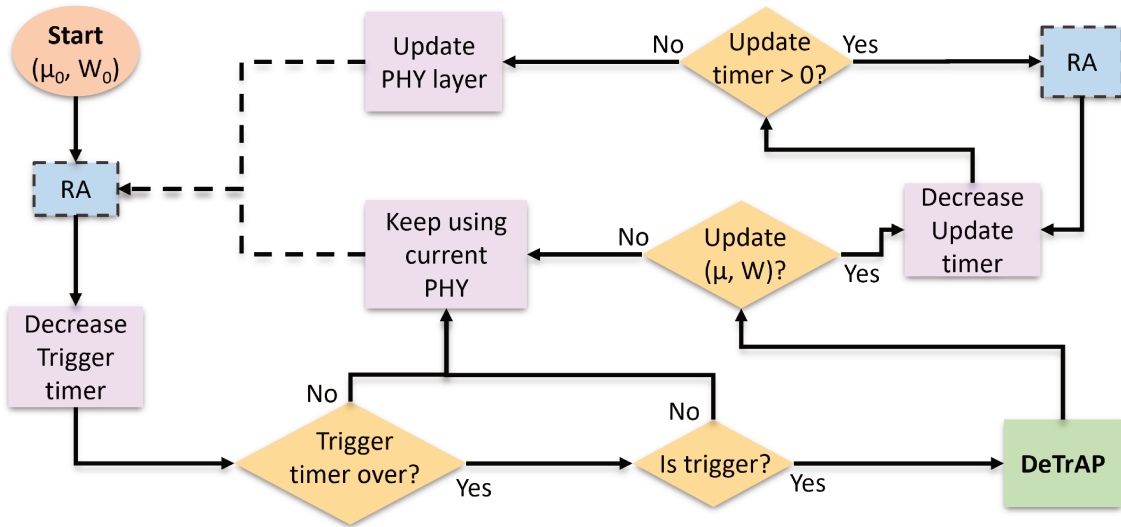


Figure 5.4 - Interaction between RA and DeTrAP

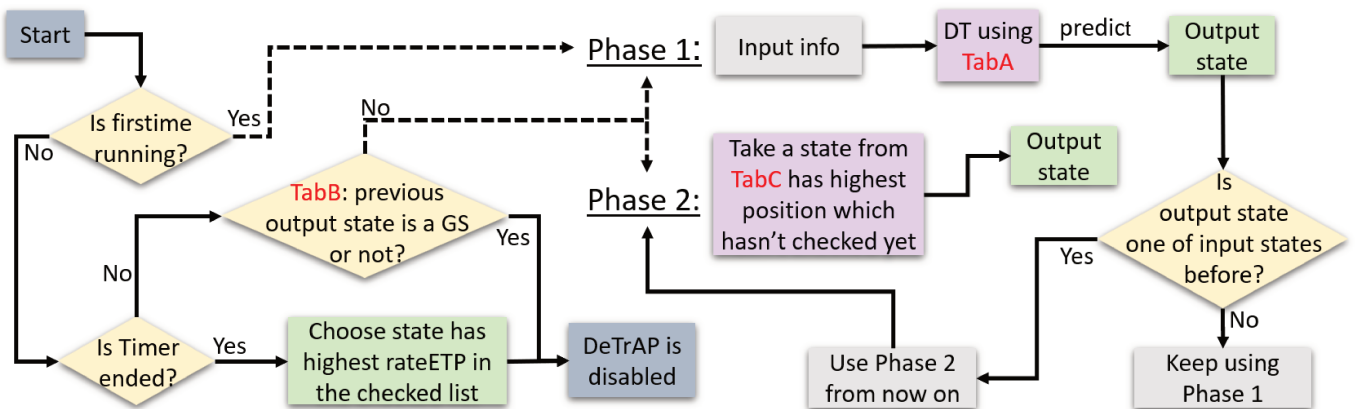


Figure 5.5 - The full algorithm of DeTrAP

in Phase 1, by feeding the information of the current environment to the DT to predict the output state based on TabA. If the predicted state output has already appeared, it means a loop may occur and affect the decision-making of DeTrAP, thus prompting it to switch to Phase 2.

In Phase 2, DeTrAP consults TabC and chooses the most frequent state output that has not been investigated. Every time DeTrAP is evoked, the information about rateETP of each current state (state input) will be saved. The rateETP of the state output of the current run will become the rateETP of the next run's state input. DeTrAP stops once it has found the GS. Whe-

ther a state output is identified as a GS depends on the TabB . Once the rateETP of the output state is computed, the rateETP is compared to Δ where $\Delta = \text{Avg}(\text{rateETP}) - \text{StDev}$ in TabB . If the $\text{rateETP} \geq \Delta$, the output state is considered the GS and DeTrAP stops.

Furthermore, DeTrAP is limited by a timer. If DeTrAP has not finished running at the end of the timer, the output state will be among those studied by DeTrAP with the highest rateETP . As there might exist special cases that were not recorded in past data, or perhaps the current environment is bad, the states that ought to be studied may reach an insufficient rateETP . In that case, we choose the state with the highest rateETP among the ones already investigated. We argue that a BS state is also a GS, but the reverse is not always true. Therefore, the chosen state may be BS if we iterate over all the states. To facilitate the computation, we run over all the remaining states to find the BS. If the chosen state is deemed a BS then it is also considered a GS.

5.5 . Performance Evaluation

We assess the performance of the proposed method using a self-developed simulator implementing the 3GPP R16 NR-V2X standard, built upon the LTEV2Vsim

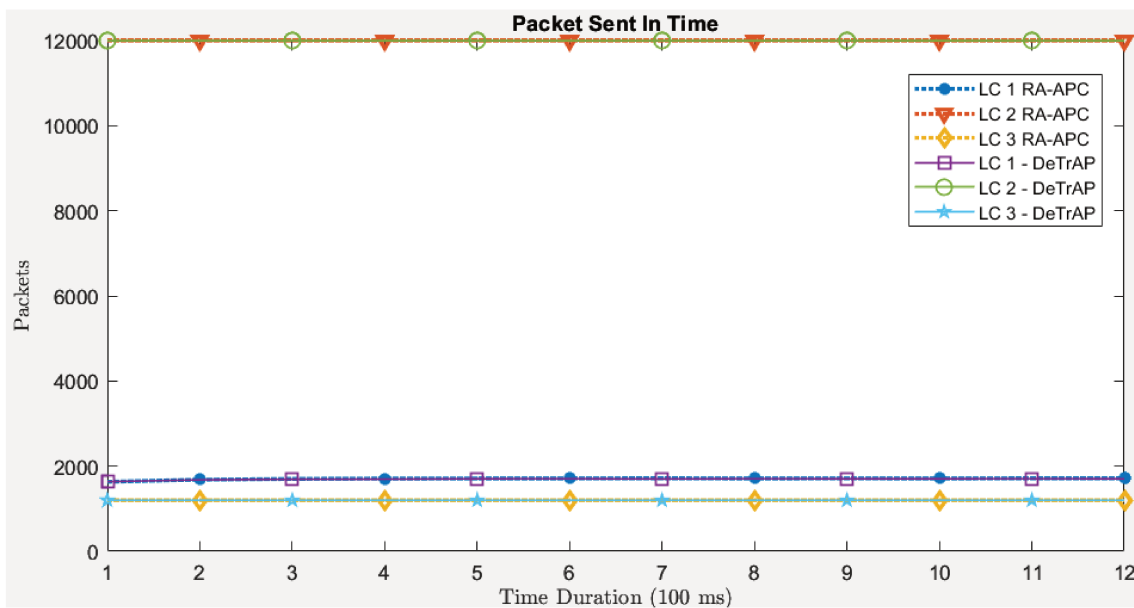


Figure 5.6 – Packet sent +/- DeTrAP

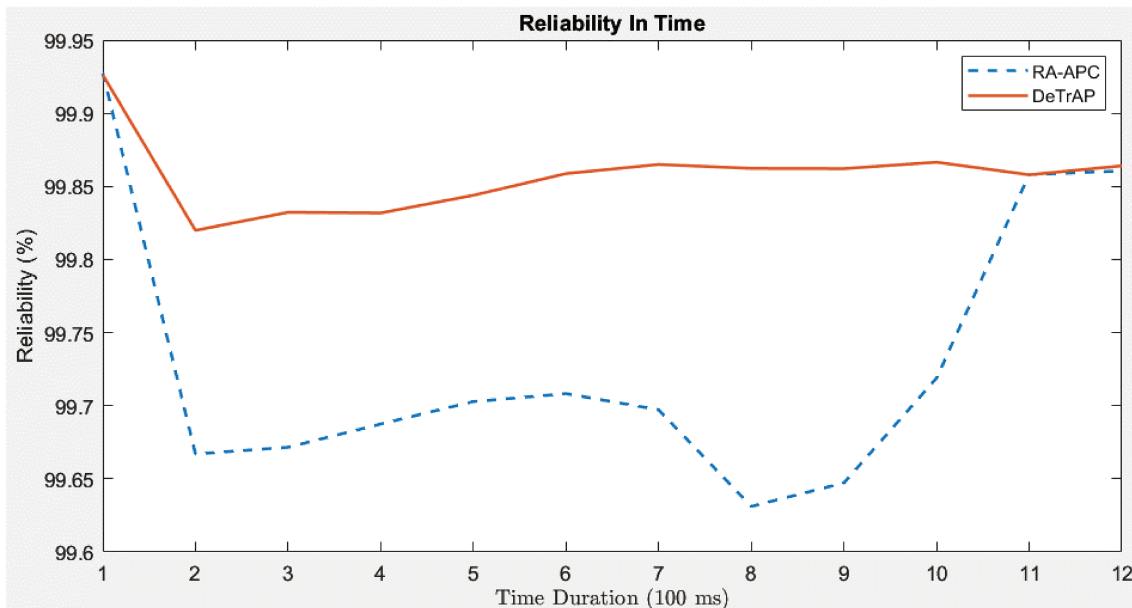


Figure 5.7 – Reliability +/- DeTrAP

v3.5 simulator¹. Table 5.5 summarizes the main network parameters.

To build the database for the first step (Figure 5.3, we run RA-APC with the appropriate parameters. We consider all density values from [100, 200, . . . , 1000] (vehicles/km) alongside 22 state inputs (Table 3.5) across seven cases (Table 5.6). For each scenario, we run 50 simulations to find the BSs. It amounts to 77000 simulations in total, the outputs of which are fed into our database, resulting in the three data sources TabA, TabB, and TabC.

Then, for each scenario, we run 10 simulations using DeTrAP to find the GS (15400 simulations in total). Table 5.7 shows the percentage of simulations that attain the GS for each case using DeTrAP on various Timers. Figure 5.8 displays the average time and probability that DeTrAP reaches the GS under Timer for all cases. For instance, if the Timer is set to 500 ms, 84.77% of 15400 simulations find the GS with an average search time of 219 ms. Therefore, DeTrAP reaches the GS on PHY layer much faster than RA-APC, which is more than 900ms.

Besides, we also study the effect of DeTrAP on the network performance compared to RA-APC. To compare RA-APC and DeTrAP, we test both algorithms on Case 7, having a density of 300 vehicles/km overall 22 states. Case

1. <https://github.com/alessandrobazzi/LTEV2Vsim>

Table 5.5 – Simulation network parameters

Name	Value
Size of map	4000m length × 21m width
Lanes	6 lanes in both directions
Frequency band	n47
Bandwidth	40 MHz
Velocity of vehicles	60 km/h
Density	[100, 200, 300 ... 1000] vehicles/km
Mode scheduling	Mode 1 Dynamic Grant
HARQ retransmissions	No
MIMO	No
DMRS pattern	2 symbols DMRS
Transmission power	23 dBm
Transmitter antenna gain	3 dB
Receiver antenna gain	3 dB
Noise figure	9 dB
Channel Model	3GPP 3-D mm-Wave [116]
CSI	Yes
Duplex Mode	Half-duplex
Mode communication	Unicast
Initial SCS - Subchannel size	All 22 states
Transport Block	1 slot × 1 or multiple subchannels
Symbol PSSCH per slot	14
Symbol for PSCCH	2
SCI 2 nd -stage type	SCI format 2-A
MCS	Table MCS 1
CQI	Table CQI 1

7 is chosen because it is the worst case that all LCs are activated. Figure 5.6 shows the number of packets successfully sent for each algorithm. For both algorithms, we see that the number of packets sent by each LC by RA-APC is the same as that by DeTrAP. Packet Sent is the packet that RA succeed to assign a TB to send.

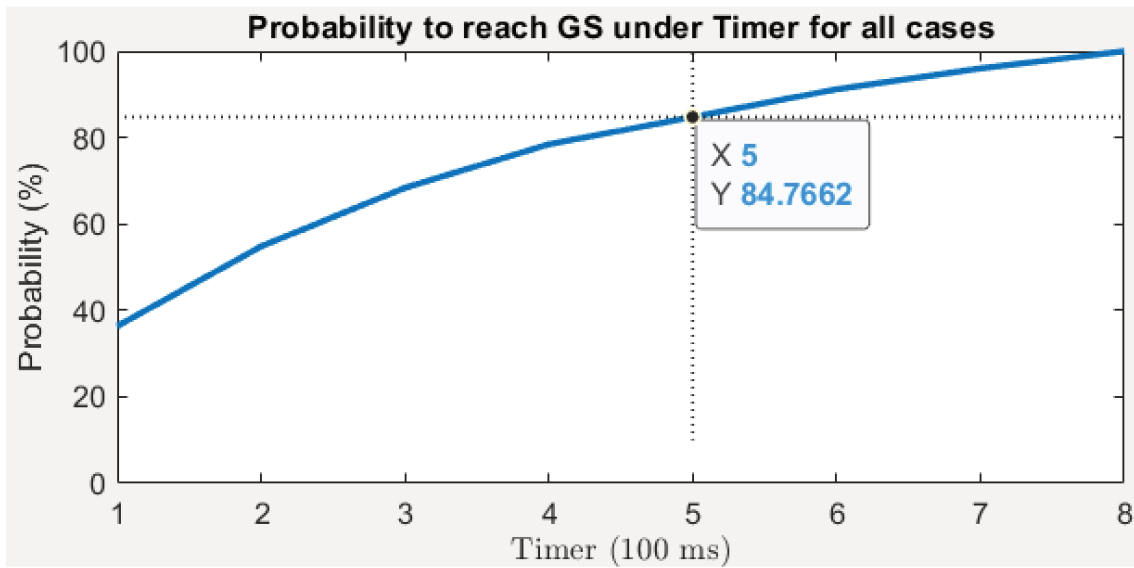


Figure 5.8 – Performance of DeTrAP under Timer

Table 5.6 – Case by combination of LCs

Case	1	2	3	4	5	6	7
LC 1	No	No	No	Yes	Yes	Yes	Yes
LC 2	No	Yes	Yes	No	No	Yes	Yes
LC 3	Yes	No	Yes	No	Yes	No	Yes

Figure 5.7 shows the average reliability of all LCs by RA-APC and DeTrAP. The reliability of DeTrAP is higher and more stable; as a result, the network performance of DeTrAP is better than RA-APC. This is explained by our proposal detecting and choosing the highest probability of obtaining a better state within a shorter time. Our proposal avoids observing all the states, in which some may yield worse performance. Meanwhile, RA-APC iterates over all states, thus attaining a suboptimal performance in some states. Moreover, we can see that the reliability of DeTrAP increases and remains stable; it is also as high as the reliability of RA-APC when the latter looks for a BS. This means the GS found by DeTrAP is as good as the BS found by RA-APC but in a shorter time, which adapt better for a dynamic nature of V2X environment.

Table 5.7 – Percentage of simulation achieved GS under Timer

Case	Timer (ms)	100	200	300	400	500	600	700	800
1	GS	566	1013	1354	1617	1834	2000	2109	2200
	Time (s)	56.6	146	248.3	353.5	462	561.6	637.9	710.7
2	GS	1033	1450	1742	1960	1986	2107	2160	2185
	Time (s)	103.3	186.7	274.3	361.5	374.5	447.1	484.2	504.2
3	GS	1056	1517	1823	2012	2044	2133	2182	2198
	Time (s)	105.6	197.8	289.6	365.2	381.2	434.6	468.9	481.7
4	GS	638	1038	1340	1585	1780	1950	2097	2200
	Time (s)	63.8	143.8	234.4	332.4	429.9	531.9	634.8	717.2
5	GS	687	1063	1368	1584	1766	1933	2074	2200
	Time (s)	68.7	143.9	235.4	321.8	412.8	513	611.7	712.5
6	GS	821	1189	1460	1670	1820	1955	2072	2178
	Time (s)	82.1	155.7	237	321	396	477	558.9	643.7
7	GS	795	1170	1442	1652	1824	1965	2088	2197
	Time (s)	79.5	154.5	236.1	320.1	406.1	490.7	576.8	664
Total GS		5596	8440	10529	12080	13054	14043	14782	15358
Percentage		36.34	54.81	68.37	78.44	84.77	91.19	95.99	99.73
Avg Time (ms)		100	133.70	166.69	196.65	219.28	246.09	268.79	288.73

5.6 . Conclusion

The contribution in this chapter proposes DeTrAP as a machine learning-based method for adapting the PHY layer configuration to address efficient resource allocation in V2X 5G NR. Built upon the previous work RA-APC, DeTrAP relies on a decision tree trained on past simulation data to find the BS (combination of μ and subchannel size W) heuristically, by eliminating the requirement to iterate the solution exhaustively space and by respecting a time limit. As a result, we expect DeTrAP to reach a GS without having to perform an exhaustive search within a short time in order to adequately address timely resource allocation for V2X communications.

We test DeTrAP on extensive simulations. The experimental results show

that DeTrAP achieves a superior network performance compared to RA-APC. DeTrAP also allows the telco operator to adapt the configuration of the PHY layer reliability faster.

6 - CONCLUSION AND FUTURE WORK

6.1 . Conclusion

To sum up, this thesis delves into the realm of adaptive numerology as it applies to resource allocation within the context of New Radio Vehicle-to-Everything (NR-V2X), particularly emphasizing on New Radio Vehicle-to-Vehicle (NR-V2V) sidelink communication. This research aimed to confront the intricate challenges associated with optimizing resource allocation within Vehicle-to-Everything (V2X) systems, while comprehensively considering the diverse communication necessities of both vehicles and infrastructural units. Following an exhaustive investigation and comprehensive analysis, we have unveiled a multitude of significant findings and contributions.

First, the thesis encompassed an in-depth investigation of the 3GPP Release 16 5G NR-V2X standard, particularly 5G NR V2V (NR-V2V). The research concentrated on the service requirements, quality of service, protocol stack, Physical layer, radio resource allocation mode, and other relevant aspects, providing understanding of their capabilities and functionalities.

Second, the thesis explored the problematic aspects of resource allocation in NR-V2X, including limited spectrum range, radio channel congestion, scalability, interoperability, etc. It highlighted the importance of implementing adaptive numerology allocation strategies that can mitigate these challenges and optimize resource utilization.

Thus, this thesis provided an in-depth review of the existing literature, research, and technologies regarding adaptive numerology in V2X communication. The manuscript discussed different approaches and algorithms mentioned in the literature, pointing out their value and limit in NR-V2X scenarios. The review provided valuable insights into state-of-the-art solutions and guided the development of the proposed adaptive numerology framework.

Based on the research findings, the thesis proposed three contributions :

Firstly, we proposed a novel algorithm named **Adaptive Physical layer Configuration, which is called APC**, to address the requirements of V2X resource allocation. APC examines how subchannel size and numerology im-

pact the system in centralized scheduling approach, in which the resource allocation is managed by the gNB, and broadcast mode communication. The primary objective of APC is to identify the best numerology and subchannel size configurations in the PHY layer to fulfill the the strictest QoS requirements for V2X communication. The **AESPR** has been implemented into the scheduler to prevent the presence of the starvation phenomenon issue. The results demonstrate that our proposal performs well in maximizing ETP and minimizing starvation for low-priority LCs.

Secondly, we improve APC by taking into account the channel state to make APC radio-aware, thus our second contribution is **Radio-Aware Adaptive Physical Layer Configuration (RA-APC)**. We studied the effects of the algorithm on Unicast communication and the flexibility of resources in terms of subchannel quantity. Our proposal, referred to as RA-APC, has been extensively simulated and achieved significant enhancements in ETP, reliability, and latency. Furthermore, in this study, we examined various combinations of numerology and subchannel size when applying RA-APC.

Finally, the convergence time required to find a good numerology and subchannel size can be further reduced by leveraging machine learning model. Precisely, we train a decision tree on the data generated by RA-APC to predict the output state given all the observational data. Our third contribution is **decision-tree-based RA-APC (DeTrAP)**. Apart from a decision tree as its core, DeTrAP also takes into consideration various densities, and the dynamic nature of V2X services. The results indicate that DeTrAP outperforms RA-APC in terms of network performance. This is achieved by reducing the time required to determine the appropriate numerology and subchannel size for different density and V2X service scenarios.

Furthermore, we have three more adding values as listed below :

1. Contribution as leader of one task in SARWS project which we explain in Appendix A on page 127.
2. Deploy 4G and 5G OpenAirInterface platform as described in Appendix B on page 129.
3. Self-developed a simulation namely 5GNRSidelinkSim, which is extended from LTEV2Vsim. This 5GNRSidelinkSim is modified, implemented 3GPP 5G NR-V2X R16 standard, and is used to run our experiments.

In summary, this thesis contributed to the issue of adaptive numerology for NR-V2X communication resource allocation. The research results and suggested methodology provide comprehensive knowledge as well as practical ideas for managing interference, allocating resources effectively, and improving the overall performance of NR-V2X systems.

6.2 . Perspectives

On-going work : In addition to the completed work in this thesis, an exciting avenue for further development in NR-V2X resource allocation lies in the implementation of reinforcement learning techniques. Specifically, reinforcement learning can enhance the adaptability of numerology and subchannel size in the PHY layer of NR-V2X. By applying reinforcement learning algorithms, we can optimize the decision-making process by dynamically adjusting the numerology and subchannel size based on real-time conditions. This eliminates the need for a database to predict the optimal "Good State" and instead relies on a reward function to guide decision-making and improve performance over time.

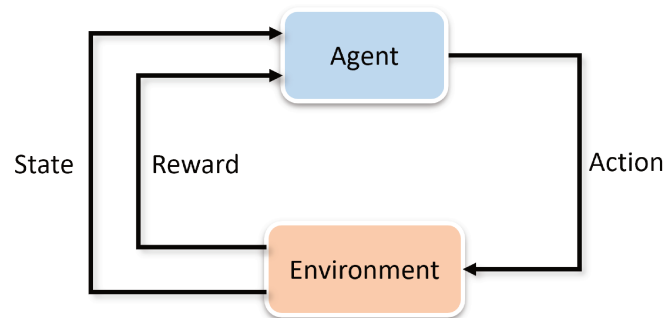


Figure 6.1 – Markov Decision Process

Reinforcement learning algorithm is based on the MDP theory [119][120] to discover the optimal policy through exploration and exploitation. State, action, transition probability, reward, and policy are the components of the MDP, as show in Figure 6.1. States denote the various configurations in which an agent can exist within its environment. Based on the current state, the agent chooses an action. Transition probabilities determine the probability

of moving from one state to another when the agent performs a particular action. Rewards show how desirable or useful a certain state or action is. A policy is a mapping between states and actions, defining the agent's behavior or strategy for selecting actions in various states. The policy guides the agent's decision-making process.

Reinforcement learning agents interact with the environment by observing the current state, choosing an action, moving to a new state, earning a reward, and adjusting their policy based on these interactions. The objective is to maximize the total rewards obtained over time.

Reinforcement learning is well-suited for the dynamic nature of the V2X environment since it allows the system to adapt and optimize its decisions in reaction to changing conditions. By comparing the results of reinforcement learning with the current DeTrAP algorithm, we are able to determine its impact on network performance and decision-making accuracy. This comparison will give us important information about how well and what other benefits there might be to adding reinforcement learning to 5G NR-V2X for flexible numerology and subchannel size.

The remaining tasks include implementing the proposed reinforcement learning algorithms in our self-developed simulator and running experiments to collect results. We aim to validate the effectiveness of this approach through intense simulation and experimentation.

The ongoing progress of reinforcement learning algorithms in the NR-V2X context shows great potential for the future. It provides opportunities to investigate advanced techniques including deep reinforcement learning or multi-agent reinforcement learning, to handle more complex decision-making scenarios.

In the near future, on one hand, in order to examine the outcomes using actual devices in a real-world environment, we will soon implement our algorithms on the Open-Air-Interface 5G platform that has already been deployed. The Open-Air-Interface is a non-profit consortium that aims to create an ecosystem for open-source software and hardware development for wireless cellular RAN and Core Network (CN) technologies based on the 3GPP standards. It was founded by EURECOM. The Universal Software Radio Peripheral (USRP) can be utilized as a base station (gNB), and a UE (smartphone) can connect to

the cellular CN via radio signal. On the other hand, we will implement and test with other schedulers in literature.

Future research may expand on the work done in this thesis by taking into consideration new, exciting study areas. **In our mid-term strategy**, by taking into account groupcast mode communication, we may, on the one hand, expand the RA-APC. The system will be able to handle more vehicles at a higher density since it will minimize the message exchange between pairs of vehicles. On the other hand, we can explore additional scenarios such as platooning, remote driving, extended sensors, and advanced driving. Hence, it would be interesting to investigate the impact of numerology on the system and enhance resource allocation in order to meet the requirements of such applications in the future. In addition, C-ITS aims to use Extremely High Frequency (EHF) above 60 GHz in Europe. There is insufficient research on the influence of numerology on the V2X system in this EHF.

A - Appendix : Celtic Next SARWS Euroepan project : Real-time location-aware road weather services composed from multi-modal data

The SARWS [124] project is a European project that utilizes C-ITS technology to enhance human comfort and safety. It aims to provide real results in a faster and more efficient manner. Through the utilization of RSU, combined RSUs and Road Weather Stations (RWS), vehicle data, road weather sensors, and ultimately mobile device data from each handheld device that can communicate and participate in traffic, this project is to expand the local data collection mechanisms from traditional road weather data sources to entirely new ones. The primary objective is to offer real-time weather services that improve the scalability, reliability, security, efficiency, safety, and sustainability of mobility and transportation.

Within the SARWS project, we served as the leader of task 3.3, which focuses on optimizing V2X protocol stack communications. The primary goal of this task is to address the design of the complete communication protocol stack for V2X. This involves exchanging data to establish weather and air quality information, like maps, without relying on infrastructure. In short, it refers to communication between vehicles (V2V) or between vehicles and infrastructure (V2I). This task primarily focuses on ITS-G5 and C-V2X (LTE-V2X and NR-V2X) communication technologies. We collaborated with the following partners CEA, Yogoko from France, Instituto de Telecomunicações, and Eurico Ferreira SA from Portugal, to contribute to the task. We are responsible for the module related to NR-V2X 3GPP Release 16 among the works. As a result, we contributed a technical report for Deliverable D3.3 entitled “Optimization of V2X protocol stack communications”.

The SARWS project accomplished its objective and finished last year after four years of collaboration.

B - Appendix : Cellular network with OpenAir-Interface platform

Open-Air-Interface platform (OAI) [125] is an open-source software platform that provides a flexible and modifiable implementation of the cellular network. It was initially developed by the French university, EURECOM. Cellular network technology, such as 4G and 5G networks, can be developed, tested, and experimented with OAI.

The advantage of this platform is its ability to interact with USRP devices, e.g. B210, X310, N200 from Ettus. USRP is a Software Defined Radio (SDR) device that serves as a customizable transceiver for designing, prototyping, and deploying radio communication systems. Consequently, simulation and emulation are possible using this platform.

Furthermore, it is an open-source software platform. Thus, we can modify the source code, implement our algorithms to do real experimentations.



Figure B.1 – USRP B210

Thus, we observed, studied, and deployed (Figure B.2) three scenarios of OAI

1. 4G cellular network : We built 4G core network (EPC) in one server, one computer with USRP B210 (Figure B.1) acted as eNB. UE was a smartphone (tested with Huawei P30 Pro, Iphone SE 2022) or a computer



Figure B.2 – OAI platform

which is connected to a USRP B210.

2. 5G Non-standalone (NSA) : from 4G platform, we deployed a gNB by using a computer connect to a USRP B210. In this scenario, UE is emulated by USRP.
3. 5G Standalone (SA) : We built 5GC then deployed a gNB by using a computer connect to a USRP B210. In this scenario, UE is emulated by USRP.

We plan to modify the OAI source code in near future in two steps :

1. Build a sidelink platform under mode 1 DG and CG.
2. Implement RA-APC and scheduler.

C - Appendix : Modulation and Coding Scheme tables

This appendix contains three MCS tables from [\[68\]](#).

Table C.1 – MCS index table 1

MCS Index	Modulation Order Q_m	Target code Rate $R \times [1024]$	Spectral efficiency
0	2	120	0.2344
1	2	157	0.3066
2	2	193	0.3770
3	2	251	0.4902
4	2	308	0.6016
5	2	379	0.7402
6	2	449	0.8770
7	2	526	1.0273
8	2	602	1.1758
9	2	679	1.3262
10	4	340	1.3281
11	4	378	1.4766
12	4	434	1.6953
13	4	490	1.9141
14	4	553	2.1602
15	4	616	2.4063
16	4	658	2.5703
17	6	438	2.5664
18	6	466	2.7305
19	6	517	3.0293
20	6	567	3.3223
21	6	616	3.6094
22	6	666	3.9023
23	6	719	4.2129
24	6	772	4.5234
25	6	822	4.8164
26	6	873	5.1152
27	6	910	5.3320
28	6	948	5.5547
29	2		reserved
30	4		reserved
31	6		reserved

Table C.2 – MCS index table 2

MCS Index	Modulation Order Q_m	Target code Rate $R \times [1024]$	Spectral efficiency
0	2	120	0.2344
1	2	193	0.3770
2	2	308	0.6016
3	2	449	0.8770
4	2	602	1.1758
5	4	378	1.4766
6	4	434	1.6953
7	4	490	1.9141
8	4	553	2.1602
9	4	616	2.4063
10	4	658	2.5703
11	6	466	2.7305
12	6	517	3.0293
13	6	567	3.3223
14	6	616	3.6094
15	6	666	3.9023
16	6	719	4.2129
17	6	772	4.5234
18	6	822	4.8164
19	6	873	5.1152
20	8	682.5	5.3320
21	8	711	5.5547
22	8	754	5.8906
23	8	797	6.2266
24	8	841	6.5703
25	8	885	6.9141
26	8	916.5	7.1602
27	8	948	7.4063
28	2		reserved
29	4		reserved
30	6		reserved
31	8		reserved

Table C.3 – MCS index table 3

MCS Index	Modulation Order Q_m	Target code Rate $R \times [1024]$	Spectral efficiency
0	2	30	0.0586
1	2	40	0.0781
2	2	50	0.0977
3	2	64	0.1250
4	2	78	0.1523
5	2	99	0.1934
6	2	120	0.2344
7	2	157	0.3066
8	2	193	0.3770
9	2	251	0.4902
10	2	308	0.6016
11	2	379	0.7402
12	2	449	0.8770
13	2	526	1.0273
14	2	602	1.1758
15	4	340	1.3281
16	4	378	1.4766
17	4	434	1.6953
18	4	490	1.9141
19	4	553	2.1602
20	4	616	2.4063
21	6	438	2.5664
22	6	466	2.7305
23	6	517	3.0293
24	6	567	3.3223
25	6	616	3.6094
26	6	666	3.9023
27	6	719	4.2129
28	6	772	4.5234
29	2		reserved
30	4		reserved
31	6		reserved

D - Appendix : Channel Quality Indicator tables

This appendix contains three CQI tables from [68].

Table D.1 – CQI table 1

CQI Index	Modulation	code rate $\times 1024$	efficiency
0		out of range	
1	QPSK	78	0.1523
2	QPSK	120	0.2344
3	QPSK	193	0.3770
4	QPSK	308	0.6016
5	QPSK	449	0.8770
6	QPSK	602	1.1758
7	16QAM	378	1.4766
8	16QAM	490	1.9141
9	16QAM	616	2.4063
10	64QAM	466	2.7305
11	64QAM	567	3.3223
12	64QAM	666	3.9023
13	64QAM	772	4.5234
14	64QAM	873	5.1152
15	64QAM	948	5.5547

Table D.2 – CQI table 2

CQI Index	Modulation	code rate $\times 1024$	efficiency
0		out of range	
1	QPSK	78	0.1523
2	QPSK	193	0.3770
3	QPSK	449	0.8770
4	16QAM	378	1.4766
5	16QAM	490	1.9141
6	16QAM	616	2.4063
7	64QAM	466	2.7305
8	64QAM	567	3.3223
9	64QAM	666	3.9023
10	64QAM	772	4.5234
11	64QAM	873	5.1152
12	256QAM	711	5.5547
13	256QAM	797	6.2266
14	256QAM	885	6.9141
15	256QAM	948	7.4063

Table D.3 – CQI table 3

CQI Index	Modulation	code rate $\times 1024$	efficiency
0		out of range	
1	QPSK	30	0.0586
2	QPSK	50	0.0977
3	QPSK	78	0.1523
4	QPSK	120	0.2344
5	QPSK	193	0.3770
6	QPSK	308	0.6016
7	QPSK	449	0.8770
8	QPSK	602	1.1758
9	16QAM	378	1.4766
10	16QAM	490	1.9141
11	16QAM	616	2.4063
12	64QAM	466	2.7305
13	64QAM	567	3.3223
14	64QAM	666	3.9023
15	64QAM	772	4.5234

E - Appendix : Use Case Group Requirement Tables

This appendix contains tables of requirements of each Use Case Group Vehicles Platooning, Advanced Driving, Extended Sensors and Remote Driving.

Table E.1 – Performance requirements for Vehicles Platooning use case group

Communication scenario description		Payload (Bytes)	Tx rate (Message/Sec)	Max end-to-end latency (ms)	Reliability (%)	Data rate (Mbps)	Min required communication range (meters) (130km/h relative speed)
Scenario	Degree						
Cooperative driving for vehicle platooning Information exchange between a group of UEs	Lowest degree of automation	300-400	30	25	90	-	-
	Low degree of automation	6500	50	20	-	-	350
	Highest degree of automation	50-1200	30	10	99.99	-	80
	High degree of automation	-	-	20	-	65	180
Reporting needed for platooning	N/A	50-1200	2	500	-	-	-
Information sharing for platooning	Lower degree of automation	6000	50	20	-	-	350
	Higher degree of automation	-	-	20	-	50	180

Table E.2 – Performance requirements for Advanced Driving use case group

Communication scenario description		Payload (Bytes)	Tx rate (Message/Sec)	Max end-to-end latency (ms)	Reliability (%)	Data rate (Mbps)	Min required communication range (meters) (130km/h relative speed)
Scenario	Degree						
Cooperative collision avoidance between UEs supporting V2X applications		2000	100	10	99.99	10	-
Information sharing for automated driving between UEs supporting V2X application.	Lower degree of automation	6500	10	100	-	-	700
	Higher degree of automation	-	-	100	-	53	360
Information sharing for automated driving between UE supporting V2X application and RSU	Lower degree of automation	6000	10	100	-	-	700
	Higher degree of automation	-	-	100	-	50	360
Emergency trajectory alignment between UEs supporting V2X application		2000	-	3	99.999	30	500
Intersection safety information between an RSU and UEs supporting V2X application.		UL : 450	UL : 50	-	-	UL : 0.25 DL : 50	-
Cooperative lane change between UEs supporting V2X applications.	Lower degree of automation	300-400	-	25	90	-	-
	Higher degree of automation	12000	-	10	-	99.99	-
Video sharing between a UE supporting V2X application and a V2X application server.		-	-	-	-	UL : 0.10	-

Table E.3 – Performance requirements for Extended Sensors use case group

Communication scenario description		Payload (Bytes)	Tx rate (Message/Sec)	Max end-to-end latency (ms)	Reliability (%)	Data rate (Mbps)	Min required communication range (meters) (130km/h relative speed)
Scenario	Degree						
Sensor information sharing between UEs supporting V2X application	Lower degree of automation	1600	10	100	99	-	1000
	Higher degree of automation	-	-	10	95	25	-
		-	-	3	99.999	50	200
		-	-	10	99.99	25	500
		-	-	50	99	10	1000
-	-	10	99.99	1000	50		
Video sharing between UEs supporting V2X application	Lower degree of automation	-	-	50	90	10	100
	Higher degree of automation	-	-	10	99.99	700	200
		-	-	10	99.99	90	400

Table E.4 – Performance requirements for Remote Driving use case group

Communication scenario description	Max end-to-end latency (ms)	Reliability (%)	Data rate (Mbps)
Information exchange between a UE supporting V2X application and a V2X Application Server	5	99.999	UL : 25 DL : 1

F - Appendix : First stage SCI structure

This appendix presents in-detail twelve fields of 1st-stage SCI.

- Priority : 3 bits. The priority value is the highest priority of the LC(s) in MAC PDU.
- Frequency resource assignment :
– $x = \lceil \log_2 ((N_{subchannel}^{SL} \times (N_{subchannel}^{SL} + 1)) / 2) \rceil$ in case sl-NumPerReserve parameter from RRC is configured to 2 or
– $x = \lceil \log_2 ((N_{subchannel}^{SL} \times (N_{subchannel}^{SL} + 1) \times (2 \times N_{subchannel}^{SL} + 1)) / 6) \rceil$ in case it is configured to 3.
- Time resource assignment : 5 in case sl-NumPerReserve parameter from RRC is configured to 2 or 9 bits in case sl-NumPerReserve is configured to 3.
- Resource reservation period : 0 if sl-MultiReserveResource parameter is not set, otherwise up to 4 bits to for maximum 16 entries in that parameter of RRC.
- DMRS pattern : 2 bits for maximum 3 entries in parameter sl-PSSCH-DMRS-TimePatternList parameter from RRC.
- 2nd-stage SCI format : 2 bits which '00' is for SCI format 2-A and '01' is for SCI format 2-B.
- Beta_offset indicator : 2 bits by parameter sl-BetaOffsets2ndSCI parameter.
- Number of DMRS port : 1 bit
- Modulation and coding scheme : 5 bits
- Additional MCS table indicator : 0, 1 or 2 depends on parameter sl-Additional-MCS-Table parameter.
- PSFCH overhead indication : 0 or 1 bit depends on parameter sl-PSFCH-Period value.
- Reserved : from 2 to 4 bits, which is set by sl-NumReservedBits parameter.

G - Appendix : Transport Block Size determination

This appendix contains the table for calculating TBS.

Table G.1 – TBS for $N_{info} \leq 3824$

Index	TBS	Index	TBS
1	24	48	768
2	32	49	808
3	40	50	848
4	48	51	888
5	56	52	928
6	64	53	984
7	72	54	1032
8	80	55	1064
9	88	56	1128
10	96	57	1160
11	104	58	1192
12	112	59	1224
13	120	60	1256
14	128	61	1288
15	136	62	1320
16	144	63	1352
17	152	64	1416
18	160	65	1480
19	168	66	1544
20	176	67	1608
21	184	68	1672
22	192	69	1736
23	208	70	1800
24	224	71	1864
25	240	72	1928
26	256	73	2024
27	272	74	2088
28	288	75	2152

Table G.1 – (continued)

Index	TBS	Index	TBS
29	304	76	2216
30	320	77	2280
31	336	78	2408
32	352	79	2472
33	368	80	2536
34	384	81	2600
35	408	82	2664
36	432	83	2728
37	456	84	2792
38	480	85	2856
39	504	86	2976
40	528	87	3104
41	552	88	3240
42	576	89	3368
43	608	90	3496
44	640	91	3624
45	672	92	3752
46	704	93	3824
47	736	-	-

Bibliographie

- [1] E. C. of Auditors, *Urban mobility in the EU*. Accessed : April, 2019. adresse : https://www.eca.europa.eu/lists/ecadocuments/ap19_07/ap_urban_mobility_en.pdf.
- [2] 5GAA, *5GAA support to V2X pilots and projects* Accessed : 2018. adresse : <https://5g-ppp.eu/wp-content/uploads/2018/09/27-Michael-Neaves.pdf>.
- [3] I. 8. p, *IEEE standard for information technology-Local and metropolitan area networks-Specific requirements-Part 11 : Wireless LAN medium access control (MAC) and physical layer (PHY) specifications amendment 5 : Enhancements for higher throughput*, 2009.
- [4] Y. J. Li, « An Overview of the DSRC/WAVE Technology, » *Quality, Reliability, Security and Robustness in Heterogeneous Networks*, p. 544, 2011.
- [5] I. S. Association et al., *IEEE 802.11 p-2010-IEEE standard for information technology-local and metropolitan area networks-specific requirements-part 11 : Wireless LAN medium access control (MAC) and physical layer (PHY) specifications amendment 6 : Wireless access in vehicular environments*, 2019.
- [6] ETSI, « Intelligent Transport Systems (ITS); Access layer specification for Intelligent Transport Systems operating in the 5 GHz frequency band, » European Telecommunications Standards Institute (ETSI), Standard 302 663, nov. 2012, V1.2.0. adresse : http://www.etsi.org/deliver/etsi_en/302600_302699/302663/01.02.00_20/en_302663v010200a.pdf.
- [7] I. C. Msadaa, P. Cataldi et F. Filali, « A comparative study between 802.11 p and mobile WiMAX-based V2I communication networks, » in *2010 fourth international conference on next generation mobile applications, services and technologies*, IEEE, 2010, p. 186-191.

- [8] F. telecom (FRANCE), *The WAVE Communications Stack : IEEE 802.11p, 1609.4 and, 1609.3* Accessed : 2007. adresse : http://herve.boeglen.free.fr/Files_IUT/wave_com_stack.PDF.
- [9] T. Etsi, « Intelligent transport systems (its); decentralized congestion control mechanisms for intelligent transport systems operating in the 5 ghz range; access layer part, » *ETSI TS*, t. 102, n° 687, p. V1, 2011.
- [10] I. ETSI, « Intelligent Transport Systems (ITS); Radiocommunications equipment operating in the 5 855 MHz to 5 925 MHz frequency band; Harmonised Standard covering the essential requirements of article 3.2 of Directive 2014/53/EU, » *EN*, t. 302, n° 571, p. V2, 2016.
- [11] IEEE, *IEEE P802.11—Next Generation V2X Study Group* Accessed : May 30, 2019. adresse : http://www.ieee802.org/11/Reports/tgbd_update.htm.
- [12] I. 8. bd, *802.11bd-2022 - IEEE Standard for Information Technology–Telecommunications and Information Exchange between Systems Local and Metropolitan Area Networks–Specific Requirements Part 11 : Wireless LAN Medium Access Control (MAC) and Physical Layer (PHY) Specifications Amendment 5 : Enhancements for Next Generation V2X*. adresse : <https://ieeexplore.ieee.org/document/10063942>.
- [13] 3rd Generation Partnership Project (3GPP), « Proximity-based services (ProSe); Stage 2, » 3rd Generation Partnership Project (3GPP), Technical specification (TS) 23.303, déc. 2016, v13.6.0. adresse : https://www.3gpp.org/ftp/Specs/archive/23_series/23.303/.
- [14] 3rd Generation Partnership Project (3GPP), « Technical Specifications and Technical Reports for a UTRAN-based 3GPP system, » 3rd Generation Partnership Project (3GPP), Technical specification (TS) 21.101, mars 2016, v12.0.0. adresse : https://www.3gpp.org/ftp/Specs/archive/21_series/21.101/.

- [15] 3rd Generation Partnership Project (3GPP), « Technical Specifications and Technical Reports for a UTRAN-based 3GPP system, » 3rd Generation Partnership Project (3GPP), Technical specification (TS) 21.101, déc. 2016, v13.0.0. adresse : https://www.3gpp.org/ftp/Specs/archive/21_series/21.101/.
- [16] 3rd Generation Partnership Project (3GPP), « Architecture enhancements for V2X services, » 3rd Generation Partnership Project (3GPP), Technical specification (TS) 23.285, sept. 2016, v14.0.0. adresse : https://www.3gpp.org/ftp/Specs/archive/23_series/23.285/.
- [17] 3rd Generation Partnership Project (3GPP), « Release 14 Description; Summary of Rel-14 Work Items, » 3rd Generation Partnership Project (3GPP), Technical report (TR) 21.914, juin 2018, v14.0.0. adresse : https://www.3gpp.org/ftp/Specs/archive/21_series/21.914/.
- [18] 3rd Generation Partnership Project (3GPP), « Service requirements for V2X services, » 3rd Generation Partnership Project (3GPP), Technical specification (TS) 22.185, mars 2016, v14.0.0. adresse : https://www.3gpp.org/ftp/Specs/archive/22_series/22.185/.
- [19] 3rd Generation Partnership Project (3GPP), « Release 15 Description; Summary of Rel-15 Work Items, » 3rd Generation Partnership Project (3GPP), Technical report (TR) 21.915, oct. 2019, v15.0.0. adresse : https://www.3gpp.org/ftp/Specs/archive/21_series/21.915/.
- [20] R. Molina-Masegosa et J. Gozalvez, « LTE-V for sidelink 5G V2X vehicular communications : A new 5G technology for short-range vehicle-to-everything communications, » *IEEE Vehicular Technology Magazine*, t. 12, n° 4, p. 30-39, 2017.
- [21] 3rd Generation Partnership Project (3GPP), « System architecture for the 5G System (5GS), » 3rd Generation Partnership Project (3GPP), Technical Specification (TS) 23.501, déc. 2017, v15.0.0. adresse : https://www.3gpp.org/ftp/Specs/archive/23_series/23.501/.

- [22] 3rd Generation Partnership Project (3GPP), « Study on NR Vehicle-to-Everything (V2X), » 3rd Generation Partnership Project (3GPP), Technical report (TR) 38.885, mars 2019, v16.0.0. adresse : https://www.3gpp.org/ftp/Specs/archive/38_series/38.885/.
- [23] 3rd Generation Partnership Project (3GPP), « Architecture enhancements for 5G System (5GS) to support Vehicle-to-Everything (V2X) services, » 3rd Generation Partnership Project (3GPP), Technical specification (TS) 23.287, sept. 2019, v16.0.0. adresse : https://www.3gpp.org/ftp/Specs/archive/23_series/23.287/.
- [24] 3rd Generation Partnership Project (3GPP), « Release 16 Description; Summary of Rel-16 Work Items, » 3rd Generation Partnership Project (3GPP), Technical report (TR) 21.916, juin 2021, v16.0.0. adresse : https://www.3gpp.org/ftp/Specs/archive/21_series/21.916/.
- [25] 3rd Generation Partnership Project (3GPP), « Release 17 Description; Summary of Rel-17 Work Items, » 3rd Generation Partnership Project (3GPP), Technical report (TR) 21.917, jan. 2023, v16.0.1. adresse : https://www.3gpp.org/ftp/Specs/archive/21_series/21.917/.
- [26] 3rd Generation Partnership Project (3GPP), « Study on architecture enhancements for 3GPP support of advanced Vehicle-to-Everything (V2X) services; Phase 2, » 3rd Generation Partnership Project (3GPP), Technical report (TR) 23.776, mars 2021, v17.0.0. adresse : https://www.3gpp.org/ftp/Specs/archive/23_series/23.776/.
- [27] 3rd Generation Partnership Project (3GPP), « Vehicle-to-Everything (V2X) services in 5G System (5GS); Stage 3, » 3rd Generation Partnership Project (3GPP), Technical specification (TS) 24.587, jan. 2023, v17.8.0. adresse : https://www.3gpp.org/ftp/Specs/archive/24_series/24.587/.
- [28] 3rd Generation Partnership Project (3GPP), « Vehicle-to-Everything (V2X) services in 5G System (5GS); User Equipment (UE) policies; Stage 3, » 3rd Generation Partnership Project (3GPP), Technical

- specification (TS) 24.588, jan. 2023, v17.2.0. adresse : https://www.3gpp.org/ftp/Specs/archive/24_series/24.588/.
- [29] 3rd Generation Partnership Project (3GPP), « Application layer support for Vehicle-to-Everything (V2X) services; Functional architecture and information flows, » 3rd Generation Partnership Project (3GPP), Technical specification (TS) 23.286, juin 2022, v17.4.0. adresse : https://www.3gpp.org/ftp/Specs/archive/23_series/23.286/.
- [30] 3rd Generation Partnership Project (3GPP), « V2X Application Enabler (VAE) Services; Stage 3, » 3rd Generation Partnership Project (3GPP), Technical specification (TS) 29.486, sept. 2022, v17.6.0. adresse : https://www.3gpp.org/ftp/Specs/archive/29_series/29.486/.
- [31] 3rd Generation Partnership Project (3GPP), « Vehicle-to-Everything (V2X) Application Enabler (VAE) layer; Protocol aspects; Stage 3, » 3rd Generation Partnership Project (3GPP), Technical specification (TS) 24.486, avr. 2023, v17.6.0. adresse : https://www.3gpp.org/ftp/Specs/archive/24_series/24.486/.
- [32] 3rd Generation Partnership Project (3GPP), « Study on application layer support for V2X services, » 3rd Generation Partnership Project (3GPP), Technical report (TR) 23.795, déc. 2018, v16.1.0. adresse : https://www.3gpp.org/ftp/Specs/archive/23_series/23.795/.
- [33] 3rd Generation Partnership Project (3GPP), « Study on enhancements to application layer support for V2X services, » 3rd Generation Partnership Project (3GPP), Technical report (TR) 23.764, déc. 2020, v17.1.0. adresse : https://www.3gpp.org/ftp/Specs/archive/23_series/23.764/.
- [34] 3rd Generation Partnership Project (3GPP), « Northbound Application Programming Interface (API) for Multimedia Broadcast/Multicast Service (MBMS) at the xMB reference point, » 3rd Generation Partnership Project (3GPP), Technical specification (TS) 26.348, juin 2022, v17.1.0. adresse : https://www.3gpp.org/ftp/Specs/archive/26_series/26.348/.

- [35] 3rd Generation Partnership Project (3GPP), « Multimedia Broadcast/Multicast Service (MBMS); Protocols and codecs, » 3rd Generation Partnership Project (3GPP), Technical specification (TS) 26.346, mars 2023, v17.3.0. adresse : https://www.3gpp.org/ftp/Specs/archive/26_series/26.346/.
- [36] 3rd Generation Partnership Project (3GPP), « Multimedia Broadcast/Multicast Service (MBMS); Architecture and functional description, » 3rd Generation Partnership Project (3GPP), Technical specification (TS) 23.246, mars 2022, v17.0.0. adresse : https://www.3gpp.org/ftp/Specs/archive/23_series/23.246/.
- [37] 3GPP, *The 5G standard Accessed : 2023*. adresse : https://www.3gpp.org/ftp/Inbox/Marcoms/3GPP_Poster%5C%20v2.pdf.
- [38] S. Eichler, « Performance evaluation of the IEEE 802.11 p WAVE communication standard, » in *2007 IEEE 66th Vehicular Technology Conference*, IEEE, 2007, p. 2199-2203.
- [39] C. Campolo, A. Vinel, A. Molinaro et Y. Koucheryavy, « Modeling broadcasting in IEEE 802.11 p/WAVE vehicular networks, » *IEEE Communications letters*, t. 15, n^o 2, p. 199-201, 2010.
- [40] K. Bilstrup, E. Uhlemann, E. G. Strom et U. Bilstrup, « Evaluation of the IEEE 802.11 p MAC method for vehicle-to-vehicle communication, » in *2008 IEEE 68th Vehicular Technology Conference*, IEEE, 2008, p. 1-5.
- [41] C. Han, M. Dianati, R. Tafazolli, R. Kernchen et X. Shen, « Analytical study of the IEEE 802.11 p MAC sublayer in vehicular networks, » *IEEE Transactions on Intelligent Transportation Systems*, t. 13, n^o 2, p. 873-886, 2012.
- [42] H. King, K. Nolan et M. Kelly, « Interoperability between DSRC and LTE for VANETs, » in *2018 IEEE 13th International Symposium on Industrial Embedded Systems (SIES)*, IEEE, 2018, p. 1-8.
- [43] Z. Khan, P. Fan, F. Abbas, H. Chen et S. Fang, « Two-level cluster based routing scheme for 5G V2X communication, » *IEEE Access*, t. 7, p. 16 194-16 205, 2019.

- [44] G. Cecchini, A. Bazzi, B. M. Masini et A. Zanella, « Performance comparison between IEEE 802.11 p and LTE-V2V in-coverage and out-of-coverage for cooperative awareness, » in *2017 IEEE Vehicular Networking Conference (VNC)*, IEEE, 2017, p. 109-114.
- [45] A. Bazzi, G. Cecchini, M. Menarini, B. M. Masini et A. Zanella, « Survey and perspectives of vehicular Wi-Fi versus sidelink cellular-V2X in the 5G era, » *Future Internet*, t. 11, n° 6, p. 122, 2019.
- [46] R. Molina-Masegosa, J. Gozalvez et M. Sepulcre, « Comparison of IEEE 802.11 p and LTE-V2X : An evaluation with periodic and aperiodic messages of constant and variable size, » *IEEE Access*, t. 8, p. 121 526-121 548, 2020.
- [47] G. P. W. NBA, J. Haapola et T. Samarasinghe, « A discrete-time Markov chain based comparison of the MAC layer performance of C-V2X mode 4 and IEEE 802.11 p, » *IEEE Transactions on Communications*, t. 69, n° 4, p. 2505-2517, 2020.
- [48] V. Mannoni, V. Berg, S. Sesia et E. Perraud, « A comparison of the V2X communication systems : ITS-G5 and C-V2X, » in *2019 IEEE 89th Vehicular Technology Conference (VTC2019-Spring)*, IEEE, 2019, p. 1-5.
- [49] G. Naik, B. Choudhury et J.-M. Park, « IEEE 802.11 bd & 5G NR V2X : Evolution of radio access technologies for V2X communications, » *IEEE access*, t. 7, p. 70 169-70 184, 2019.
- [50] 3rd Generation Partnership Project (3GPP), « Service Enabler Architecture Layer for Verticals (SEAL); Application Programming Interface (API) specification; Stage 3, » 3rd Generation Partnership Project (3GPP), Technical specification (TS) 29.549, déc. 2022, v17.7.0. adresse : https://www.3gpp.org/ftp/Specs/archive/29_series/29.549/.
- [51] 3rd Generation Partnership Project (3GPP), « Location Management - Service Enabler Architecture Layer for Verticals (SEAL); Protocol specification, » 3rd Generation Partnership Project (3GPP), Technical specification (TS) 24.545, jan. 2023, v17.5.0. adresse : https://www.3gpp.org/ftp/Specs/archive/24_series/24.545/.

- [52] 3rd Generation Partnership Project (3GPP), « Group Management - Service Enabler Architecture Layer for Verticals (SEAL); Protocol specification, » 3rd Generation Partnership Project (3GPP), Technical specification (TS) 24.544, jan. 2023, v17.4.0. adresse : https://www.3gpp.org/ftp/Specs/archive/24_series/24.544/.
- [53] 3rd Generation Partnership Project (3GPP), « Configuration management - Service Enabler Architecture Layer for Verticals (SEAL); Protocol specification, » 3rd Generation Partnership Project (3GPP), Technical specification (TS) 24.546, jan. 2023, v17.5.0. adresse : https://www.3gpp.org/ftp/Specs/archive/24_series/24.546/.
- [54] 3rd Generation Partnership Project (3GPP), « Identity management - Service Enabler Architecture Layer for Verticals (SEAL); Protocol specification, » 3rd Generation Partnership Project (3GPP), Technical specification (TS) 24.547, avr. 2023, v17.3.0. adresse : https://www.3gpp.org/ftp/Specs/archive/24_series/24.547/.
- [55] 3rd Generation Partnership Project (3GPP), « Security aspects of Service Enabler Architecture Layer (SEAL) for verticals, » 3rd Generation Partnership Project (3GPP), Technical specification (TS) 33.434, sept. 2022, v17.3.0. adresse : https://www.3gpp.org/ftp/Specs/archive/33_series/33.434/.
- [56] 3rd Generation Partnership Project (3GPP), « Network Resource Management - Service Enabler Architecture Layer for Verticals (SEAL); Protocol specification, » 3rd Generation Partnership Project (3GPP), Technical specification (TS) 24.548, avr. 2023, v17.4.0. adresse : https://www.3gpp.org/ftp/Specs/archive/24_series/24.548/.
- [57] 3rd Generation Partnership Project (3GPP), « NR; Radio Resource Control (RRC); Protocol specification, » 3rd Generation Partnership Project (3GPP), Technical specification (TS) 38.331, avr. 2022, v16.8.0. adresse : https://www.3gpp.org/ftp/Specs/archive/38_series/38.331/.

- [58] 3rd Generation Partnership Project (3GPP), « NR; NR and NG-RAN Overall description; Stage-2, » 3rd Generation Partnership Project (3GPP), Technical specification (TS) 38.300, jan. 2021, v16.4.0. adresse : https://www.3gpp.org/ftp/Specs/archive/38_series/38.300/.
- [59] 3rd Generation Partnership Project (3GPP), « Evolved Universal Terrestrial Radio Access (E-UTRA) and NR; Service Data Adaptation Protocol (SDAP) specification, » 3rd Generation Partnership Project (3GPP), Technical specification (TS) 37.324, juill. 2021, v16.3.0. adresse : https://www.3gpp.org/ftp/Specs/archive/37_series/37.324/.
- [60] 3rd Generation Partnership Project (3GPP), « NR; Packet Data Convergence Protocol (PDCP) specification, » 3rd Generation Partnership Project (3GPP), Technical specification (TS) 38.323, mars 2021, v16.3.0. adresse : https://www.3gpp.org/ftp/Specs/archive/38_series/38.323/.
- [61] 3rd Generation Partnership Project (3GPP), « NR; Radio Link Control (RLC) protocol specification, » 3rd Generation Partnership Project (3GPP), Technical specification (TS) 38.322, juill. 2022, v16.3.0. adresse : https://www.3gpp.org/ftp/Specs/archive/38_series/38.322/.
- [62] 3rd Generation Partnership Project (3GPP), « NR; Medium Access Control (MAC) protocol specification, » 3rd Generation Partnership Project (3GPP), Technical specification (TS) 38.321, avr. 2022, v16.8.0. adresse : https://www.3gpp.org/ftp/Specs/archive/38_series/38.321/.
- [63] 3rd Generation Partnership Project (3GPP), « NR; Physical layer; General description, » 3rd Generation Partnership Project (3GPP), Technical specification (TS) 38.201, jan. 2020, v16.0.0. adresse : https://www.3gpp.org/ftp/Specs/archive/38_series/38.201/.
- [64] 3rd Generation Partnership Project (3GPP), « NR; Services provided by the physical layer, » 3rd Generation Partnership Project (3GPP), Technical specification (TS) 38.202, jan. 2022, v16.3.0.

adresse : https://www.3gpp.org/ftp/Specs/archive/38_series/38.202/.

- [65] 3rd Generation Partnership Project (3GPP), « NR; Physical channels and modulation, » 3rd Generation Partnership Project (3GPP), Technical specification (TS) 38.211, jan. 2022, v16.8.0. adresse : https://www.3gpp.org/ftp/Specs/archive/38_series/38.211/.
- [66] 3rd Generation Partnership Project (3GPP), « NR; Multiplexing and channel coding, » 3rd Generation Partnership Project (3GPP), Technical specification (TS) 38.212, jan. 2022, v16.8.0. adresse : https://www.3gpp.org/ftp/Specs/archive/38_series/38.212/.
- [67] 3rd Generation Partnership Project (3GPP), « NR; Physical layer procedures for control, » 3rd Generation Partnership Project (3GPP), Technical specification (TS) 38.213, jan. 2022, v16.8.0. adresse : https://www.3gpp.org/ftp/Specs/archive/38_series/38.213/.
- [68] 3rd Generation Partnership Project (3GPP), « NR; Physical layer procedures for data, » 3rd Generation Partnership Project (3GPP), Technical specification (TS) 38.214, jan. 2020, v16.0.0. adresse : https://www.3gpp.org/ftp/Specs/archive/38_series/38.214/.
- [69] 3rd Generation Partnership Project (3GPP), « NR; Physical layer measurements, » 3rd Generation Partnership Project (3GPP), Technical specification (TS) 38.215, avr. 2022, v16.5.0. adresse : https://www.3gpp.org/ftp/Specs/archive/38_series/38.215/.
- [70] 3rd Generation Partnership Project (3GPP), « NR; User Equipment (UE) radio transmission and reception; Part 1 : Range 1 Standalone, » 3rd Generation Partnership Project (3GPP), Technical specification (TS) 38.101-1, oct. 2021, v16.9.0. adresse : https://www.3gpp.org/ftp/Specs/archive/38_series/38.101-1/.

- [71] 3rd Generation Partnership Project (3GPP), « Overall description of Radio Access Network (RAN) aspects for Vehicle-to-everything (V2X) based on LTE and NR, » 3rd Generation Partnership Project (3GPP), Technical report (TR) 37.985, avr. 2022, v16.1.0. adresse : https://www.3gpp.org/ftp/Specs/archive/37_series/37.985/.
- [72] Q. Zhao, X. Ma et X. Liu, « Analysis of doppler effect of vehicle noise on environmental noise, » in *2020 5th International Conference on Information Science, Computer Technology and Transportation (ISCTT)*, IEEE, 2020, p. 589-592.
- [73] 3rd Generation Partnership Project (3GPP), « Service requirements for enhanced V2X scenarios, » 3rd Generation Partnership Project (3GPP), Technical specification (TS) 22.186, sept. 2018, v16.0.0. adresse : https://www.3gpp.org/ftp/Specs/archive/22_series/22.186/.
- [74] 3rd Generation Partnership Project (3GPP), « Study on enhancement of 3GPP support for 5G V2X services, » 3rd Generation Partnership Project (3GPP), Technical report (TR) 22.886, déc. 2018, v16.2.0. adresse : https://www.3gpp.org/ftp/Specs/archive/22_series/22.886/.
- [75] SAE, *Taxonomy and Definitions for Terms Related to Driving Automation Systems for On-Road Motor Vehicles Accessed : 2021*. adresse : https://www.sae.org/standards/content/j3016_202104/.
- [76] J. Gao, M. R. Khandaker, F. Tariq, K.-K. Wong et R. T. Khan, « Deep neural network based resource allocation for V2X communications, » in *2019 IEEE 90th Vehicular Technology Conference (VTC2019-Fall)*, IEEE, 2019, p. 1-5.
- [77] O. Elgarhy, O. Yener et M. M. Alam, « Performance evaluation of 5G NR sidelink for V2X scenarios, » in *2022 18th Biennial Baltic Electronics Conference (BEC)*, IEEE, 2022, p. 1-5.
- [78] S. Xiaoqin, M. Juanjuan, L. Lei et Z. Tianchen, « Maximum-throughput sidelink resource allocation for NR-V2X networks with the energy-efficient CSI transmission, » *IEEE Access*, t. 8, p. 73 164-73 172, 2020.

- [79] D. M. Soleymani, L. Ravichandran, M. R. Gholami, G. Del Galdo et M. Harounabadi, « Energy-Efficient Autonomous Resource Selection for Power-Saving Users in NR V2X, » in *2021 IEEE 32nd Annual International Symposium on Personal, Indoor and Mobile Radio Communications (PIMRC)*, IEEE, 2021, p. 972-978.
- [80] V. Todisco, S. Bartoletti, C. Campolo, A. Molinaro, A. O. Berthet et A. Bazzi, « Performance analysis of sidelink 5G-V2X mode 2 through an open-source simulator, » *IEEE Access*, t. 9, p. 145 648-145 661, 2021.
- [81] Y. Yoon et H. Kim, « A stochastic reservation scheme for aperiodic traffic in NR V2X communication, » in *2021 IEEE Wireless Communications and Networking Conference (WCNC)*, IEEE, 2021, p. 1-6.
- [82] A. Molina-Galan, B. Coll-Perales et J. Gozalvez, « Re-Evaluation Strategies for 5G NR V2X Communications, » in *2022 IEEE 96th Vehicular Technology Conference (VTC2022-Fall)*, IEEE, 2022, p. 1-5.
- [83] Z. Ali, S. Lagén, L. Giupponi et R. Rouil, « 3GPP NR V2X mode 2 : overview, models and system-level evaluation, » *IEEE Access*, t. 9, p. 89 554-89 579, 2021.
- [84] M. Segata, P. Arvani et R. L. Cigno, « A critical assessment of C-V2X resource allocation scheme for platooning applications, » in *2021 16th Annual Conference on Wireless On-demand Network Systems and Services Conference (WONS)*, IEEE, 2021, p. 1-8.
- [85] S. Hegde, O. Blume, R. Shrivastava et H. Bakker, « Enhanced resource scheduling for platooning in 5G V2X systems, » in *2019 IEEE 2nd 5G World Forum (5GWF)*, IEEE, 2019, p. 108-113.
- [86] J. Kim, Y.-J. Choi, G. Noh et H. Chung, « On the Feasibility of Remote Driving Applications Over Mmwave 5 G Vehicular Communications : Implementation and Demonstration, » *IEEE Transactions on Vehicular Technology*, 2022.

- [87] T. Zugno, M. Drago, M. Giordani, M. Polese et M. Zorzi, « NR V2X communications at millimeter waves : An end-to-end performance evaluation, » in *GLOBECOM 2020-2020 IEEE Global Communications Conference*, IEEE, 2020, p. 1-6.
- [88] A. Reyhanoglu et al., « Machine Learning Aided NR-V2X Quality of Service Predictions, » in *2023 IEEE Vehicular Networking Conference (VNC)*, IEEE, 2023, p. 183-186.
- [89] L. Cao et H. Yin, « Resource allocation for vehicle platooning in 5G NR-V2X via deep reinforcement learning, » in *2021 IEEE International Black Sea Conference on Communications and Networking (BlackSeaCom)*, IEEE, 2021, p. 1-7.
- [90] M. Parvini, M. R. Javan, N. Mokari, B. Abbasi et E. A. Jorswieck, « Aol-aware resource allocation for platoon-based C-V2X networks via multi-agent multi-task reinforcement learning, » *IEEE Transactions on Vehicular Technology*, 2023.
- [91] H. Ye, G. Y. Li et B.-H. F. Juang, « Deep reinforcement learning based resource allocation for V2V communications, » *IEEE Transactions on Vehicular Technology*, t. 68, n° 4, p. 3163-3173, 2019.
- [92] H. Ye et G. Y. Li, « Deep reinforcement learning for resource allocation in V2V communications, » in *2018 IEEE International Conference on Communications (ICC)*, IEEE, 2018, p. 1-6.
- [93] M. C. Lucas-Estañ et al., « Analysis of 5G RAN Configuration to Support Advanced V2X Services, » in *2021 IEEE 93rd Vehicular Technology Conference (VTC2021-Spring)*, IEEE, 2021, p. 1-5.
- [94] M. C. Lucas-Estañ et al., « On the scalability of the 5G RAN to support advanced V2X services, » in *2020 IEEE Vehicular Networking Conference (VNC)*, IEEE, 2020, p. 1-4.
- [95] F. Romeo, C. Campolo, A. Molinaro et A. O. Berthet, « DENM repetitions to enhance reliability of the autonomous mode in NR V2X sidelink, » in *2020 IEEE 91st Vehicular Technology Conference (VTC2020-Spring)*, IEEE, 2020, p. 1-5.

- [96] J. Yan et J. Härri, « On the Feasibility of URLLC for 5G-NR V2X Sidelink Communication at 5.9 GHz, » in *GLOBECOM 2022-2022 IEEE Global Communications Conference*, IEEE, 2022, p. 3599-3604.
- [97] F. Romeo, C. Campolo, A. Molinaro, A. O. Berthet et A. Bazzi, « Supporting Sporadic DENM Traffic over 5G-V2X Sidelink in the Autonomous Mode, » in *2021 IEEE 94th Vehicular Technology Conference (VTC2021-Fall)*, IEEE, 2021, p. 1-5.
- [98] F. Romeo, C. Campolo, A. O. Berthet et A. Molinaro, « Improving the DENM reliability over 5G-V2X sidelink through repetitions and diversity combining, » in *2021 IEEE 4th 5G World Forum (5GWF)*, IEEE, 2021, p. 352-357.
- [99] K. Sehla, T. M. T. Nguyen, G. Pujolle et P. B. Velloso, « Resource allocation modes in C-V2X : from LTE-V2X to 5G-V2X, » *IEEE Internet of Things Journal*, t. 9, n° 11, p. 8291-8314, 2022.
- [100] A. A. Zaidi et al., « Waveform and numerology to support 5G services and requirements, » *IEEE Communications Magazine*, t. 54, n° 11, p. 90-98, 2016.
- [101] N. Patriciello, S. Lagen, L. Giupponi et B. Bojovic, « 5G new radio numerologies and their impact on the end-to-end latency, » in *2018 IEEE 23rd international workshop on computer aided modeling and design of communication links and networks (CAMAD)*, IEEE, 2018, p. 1-6.
- [102] A. A. Zaidi, R. Baldemair, V. Molés-Cases, N. He, K. Werner et A. Cedergren, « OFDM numerology design for 5G new radio to support IoT, eMBB, and MBSFN, » *IEEE Communications Standards Magazine*, t. 2, n° 2, p. 78-83, 2018.
- [103] F. Abinader et al., « Impact of bandwidth part (BWP) switching on 5G NR system performance, » in *2019 IEEE 2nd 5G World Forum (5GWF)*, IEEE, 2019, p. 161-166.
- [104] T. Bag, S. Garg, Z. Shaik et A. Mitschele-Thiel, « Multi-numerology based resource allocation for reducing average scheduling latencies for 5G NR wireless networks, » in *2019 European Confe-*

- rence on Networks and Communications (EuCNC)*, IEEE, 2019, p. 597-602.
- [105] S. Khabaz, K. O. Boulila, T. M. T. Nguyen, G. Pujolle, M. El Aoun et P. B. Velloso, « A Comprehensive Study of the Impact of 5G Numerologies on V2X Communications, » in *2022 13th International Conference on Network of the Future (NoF)*, IEEE, 2022, p. 1-9.
- [106] D. Wang, O. Saraci, R. R. Sattiraju, Q. Zhou et H. D. Schotten, « Effect of Variable Physical Numerologies on Link-Level Performance of 5G NR V2X, » in *2022 IEEE 8th International Conference on Computer and Communications (ICCC)*, 2022, p. 291-296. doi : [10.1109/ICCC56324.2022.10065622](https://doi.org/10.1109/ICCC56324.2022.10065622).
- [107] G. M. N. Ali, S. A. Sharief, M. N. Sadat et M. S. Miah, « Performance Analysis of 5G New Radio V2X Communication, » in *2023 IEEE Wireless and Microwave Technology Conference (WAMICON)*, IEEE, 2023, p. 1-4.
- [108] J. Valgas, D. Martin-Sacristan et J. Monserrat, « 5G New Radio Numerologies and their Impact on V2X Communications, » in *Waves*, 2018, p. 15-22.
- [109] C. Campolo, A. Molinaro, F. Romeo, A. Bazzi et A. O. Berthet, « 5G NR V2X : On the impact of a flexible numerology on the autonomous sidelink mode, » in *2019 IEEE 2nd 5G World Forum (5GWF)*, IEEE, 2019, p. 102-107.
- [110] Z. Ali, S. Lagén et L. Giupponi, « On the impact of numerology in NR V2X Mode 2 with sensing and random resource selection, » in *2021 IEEE Vehicular Networking Conference (VNC)*, IEEE, 2021, p. 151-157.
- [111] S. Khabaz, K. O. Boulila, T. M. T. Nguyen, G. Pujolle, M. El Aoun et P. B. Velloso, « A New Priority and Satisfaction-based Resource Allocation Algorithm with Mixed Numerology for 5G-V2X communications, » in *2022 14th IFIP Wireless and Mobile Networking Conference (WMNC)*, IEEE, 2022, p. 85-92.

- [112] 3rd Generation Partnership Project (3GPP), « NR; User Equipment (UE) radio access capabilities, » 3rd Generation Partnership Project (3GPP), Technical specification (TS) 38.306, avr. 2020, v16.0.0. adresse : https://www.3gpp.org/ftp/Specs/archive/38_series/38.306/.
- [113] Matlab, *5G NR CQI reporting Accessed : 2021*. adresse : <https://ch.mathworks.com/help/5g/ug/5g-nr-cqi-reporting.html>.
- [114] H. Ji, S. Park, J. Yeo, Y. Kim, J. Lee et B. Shim, « Ultra-reliable and low-latency communications in 5G downlink : Physical layer aspects, » *IEEE Wireless Communications*, t. 25, n° 3, p. 124-130, 2018.
- [115] "<https://github.com/alessandrobazzi/LTEV2Vsim>", 2020.
- [116] 3rd Generation Partnership Project (3GPP), « Study on channel model for frequencies from 0.5 to 100 GHz, » 3rd Generation Partnership Project (3GPP), Technical report (TR) 38.901, jan. 2020, v16.1.0. adresse : https://www.3gpp.org/ftp/Specs/archive/38_series/38.901/.
- [117] A. L. Samuel, « Some Studies in Machine Learning Using the Game of Checkers, » *IBM Journal of Research and Development*, t. 3, n° 3, p. 210-229, juill. 1959, Conference Name : IBM Journal of Research and Development, issn : 0018-8646. doi : [10.1147/rd.33.0210](https://doi.org/10.1147/rd.33.0210).
- [118] F. Emmert-Streib et M. Dehmer, « Taxonomy of machine learning paradigms : A data-centric perspective, » en, *WIREs Data Mining and Knowledge Discovery*, t. 12, n° 5, e1470, 2022, _eprint : <https://onlinelibrary.wiley.com/doi/pdf/10.1002/widm.1470>, issn : 1942-4795. doi : [10.1002/widm.1470](https://doi.org/10.1002/widm.1470). adresse : <https://onlinelibrary.wiley.com/doi/abs/10.1002/widm.1470> (visité le 08/03/2023).
- [119] R. Bellman, « A Markovian decision process, » *Journal of mathematics and mechanics*, p. 679-684, 1957.
- [120] R. A. Howard, « Dynamic programming and markov processes., » 1960.

- [121] L. Rokach et O. Maimon, *Data Mining with Decision Trees*, 2nd. WORLD SCIENTIFIC, 2014. doi : [10.1142/9097](https://doi.org/10.1142/9097). eprint : <https://www.worldscientific.com/doi/pdf/10.1142/9097>. adresse : <https://www.worldscientific.com/doi/abs/10.1142/9097>.
- [122] L. E. Raileanu et K. Stoffel, « Theoretical comparison between the gini index and information gain criteria, » *Annals of Mathematics and Artificial Intelligence*, t. 41, p. 77-93, 2004.
- [123] H. M. Sani, C. Lei et D. Neagu, « Computational complexity analysis of decision tree algorithms, » in *Artificial Intelligence XXXV : 38th SGA1 International Conference on Artificial Intelligence, AI 2018, Cambridge, UK, December 11-13, 2018, Proceedings 38*, Springer, 2018, p. 191-197.
- [124] S. project, *Real-time location-aware road weather services composed from multi-modal data (SARWS) project* Accessed : 2022. adresse : <https://sarws.eu/>.
- [125] OpenAirInterface, *OpenAirInterface website* Accessed : 2023. adresse : <https://openairinterface.org>.